NASA CONTRACTOR
REPORT

NASA CR-61233

July 1968

NASA CR-61233

GPO PRICE $ _____

CSFTI PRICE(S) $ _____

Hard copy (HC) 3.00

Microfiche (MF) .65

ff 653 July 65

STUDY ON EXHAUST PLUME RADIATION PREDICTIONS
Final Report

Prepared under Contract No. NAS 8-21082 by
GENERAL DYNAMICS
Convair Division

For

NASA-GEORGE C. MARSHALL SPACE FLIGHT CENTER
Huntsville, Alabama

July 1968

NASA CR-61233

STUDY ON
EXHAUST PLUME RADIATION PREDICTIONS
(Final Report originally published Nov. 1967)

Prepared under Contract No. NAS 8-21082 by
GENERAL DYNAMICS
Convair Division

For

Aero-Astrodynamics Laboratory

NASA-GEORGE C. MARSHALL SPACE FLIGHT CENTER

TABLE OF CONTENTS

Section		Page
	LIST OF ILLUSTRATIONS	iv
	SUMMARY	x
1	INTRODUCTION	1-1
2	EXPERIMENTAL PROCEDURE	2-1
3	DATA ANALYSIS	3-1
4	RESULTS	4-1
	4.1 THE ABSORPTION COEFFICIENTS OF H_2O	4-1
	4.2 THE INVERSE OF THE LINE SPACINGS	4-1
	4.3 COMPARISON WITH EXPERIMENTAL DATA	4-5
	4.4 ERROR LIMITS	4-5
	4.5 INHOMOGENEOUS GAS MEASUREMENTS	4-8
5	THEORETICAL SENSITIVITY STUDY	5-1
6	REFERENCES	6-1
7	FIGURES	7-1
8	TABLES	8-1

LIST OF ILLUSTRATIONS

Figure	Caption	Page
1	Photograph of twenty burner sections installed inside the tank.	7-1
2	Curve of growth at 2000°K for ω = 3500 cm^{-1} in terms of $\left(u/\ell n\ (1/1-\epsilon)\right)^2$ versus u. Previous data are indicated by (□), the present data by (Δ).	7-2
3	Comparison of the total emissivity between 1150 and 5900 cm^{-1} at 2500°K, based on previous k and a (solid line) and based on present k and (1/d) (dashed line) at p_T = 0.1 atm as a function of pL(cm-atm) for 50% H_2O and 50% N_2.	7-3
3a	Comparison of the total emissivity between 1150 and 5900 cm^{-1} at 1500°K, based on previous k and a (solid line) and based on present k and (1/d) (dashed line) at p_T = 0.1 atm as a function of pL(cm-atm) for 50% H_2O and 50% N_2.	7-4
4	Comparison of previous k (*) and present k (solid line) at 300°K.	7-5
5	Comparison of previous k (*) and present k (solid line) at 600°K.	7-6
6	Comparison of previous k (*) and present k (solid line) at 1000°K.	7-7
7	Comparison of previous k (*) and present k (solid line) at 1500°K.	7-8
8	Comparison of previous k (*) and present k (solid line) at 2000°K.	7-9

LIST OF ILLUSTRATIONS (CON'T)

Figure	Caption	Page
9	Comparison of previous k (*) and present k (solid line) at 2500°K.	7-10
10	Comparison of previous k (*) and present k (solid line) at 3000°K.	7-11
11	Plot of $(1/d_{LR})$ versus T at 1500 cm^{-1} (A), 1525 (B), 1550 (C), and 1575 cm^{-1} (D).	7-12
12	Plot of $(1/d_{LR})$ versus T at 2000 cm^{-1} (A), 2025 (B), 2050 (C), and 2075 cm^{-1} (D).	7-13
13	Plot of $(1/d_{LR})$ versus T at 2500 cm^{-1} (A), 2525 (B), 2550 (C), and 2575 cm^{-1} (D).	7-14
14	Plot of $(1/d_{LR})$ versus T at 3000 cm^{-1} (A), 3025 (B), 3050 (C), and 3075 cm^{-1} (D).	7-15
15	Plot of $(1/d_{LR})$ versus T at 3500 cm^{-1} (A), 3525 (B), 3550 (C), and 3575 cm^{-1} (D).	7-16
16	Plot of $(1/d_{LR})$ versus T at 4000 cm^{-1} (A), 4025 (B), 4050 (C), and 4075 cm^{-1} (D).	7-17
17	Plot of $(1/d_{LR})$ versus T at 4500 cm^{-1} (A), 4525 (B), 4550 (C), and 4575 cm^{-1} (D).	7-18
18	Plot of $(1/d_{LR})$ versus T at 5000 cm^{-1} (A), 5025 (B), 5050 (C), and 5075 cm^{-1} (D).	7-19
19	Plot of $(1/d_{LR})$ versus T at 5500 cm^{-1} (A), 5525 (B), 5550 (C), and 5575 cm^{-1} (D).	7-20
20	Plot of $(1/d_{LR})$ versus T at 6000 cm^{-1} (A), 6025 (B), 6050 (C), and 6075 cm^{-1} (D).	7-21

LIST OF ILLUSTRATIONS (CON'T)

Figure	Caption	Page
21	Plot of $(1/d_{LR})$ versus ω between 1150 cm^{-1} and 7500 cm^{-1} for T = 600°, 1000°, 1500°, 2000°, 2500°, and 3000°K. The extrapolated regions are indicated by dashed lines.	7-22
22	Integrated emissivity between 1150 and 7500 cm^{-1} versus pL, based on (1/d) from Table II (solid line) and (1/d) as a sinusoidal function of ω (dashed line) for 1500° and 2500°K. Total pressure is 0.1 atm, 50% H_2O and 50% N_2. Note: The values for the 2500°K case must be multiplied by 10.	7-23
23	Integrated band emissivities at 1500°K versus pL, based on (1/d) from Table II (solid line) and on (1/d) as a sinusoidal function of ω (dashed line). Total pressure is 0.1 atm, 50% H_2O and 50% N_2.	7-24
24	Integrated band emissivities at 2500°K versus pL, based on (1/d) from Table II (solid line) and on (1/d) as a sinusoidal function of ω (dashed line). Total pressure is 0.1 atm, 50% H_2O and 50% N_2.	7-25
25	Comparison between experimental (solid line) and computed spectra (*) at 1500°K and 2' pathlength.	7-26
26	Comparison between experimental (solid line) and computed spectra (*) at 2500°K and 2' pathlength.	7-27
27	Comparison between experimental (solid line) and computed spectra (*) at 1500°K and 5' pathlength.	7-28
28	Comparison between experimental (solid line) and computed spectra (*) at 2500°K and 5' pathlength.	7-29

LIST OF ILLUSTRATIONS (CON'T)

Figure	Caption	Page
29	Comparison between experimental (solid line) and computed spectra (*) at 1500°K and 10' pathlength.	7-30
30	Comparison between experimental (solid line) and computed spectra (*) at 2500°K and 10' pathlength.	7-31
31	Comparison between experimental (solid line) and computed spectra (*) at 1500°K and 20' pathlength.	7-32
32	Comparison between experimental (solid line) and computed spectra (*) at 2500°K and 20' pathlength.	7-33
33	Comparison with experimental results obtained by Simmons (solid line) at 1020 ± 7°K for different pressures of H_2O at a pathlength of 60 cm.	7-34
34	Comparisons with experimental results obtained by Simmons (solid line) at 1177 ± 6°K for different pressures of H_2O at a pathlength of 60 cm.	7-35
35	Error in ϵ due to uncertainty of ± 3% in T versus ω for three different temperatures.	7-36
36	RMS scatter of experimental values to curve of growth at T = 2750°K.	7-37
37	RMS scatter of experimental values to curve of growth at T = 2000°K.	7-38
38	RMS scatter of experimental values to curve of growth at T = 1250°K.	7-39

Figure	Caption	Page
39	Radiance from four slabs (ℓ = 150 cm each) in watts/$cm^2 cm^{-1}$. Solid line is the experimental curve. Calculated values from Model 3 are given by (□), from Model 3a are given by (X). Conditions for T and c are given in Section 4.5.	7-40
40	Radiance from four slabs (ℓ = 150 cm each) in watts/$cm^2 cm^{-1}$. Solid line is the experimental curve. Calculated values from Model 3 are given by (□), from Model 3a are given by (X). Conditions for T and c are given in Section 4.5.	7-41
41	Radiance from four slabs (ℓ = 150 cm each) in watts/$cm^2 cm^{-1}$. Solid line is the experimental curve. Calculated values from Model 3 are given by (□), from Model 3a are given by (X). Conditions for T and c are given in Section 4.5.	7-42
42	Graph of $e_n(x_E)$ vs x_E for n = 1.8 (dashed), n = 2.0 (solid), and n = 2.2 (dotted). For a Lorentz shape n = 2; a line with n < 2 has above-Lorentzian wings; a line with n > 2 has below-Lorentzian wings.	7-43
43	Line intensity probability distribution functions. Solid line: $P(S) \propto S^{-1}$. Dotted lines: $P(S) \propto [\ell n\ (S_M/S)]^m\ S^{-1}$, for m = 1, 2, 3. Dashed line: $P(S) \propto S^{-2}$. All P(S) = 0 outside of region $(S_M/R \leq S \leq S_M)$.	7-44

Figure	Caption	Page
44	Curves of growth for random Lorentz band models. Solid line: $P(S) = \delta(S-S_E)$. Dotted line: $P(S) \propto S^{-1} \exp(-S/\pi S_E)$. Dashed line: $P(S) \propto S^{-2} [(S_M+S)\exp(-S/S_M) - (S_M-RS)\exp(-RS/S_M)]$ for $R = 10^6$.	7-45

SUMMARY

This report documents research performed under Contract NAS 8-21082 between 1 January 1967 and 31 October 1967. The object of this program is to measure the absorption coefficients and fine structure parameters of water vapor at wavelengths between 1 and 10 μ and at temperatures between 1200° and 3000°K and to incorporate these into a practical analytic procedure which may be used for the evaluation of the radiative base heating of Saturn V and other launch vehicles. Scientific and technical personnel who spent appreciable amounts of their time on this study were C. B. Ludwig (Principal Investigator and Project Leader), J. A. L. Thomson, W. Malkmus, M. L. Streiff, C. N. Abeyta, R. Janda, and D. Suttie. The Contract Monitor was R. M. Huffaker, Aerodynamics Branch, National Aeronautics and Space Administration, Marshall Space Flight Center, Huntsville, Alabama.

A uniform volume of high temperature water vapor was produced above the combustion zone of a long three inch wide flat burner which was constructed for these measurements. Emission and absorption measurements were made with a pathlength of 20 feet.

The results obtained under the present program have been combined with previous data in order to generate tables of water vapor absorption coefficients covering the spectral region 50 to 9300 cm^{-1} and the temperature interval 300° to 3000°K. The representation of the inverse of the line spacing covers the intervals 1150 to 7500 cm^{-1} in the temperature range from 600° to 3000°K.

Several nonisothermal measurements with four five-foot sections at different temperatures were made to test the nonisothermal radiance calculation procedure.

A theoretical study of the sensitivity of band models to deviations of the line shape from the assumed Lorentz shape was made and plausible line intensity distribution functions were investigated.

SECTION 1

INTRODUCTION

Measurements of hot water vapor absorption up to a pathlength of ten feet were carried out previously. Assuming the applicability of the statistical band model, values for the absorption coefficients and fine structure parameters were obtained.

The purpose of the research reported here is the extension of these measurements to twenty feet, in order to obtain more reliable values of the fine structure parameter in spectral regions where the square-root region of water vapor becomes better defined only at longer pathlengths. These spectral regions include the troughs between the vibration-rotation bands and the higher order bands at elevated temperatures.

Of course, at and near the bottom of the troughs, much longer pathlengths than the present twenty feet are needed to bring the water absorption into the square-root regions. However, the present results are sufficient as to extrapolate with confidence the values of the fine structure parameter into these trough regions, thereby eliminating the uncertainty existing in the previously reported values.

New values of the absorption coefficients k and the reciprocal of the average line spacing d are reported. The decision to present $1/d$ rather than "a" was dictated by the desire to reduce the complexity in the calculation of ϵ at other than the present conditions. The representation of the line half width γ as a function of self and foreign gas broadening, temperature, and pressure is the same as given in Refs. 1 and 2.

The new values of k are very similar to the values reported previously. The new values of the fine structure parameter a (and therefore $1/d = a/\gamma$)

are similar to the previous band-averaged values of a for the 6.3- and 2.7-μ band at all temperatures, for the 1.8- and 1.14-μ band only at temperatures below 1500°K. Higher values of a are obtained for these bands at higher temperatures (> 1500°K) and in the troughs. In order to facilitate the computational procedures in complex programs, it is desirable to represent the frequency dependent term 1/d by simple equations. Previously, band-averaged values were suggested. We propose now to replace the band-averaged values with a sinusoidal function, which simulates much more closely the measured and extrapolated values of 1/d. While this does not render the computations more difficult, it gives better values of ε at long and non-homogeneous pathlengths than by using band-averaged values.

In addition to these measurements, the independent control of four separate five-feet sections was utilized to make inhomogeneous measurements. The comparison with calculations using the present set of k and 1/d and the Curtis-Godson approximation gives good agreement, even for the extreme case, where the radiation of 5 feet of H_2O at 2500°K is passing through 15 feet of H_2O at 1200°K. Although we estimate that the calculation of the spectral and total emissivities of water vapor above 1200°K is accurate to within ± 20% for homogeneous and inhomogeneous paths at most of the conditions relevant to the exhaust of the Saturn V, certain additional studies must be made to verify this confidence level to temperatures below 1200°K and to more extreme inhomogeneous paths. The first task can be carried out through the analysis of the extensive experimental data taken by Rocketdyne[3] and by the University of Michigan.[4] The second task requires a combination of experimental and theoretical investigations. More extreme inhomogeneous

path measurements must be taken and work on different models for use in the Curtis-Godson approximation must be continued.

SECTION 2

EXPERIMENTAL PROCEDURE

The installation of the ten-foot burner was described previously.[1] For the present program, ten feet of burner with the necessary propellant, cooling and control system were added. A photograph of the completed burner inside the tank is shown in Fig. 1. At both sides of the burner, the manifolds connecting five one-foot sections can be seen. The four infrared safety devices (one for each five-foot section) are located outside the tank and cannot be seen in the figure, except one hole in the tank wall near the entrance, through which the collimated radiation passes. The infrared safety devices consist of a PbS detector, an amplifier, and a relay, which governs the two main control valves for the propellants. If the radiation drops below a previous set level, the main control valves are shut and a nitrogen purge is initiated. In addition, the output of these amplifiers is displayed on a Sanborn recorder in order to check the constancy of the radiation during a spectral scan. The maximum variation of the output level was within the accuracy of the control gages (± 2%). The check of the homogeneity was again made with a thermocouple, traveling the total length along the line of sight. The RMS value of the variations was less than 5%.

A total of 24 runs were made. In order to establish consistency with the previous runs, six runs with a five-foot pathlength using different five-foot sections, six runs with a ten-foot pathlength, and twelve runs with a twenty-foot pathlength were made. During the course of these runs, one error was discovered, which existed in some of the previous runs made last

year at ten-foot pathlengths. A discussion of this is given in the next section.

SECTION 3

DATA ANALYSIS

The same data reduction procedure as described in Ref. 1 was used. Previous runs at 2', 5', and 10' together with new runs at 5', 10', and 20' were used. The spectral emissivities were averaged over 25 cm^{-1} intervals. The averaged emissivities were then least-square fitted to 2nd degree polynomials as functions of the temperature. The RMS of the deviation to these fits was about the same as was found previously, less than ± 5% in the bands, but somewhat greater in the troughs, where the signal-to-noise ratio was smaller. However, the errors in the 20' trough measurements were less than the corresponding measurements at smaller pathlengths.

From the curve-fitted data, the emissivities were calculated at specified temperatures between 1250° and 2750°K. Using the statistical model with exponential line intensity distribution, the parameters k and a were obtained from the curves of growth at each ω. The curves of growth $\ell n(1/1-\epsilon)$ were transformed into linear functions of u:

$$\left(u/\ell n\ (1/1-\epsilon)\right)^2 = k^{-2} + u(4ak)^{-1} \quad . \tag{1}$$

From the intercept with the ordinate and from the slope, the values of k and a, respectively, are obtained.

In comparing these data with the previous ones, given in Ref. 1, the following observations are made.

1. The absorption coefficients are essentially the same, except in the troughs.
2. The fine structure parameters "a" are larger for the higher order bands and for the trough regions between the bands. The reason for the difference is twofold: first, the 20' burner data improved the determination of the square-root region, which was previously well-defined only for the regions having the largest values of k; second, some of the previous 10' burner data were in error by about 20%.

This error occurred through a wrong calibration in the propellant system which influenced the determination of the temperature. After the data were corrected and new 10' data obtained as a check, they were then used in the present data reduction, which subsequently gave higher values of a. As an example, the curve of growth at 2000°K for $\omega = 3500$ cm^{-1} is plotted in Fig. 2. The previous data are given by (□), and the resulting curve of growth (least-square fit) is given by the dashed line. The present data are given by (Δ) and the curve of growth is given by the solid line. The present curve has a smaller slope and, therefore, a greater value of "a" for the same k. At the same time, the σ (RMS of the scatter of data points) is much reduced.

As in the previous data reduction, where the largest pathlength was 10', the present data up to 20' are still not sufficient to determine the fine structure parameter in the troughs between the bands. These regions were presented in Ref. 1 as dotted lines because of this uncertainty. However, a certain consistency in the data let us believe that "a" was small in these regions. We are now convinced that the consistency was fortuitous. The

present data indicate a rise of "a" toward the wings of the bands so that the actual minima of "a" occur in the center of the bands (excluding the Q-branch) and not in the troughs.

Although the absolute levels of "a" and the dependence of "a" on the wavelength are different as compared with the results given in Ref. 1, the difference in the total emissivity based on the two different sets of "a" is small and is within the uncertainty limits of the band model parameters. In Figs. 3 and 3a, the total emissivities between 1150 and 5900 cm^{-1} at 2500^{o} and $1500^{o}K$, respectively, are computed based on previous k and band-averaged a's and on present k and 1/d at a total pressure of 0.1 atm and 50% H_2O and 50% N_2 mixture. The abscissa is the pathlength from 0.1 to 10^5 cm-atm. The maximum deviation of about 25% occurs at around 100 cm-atm for $1500^{o}K$.

SECTION 4

RESULTS

In this section, we present the results of the absorption coefficients and the fine structure parameter in graphical and tabular form. Comparisons between experimental and calculated data, error considerations and results of inhomogeneous data are also given.

4.1 THE ABSORPTION COEFFICIENTS OF H_2O

Data were obtained in the temperature range from 1250° to 2750°K. Extrapolations were made to 1000° and 3000°K. Previous data at 300° and 600°K were re-examined and changes incorporated where necessary. Comparisons of the new data versus previous data[1] are shown in Figs. 4-10 at the temperatures of 300°, 600°, 1000°, 1500°, 2000°, 2500°, and 3000°K. The major differences occur in the troughs only. The change of the trough values at 4600 cm^{-1} for 1000°K comes through an error in the previous data. No experimental data exist for the trough values at the temperatures of 600° and 300°K. The new data are logical extrapolations from the high temperature results. The results are given also in tabular form in Table I.

4.2 THE INVERSE OF THE LINE SPACINGS

While the format and the actual values of the absorption coefficients are changed very little, the representation of the fine structure parameter has been changed. In the case for pure collision broadening for H_2O spectral lines, we write

$$a_c = \gamma_c^{H_2O}/d \qquad (2)$$

where

$$\gamma_c^{H_2O} = \sum_j \left[\left(\gamma_j^{H_2O} \right)_{STP} p_j \left(\frac{273}{T} \right)^{1/2} \right] + \left(\gamma^{*H_2O}_{H_2O} \right)_{STP} p_{H_2O} \left(\frac{273}{T} \right) \quad . \quad (3)$$

Preliminary data of the individual line half widths for different broadeners are the following (the same as given in Ref. 2). The data in parentheses are guesses.

$$\gamma^{*H_2O}_{H_2O} = 0.44$$

$$\gamma^{H_2O}_{H_2O} = (0.09)$$

$$\gamma^{H_2O}_{N_2} = 0.09$$

$$\gamma^{H_2O}_{O_2} = 0.04$$

$$\gamma^{H_2O}_{H_2} = (0.05)$$

$$\gamma^{H_2O}_{CO_2} = 0.12$$

$$\gamma^{H_2O}_{CO} = (0.10)$$

Values of the inverse of the line spacings (1/d) are given in this report. These are identical to the $(1/d_{LR})$, used in Model 3a. For Model 3, values of $1/d_o$ are used, where

$$\frac{1}{d_{LR}} = \frac{1}{d_o} \frac{1+e^{-\theta/2T}}{1-e^{-\theta/2T}} \quad (4)$$

with $\theta = 2300°K$. For a binary mixture, Eq. (2) reduces to

$$\gamma_c^{H_2O} = p_T \left[c\left(0.44 \left(\frac{273}{T}\right) + 0.09 \left(\frac{273}{T}\right)^{1/2}\right) + (1-c) \left(\frac{273}{T}\right)^{1/2} \gamma_j^{H_2O} \right] \quad (5)$$

which has been used (with $\gamma_j^{H_2O} = \gamma_{O_2}^{H_2O} = 0.04$) to reduce our experimental data of "a" to the values of $1/d$ $(= 1/d_{LR})$. The concentration c for our conditions was calculated from a thermochemical equilibrium model.

The reduction of the experimental values of "a" to the parameter $1/d$ assumes the validity of the representation of the collision half width through Eq. (3) or Eq. (5) and the three individual half widths $\gamma_{H_2O}^{*H_2O}$, $\gamma_{H_2O}^{H_2O}$, and $\gamma_{O_2}^{H_2O}$. If in the future a new representation of $\gamma_c^{H_2O}$ and/or new individual half widths are found to be more applicable, the fine structure parameter "a" can be obtained through Eq. (5) and the values of $1/d$ listed in this report. The concentration c is given by

$$c = -.1002 + .2802 \times 10^{-3} T^1 - .1089 \times 10^{-6} T^2 + .0291 \times 10^{-9} T^3 \quad (6)$$

Data were obtained for the temperature range from 1250° to 2750°K in the approximate spectral regions:

$$1150 - 2200 \text{ cm}^{-1}$$

$$3200 - 4100 \text{ cm}^{-1}$$

$$4750 - 5700 \text{ cm}^{-1}$$

$$6700 - 7500 \text{ cm}^{-1}$$

These spectral regions correspond to the major portions of the four vibration-rotation bands of H_2O. In all cases, the values of 1/d increase toward the wings of the bands and become undetermined in the center of the troughs and the values of 1/d were extrapolated into the trough regions. Since the plots of the experimentally determined values of 1/d versus temperatures were smooth curves (see Figs. 11-20), they were extrapolated to 600°K and to 3000°K. A verification of these extrapolations to 600°K will be made in the future through the use of Simmons and Rocketdyne data.

The set of 1/d versus ω for T = 600°, 1000°, 1500°, 2000°, 2500°, and 3000°K is shown in Fig. 21, where all regions, which were extrapolated by us, are given as dashed lines. A list of the values is given in Table II.

In order to reduce the number of values to be stored in a computer program, the 1/d were represented by a sinusoidal function:

$$\ell n\, 1/d = A \sin (B\omega + C) + D(T) \qquad (7)$$

where

$$A = .7941$$

$$B = .0036$$

$$C = -8.043$$

$$D(T) = -2.295 + .3004 \times 10^{-2}\, T - .366 \times 10^{-6}\, T^2$$

In order to check this approximation, integrated emissivities were calculated based on (1/d) from Table II and on (1/d) from Eq. (7). The calculations were performed for a gas mixture of 50% H_2O and 50% N_2 at a total pressure of 0.1 atm. The optical path ranged from 0.1 cm-atm to 10^5 cm-atm. In Fig. 22, the total emissivities integrated from 1150 to 7500 cm^{-1} are compared. In Figs. 23 and 24, the band emissivities at 1500° and 2500°K,

respectively, are compared. The difference between the results is small.

4.3 COMPARISON WITH EXPERIMENTAL DATA

The consistency of our results was checked by comparing the experimentally measured emissivities with calculated values using the k and 1/d from Tables I and II. The results are shown to be consistent (see Figs. 25-32) for all pathlengths (2, 5, 10, and 20 feet) at two representative temperatures (1500° and 2500°K).

As an independent check, comparisons with Simmons' data are made for temperatures greater than 1000°K. The results are given in Figs. 33 and 34.

4.4 ERROR LIMITS

It is difficult to assign specific error limits to the data we presented, because they depend on many different parameters. We can estimate the precision with which the data were taken. From the knowledge of the statistical scatter, the accuracy of the intermediate and the final results can be estimated. It was found that both precision and accuracy depend upon the spectral regions, the temperature and the pathlengths. In addition to these considerations, the uncertainty of the models themselves must be assessed.

In order to give some overall error limits, we estimate the calculation of integrated radiancies (or total engineering emissivities) based on the data presented here to be within ± 5% for $pL \leq 20$ ft-atm. For greater pathlengths, the uncertainty is surely greater because it depends then more on the individual foreign gas broadener parameters, which are uncertain and, in some cases, are only guesses. For the calculation of spectral radiancies (or spectral emissivities), we estimate the overall error limits to be within

± 20%. There are several exceptions to this value. The center of the 2.7-μ band at the higher temperatures is known better than ± 10%, while all the trough regions and bands at the lower temperatures are probably known with less certainty than ± 20%.

We will now discuss the individual contributions to the overall error limits. The precision of the individual data (in μV) is largely determined by the signal-to-noise ratios of the system, the knowledge of the calibration blackbody source (energy, temperature) and the spectral calibration (micrometer drum divisions versus wavelength). The signal-to-noise ratio changes from 1 for low radiation levels to 100 for high radiation levels. Low radiation levels exist in the bottom of the troughs and in spectral region > 7000 cm^{-1} at temperatures < 1500°K, and no reliable data are obtained in these regions. The precision in determining the blackbody temperature is within ± 1°K. The spectral calibration is precise within ± 3 cm^{-1}.

The accuracy of the spectral data depends upon the conversion of the output of the amplifier (μV) to emissivities. In the case of absorption spectra, the accuracy is determined by the precision with which the data were taken, and is, in general, poorer by a factor of 2. In the case of emission spectra, the precision with which the gas temperature is known, in addition to the precision of the amplifier output, determines the accuracy of the spectral emissivities. The temperature of the gas is known within ± 3%. This value was established through the precision of the flow meters and through the statistical scatter of many temperature determinations. The ± 3% precision in temperature means an inaccuracy of ± 5% to ± 30% in the

spectral emissivities from 3000 cm^{-1} at 3000°K to 8000 cm^{-1} at 1000°K. (See Fig. 35).

An improvement in precision is effected by the curve fitting process for ϵ versus T. We found that the RMS value of the deviations of the experimental spectral emissivities is $\leq \pm 5\%$ for the major portions of the bands and $\leq \pm 20\%$ in the troughs down to the lowest temperature of 1250°K.

The deduction of the absorption coefficients and fine structure parameters from the experimental data depends upon the knowledge of the state parameters of the gas, the pathlength, and the band model employed. As stated before, the temperature is known to within ± 3%; the total pressure was always assumed to be 1 atm; the partial pressure for water vapor and oxygen was calculated based on the assumption of chemical equilibrium, and the uncertainty is unknown; the geometric length is uncertain due to the temperature gradient at the two ends of the burner in the zones where the hot gas mixes with the cold nitrogen flow. Thermocouple readings at low temperatures and visual inspection at high temperatures, where the flame exhibits an orange color, indicates a transition zone thickness of approximately 4". At a nominal pathlength of 20 feet, these 4" amount to an error of about 2%. A value for the uncertainty in using a particular band model has not been established as yet, but will be done in the near future. A measure of the validity of the statistical model can be seen in the fit of $\left(u/\ell n\ (\frac{1}{1-\epsilon})\right)^2$ versus u to a straight line [see Eq. (1)]. Figures 36-38 show the RMS scatter (denoted by σ) in the fit of the experimental data to Eq. (1). This is not readily interpreted in terms of accuracy of k and a. If the measurements are primarily near the linear region of the curve of growth, the points in the transformed

equation [Eq. (1)] have nearly equal ordinates. Thus k is well-determined, with experimental accuracy of about $\frac{1}{2}\sigma$. The slope of Eq. (1) may be poorly determined, and the error in a may be large. If the measurements are primarily near the square-root region, the slope of Eq. (2) may be well-determined, but not the intercept. Thus, the product ka is known, but k (and, hence, a) may not be known separately with any accuracy. If the measurements are located primarily along the transitional region of the curve of growth, k and a may both be known with comparable accuracy, but with error greater than $\frac{1}{2}\sigma$. Only if the measurements extend well into both the linear and square-root regions (so that σ represents the uncertainty in k^2 as well as in the slope ka) will both k and a be determined with an accuracy of about $\frac{1}{2}\sigma$ and σ, respectively. The trend exhibited in Figs. 36-38 is to be expected. Low σ values exist in the bands and at the higher temperatures, while higher values exist in the troughs and at the low temperature.

4.5 INHOMOGENEOUS GAS MEASUREMENTS

In addition to the homogeneous measurements, the independent control of four separate five-foot sections was utilized to make inhomogeneous measurements. The experimental results are given in Figs. 39-44 in terms of $W/cm^2\ cm^{-1}$ for the following conditions.

Section	Temp Conc	Fig. 39	Fig. 40	Fig. 41
A	T	2480	1210	1210
	c	.37	.14	.14
B	T	1220	1520	1210
	c	.14	.18	.14
C	T	1180	2000	1180
	c	.13	.26	.13
D	T	2480	2480	2480
	c	.37	.37	.37

The experimental data are compared with calculated ones, using the Curtis-Godson approximation with Model 3 and 3a. The agreement of the theoretical and experimental values is within the uncertainty of the temperatures. The comparisons are made at 1 atm and the difference of the theoretical values determined by the two models is at most 12%. In addition to the calculations at 1 atm, calculations were performed at 0.1 atm, where no experimental data exist. In that case, the largest difference of the theoretical values amounted to 50% between the two models, Model 3a always being higher and, therefore, being conservative.

In conclusion, we remark that the simpler model 3a is preferable, giving good agreement with experimental data at 1 atm and conservative values at lower pressures.

SECTION 5

ANALYTICAL STUDIES

Studies have continued on optimizing the selection of band models for use in particular situations. Certain results are summarized here in regard to two topics: (a) the effect on non-Lorentz line shape and (b) the choice of line intensity distribution function.

5.1 NON-LORENTZ LINE SHAPE

Experimental studies have been successful in demonstrating deviations from Lorentz line shape in certain situations, e.g., in the troughs between the widely spaced lines of hydrogen halides,[5] and in the region beyond a sharp band head (CO_2).[6] In the former case, deviations were noted between 2 and 20 cm^{-1} from the line centers, and in the latter up to 200 cm^{-1} from the nearest line centers.

In the case of HF, above-Lorentzian shapes were noted, and the wings were empirically fitted[5] to a form $\alpha(\omega-\omega_0)^{-n}$, where n (which is 2 for Lorentz lines) was observed to be of the order of 1.8.

In the case of CO_2 and CO, the line wings about 100 cm^{-1} from the line centers were found to be below-Lorentzian in shape.[6] In these cases, the experimenters assumed an empirical factor applied to the line shape, which factor decreased experimentally with distance from the line center.

In studying the behavior of models of lines where the local properties do not vary abruptly, as near a band head, or in the far wings of a molecular band system where the local intensity may drop off exponentially, we are most concerned with the deviations in the near wings of the lines, since this may have the greatest effect on the local emissivity properties.

We will investigate the situation where the absorption coefficient in the wings of a line varies as $(\omega-\omega_0)^{-n}$:

$$k(\omega) \propto |\omega-\omega_0|^{-n} \text{ for } |\omega-\omega_0| \text{ large} \quad . \tag{1}$$

In analogy to the case of the Lorentz line shape, we assume

$$k(\omega) = \frac{a}{b^n + |\omega-\omega_0|^n} \quad , \tag{2}$$

where b has the usual meaning of half-width at half-intensity, and a is proportional to the line intensity. From the definition

$$S = \int k(\omega)\, d\omega \quad , \tag{3}$$

we obtain directly by integration

$$k(\omega) = \frac{(Sb^{n-1}/\pi)\,[\frac{1}{2}\, n \sin(\pi/n)]}{b^n + |\omega-\omega_0|^n} \quad . \tag{4}$$

For n = 2, Eq. (4) reduces to the usual Lorentz equation:

$$k(\omega) = \frac{Sb/\pi}{b^2 + (\omega-\omega_0)^2} \quad . \tag{5}$$

From the definition of equivalent width of an isolated line,

$$W = \int_0^\infty \left\{1-\exp[-k(\omega)\, u]\right\} d\omega \quad , \tag{6}$$

we have

$$W = \int_0^\infty \left\{1-\exp\left[-\frac{au}{b^n + |\omega-\omega_0|^n}\right]\right\} d\omega \quad . \tag{7}$$

This equation is not immediately integrable. However, for investigating the strong line region, we may study the asymptotic form

$$W \leq \int_0^\infty \left\{ 1 - \exp\left[- au \left| \omega - \omega_0 \right|^{-n} \right] \right\} d\omega, \qquad (8)$$

which yields

$$W \leq 2a^{\frac{1}{n}} \Gamma\left(1 - \frac{1}{n}\right) u^{\frac{1}{n}}, \qquad (9)$$

or explicitly,

$$W \leq 2\left(\frac{n}{2} \sin \frac{\pi}{n} \right)^{\frac{1}{n}} \Gamma\left(1 - \frac{1}{n}\right) (\pi)^{-\frac{1}{n}} \left(Su/b\right)^{\frac{1}{n}} b. \qquad (10)$$

An approximate form of Eq. (10) can be obtained by expanding in powers of (n-2):

$$W \leq 2(Sbu)^{\frac{1}{2}} (Su/b)^{-(n-2)/4} \left[1 + .05\,(n-2) \right]. \qquad (11)$$

For $1.7 \leq n \leq 2.3$, Eq. (11) approximates Eq. (10) within 1%, so that Eq. (11) still provides a very close upper limit. For $n = 2$, both Eq. (10) and Eq. (11) yield

$$W \leq 2(Sbu)^{\frac{1}{2}}, \qquad (12)$$

the usual equation for the "square-root" region of a Lorentz line in the strong-line approximation, i.e., when the line is strongly absorbed in the region near the line center.

We note that in the strong-line region for a line of shape given by Eq. (2), we have

$$W \propto u^{\frac{1}{n}}. \qquad (13)$$

Thus for $n = 1.8$, we have $W \propto u^{.455}$ in the strong line region.

If we consider a band composed of randomly located lines whose intensities are distributed according to some normalized intensity distribution P(S), we have

$$\bar{W} = \int W(S)\, P(S)\, dS \quad . \tag{14}$$

For the case of an exponential intensity distribution.

$$P(S) = S_0^{-1} \exp\,(-S/S_0) \quad , \tag{15}$$

and the $k(\omega)$ given by Eq. (2), we have

$$\bar{W} = S_0^{-1} \int_{S=0}^{\infty} \int_{\omega=0}^{\infty} \left\{ 1 - \exp\left[- \frac{(b^{n-1}/\pi)\,(n/2)\,\sin\,(\pi/n)Su}{b^n + |\,\omega - \omega_0\,|^n} \right] \right\}$$

$$x\,d\omega\, \exp(-S/S_0)\, dS \quad . \tag{16}$$

After lengthy manipulations, including interchange of order of integration, we obtain an exact expression:

$$\bar{W} = S_0 u \;\left[\, 1 + n \sin(\pi/n)\, S_0 u/2\pi b\right]^{\frac{1}{n} - 1} \quad . \tag{17}$$

For n = 2, we obtain the customary expression

$$\bar{W} = S_0 u \;\left[\, 1 + S_0 u/\pi b\right]^{-\frac{1}{2}} \quad . \tag{18}$$

On division by d, the mean line spacing, Equation (17) yields, in the limit of small $S_0 u/d$,

$$\frac{\bar{W}}{d} \approx \frac{S_0 u}{d} \quad , \tag{19}$$

and, in the limit of large $S_0 u/d$,

$$\frac{\overline{W}}{d} \approx \left[\frac{2\pi b/d}{n \sin(\pi/n)} \right]^{1 - 1/n} \left[\frac{S_0 u}{d} \right]^{1/n} \quad . \tag{20}$$

If we identify these asymptotic regions with those of a model[7] comprised of lines of an equivalent intensity S_E and equivalent spacing d_E (using Eq. (10)) we find

$$S_0 = S_E \left[\frac{n}{\pi} \sin\left(\frac{\pi}{n}\right) \Gamma\left(1 - \frac{1}{n}\right) \right]^{-\frac{n}{n-1}} \tag{21}$$

$$d = d_E \left[\frac{n}{\pi} \sin\left(\frac{\pi}{n}\right) \Gamma\left(1 - \frac{1}{n}\right) \right]^{-\frac{n}{n-1}} \quad . \tag{22}$$

In terms of these parameters, we have

$$\frac{\overline{W}}{d} = \frac{S_E u}{d_E} \left\{ 1 + \left[\frac{n}{\pi} \sin\left(\frac{\pi}{n}\right) \right]^{-\frac{n}{n-1}} \left[\Gamma\left(1 - \frac{1}{n}\right) \right]^{-\frac{n}{n-1}} \right.$$

$$\left. \times \frac{S_E u}{2b} \right\}^{\frac{1}{n} - 1} \quad . \tag{23}$$

On introduction of the dimensionless parameters

$$\beta_E = 2\pi b/d_E \tag{24}$$

and

$$x_E = S_E u/2\pi b \quad , \tag{25}$$

Eq. (23) becomes

$$\frac{\overline{W}}{d} = \beta_E e_n(x_E) \quad , \tag{26}$$

where

$$e_n(x_E) = x_E \left\{ 1 + \left[\frac{n}{\pi} \sin\left(\frac{\pi}{n} \right) \right]^{-\frac{n}{n-1}} \left[\Gamma\left(1 - \frac{1}{n}\right) \right]^{-\frac{n}{n-1}} \right.$$

$$\left. \times \pi\, x_E \right\}^{\frac{1}{n}-1} . \qquad (27)$$

Again, we note that for n = 2, Eq. (27) becomes

$$e_2(x_E) = x_E \left[1 + \frac{\pi}{2} x_E \right]^{-\frac{1}{2}} , \qquad (28)$$

the curve of growth previously designated[7] $e(x_E)$.

In Fig.42, the curves of growth $e_n(x_E)$ are plotted for n = 1.8 (dashed), 2.0 (solid), and 2.2 (dotted). A wide enough range of x_E is used to show the fusion of each curve with its asymptotes.

5.2 LINE INTENSITY DISTRIBUTION FUNCTIONS

The selection of an appropriate line intensity distribution function should be based at least to some extent on the theoretically anticipated distribution of intensities in the spectral region which the model is to represent, since it would be extremely arduous, if not completely impossible, to make an actual count of lines over many orders of magnitude.

Some models which are still commonly used presuppose intensity distributions which are based at least as much upon mathematical expediency as upon physical reasoning. For instance, an intensity distribution in which all lines are assigned equal intensities is clearly not an optimum description for a high-temperature molecular spectrum. However, under this assumption, the curve of growth of a random band model is identical to that of a single isolated line. Similarly the assumption of an exponential intensity distribution, while more reasonable, is not based on direct physical reasoning, but is employed because it removes the Bessel functions from the Ladenburg-Reiche function and leaves a simple algebraic form.

The distribution of intensities within a hypothetical band is frequently described by a probability distribution P(S) which is normalized:

$$\int_0^\infty P(S)\, dS = 1 \quad . \tag{29}$$

Thus the probability that any arbitrary line has an intensity between S_1 and S_2 is given by

$$\int_{S_1}^{S_2} P(S)\, dS \quad . \tag{30}$$

The probability distribution function is proportional to the number density of lines with respect to intensity

$$P(S) \propto \frac{dn}{dS} \tag{31}$$

Using the chain rule, we can write

$$\frac{dn}{dS} = \frac{dn}{dE} \quad \frac{dE}{dS} \quad . \tag{32}$$

The dominant factor in the general expression for line intensity is the Boltzmann factor. From the approximate relationship

$$S \propto \exp(-E/kT) \ , \tag{33}$$

we find

$$\frac{dE}{dS} \propto S^{-1} \quad . \tag{34}$$

As a result of effects such as nonrigidity and multiple vibrational degree of freedom, the number density of energy levels will increase with E. If we postulate an approximate power law

$$\frac{dn}{dE} \propto E^m \propto \left[\ln (S_M/S)\right]^m \qquad (m \geq 0) \tag{35}$$

we have

$$P(S) = K\, S^{-1} \left[\ln (S_M/S)\right]^m \quad . \tag{36}$$

From the normalization requirement,

$$\int_{S_M/R}^{S_M} P(S)\, dS = 1 \ , \tag{37}$$

where S_M is the maximum and S_M/R the minimum intensity, we have

$$K = (m+1)/(\ln R)^{m+1} \quad . \tag{38}$$

We then have, explicitly,

$$P(S) = (m+1)\, S^{-1} \left[\ln(S_M/S)\right]^m / (\ln R)^{m+1} . \qquad (39)$$

For m = 0, this expression reduces to

$$P(S) = S^{-1}/\ln R, \qquad (40)$$

which case has been discussed previously.[7]

The average value of S is given by

$$\bar{S} = \int SP(S)\, ds = (m+1)(\ln R)^{-m-1} \int_{S_M/R}^{S_M} \left[\ln S_M/S\right]^m dS , \qquad (41)$$

which, for large R, is

$$\bar{S} = S_M\, \Gamma(m+2)/(\ln R)^{m+1} \qquad (42)$$

Similarly, the average value of $S^{\frac{1}{2}}$ is given by

$$\overline{S^{\frac{1}{2}}} = \int S^{\frac{1}{2}} P(S)\, dS = (m+1)(\ln R)^{-m-1} \int_{S_M/R}^{S_M} \left[\ln S_M/S\right]^m S^{-\frac{1}{2}}\, dS , \qquad (43)$$

which, for large R, is

$$\overline{S^{\frac{1}{2}}} = S_M^{\frac{1}{2}}\, \Gamma(m+2)\, 2^{m+1} / (\ln R)^{m+1} .$$

By defining the parameters S_E and d_E such that

$$S_E/d_E = \bar{S}/d \qquad (45)$$

and

$$S_E^{\frac{1}{2}}/d_E = \overline{S^{\frac{1}{2}}}/d , \qquad (46)$$

we obtain

$$S_E = S_M/4^{m+1} \tag{47}$$

and

$$d_E = d\,(\ln R)^{m+1} / 4^{m+1}\,\Gamma(m+2) \quad . \tag{48}$$

The probability distribution functions for $R = 10^6$ and $m = 0,1,2,$ and 3 are shown in Fig.43. Note that in the region of smallest intensities the slope is somewhat steeper than -1. If we define

$$x = \ln (S_M/S) \tag{49}$$

and

$$y = \ln P(S) \quad , \tag{50}$$

Eq. (39) becomes

$$y = \ln \left[(m+1)/S_M\,(\ln R)^{m+1}\right] - x + m \ln x \quad , \tag{51}$$

from which we find

$$\frac{dy}{dx} = -1 + mx^{-1} \quad . \tag{52}$$

Thus for $x \approx -14$ ($S = S_M/R$) and $m = 3$, the slope $\frac{dy}{dx} \approx -1.2$.

It does not appear possible to obtain closed form expressions for the curves of growth associated with P(S) of the form of Eq. (39). We can, however, note a P(S) which is proportional to S^{-2} (shown in Fig. 43 as a dashed curve, with slope -2) is far more heavily biased toward the lower intensities than the curves shown for $m = 1,2,3$. The normalized distribution is expressed by

$$P(S) = S_M (R-1)^{-1} S^{-2} \qquad (S_M/R \leq S \leq S_M)$$

$$= 0 \qquad \text{(otherwise)} \quad . \tag{53}$$

If this expression is convoluted with an exponential distribution (for convenience), which broadens the distribution of intensities even further, the resulting distribution is given by

$$P(S) = (R-1)^{-1} S^{-2} \left[(S_M + S) \exp(-S/S_M) - (S_M + RS) \exp(-RS/S_M) \right] . \tag{54}$$

By following the same procedure as in Ref. 7, we obtain the following explicit expression for the curve of growth resulting from the P(S) of Eq. (54):

$$\bar{W}/a = \beta_E F_2 (X_E), \tag{55}$$

where

$$F_2(X_E) = \frac{X_E}{\ln R} \ln \left\{ \frac{\left[1+2\pi R X_E/(\ln R)^2\right]^{\frac{1}{2}} - 1}{\left[1+2\pi R X_E/(\ln R)^2\right]^{\frac{1}{2}} + 1} \cdot \frac{\left[1+2\pi X_E/(\ln R)^2\right]^{\frac{1}{2}} + 1}{\left[1+2\pi X_E/(\ln R)^2\right]^{\frac{1}{2}} - 1} \right\} , \tag{56}$$

and β_E and X_E have the meanings defined previously.

This curve of growth is shown in Fig. (44) as a dashed line. For comparison, the Ladenburg-Reiche curve (solid curve) corresponding to $P(S) = \delta(S - S_E)$ and the curve[3] $h(X_E)$ corresponding to $P(S) = (S \ln R)^{-1} \exp(-S/\pi S_E)$ (dotted curve) are also shown. The mutual asymptotes are shown as solid lines.

The curve $F_2 (X_E)$ provides only a gross lower limit to the curves of growth which would correspond to the P(S) of Eq. (39), shown in Fig. (43).

SECTION 6

REFERENCES

1. "Study on Exhaust Plume Radiation Predictions, Interim Progress Report," Report No. GDC-DBE66-001, Space Science Laboratory, General Dynamics/Convair, San Diego, Calif., January 1966.
2. "Study on Exhaust Plume Radiation Predictions, Final Report," Report No. GDC-DBE66-017, Space Science Laboratory, General Dynamics/Convair, San Diego, Calif., December 1966.
3. W. F. Herget, J. S. Muirhead, and S. A. Golden, "Band Model Parameters of H_2O," Report No. R-6916, Rocketdyne, 27 January 1967.
4. F. S. Simmons, Appl. Opt. 5, 1801 (1966).
5. G. A. Kuipers, J. Mol. Spectry. 2, 75 (1958).
   D. F. Smith, J. Mol. Spectry. 3, 473 (1959).
   W. F. Herget et al., J. Opt. Soc. Am. 52, 1113 (1962).
6. E. K. Plyler et al., J. Opt. Soc. Am. 52, 1017 (1962).
   W. S. Benedict et al., Astrophys. J. 135, 277 (1962).
7. W. Malkmus, J. Opt. Soc. Am. 57, 323 (1967).

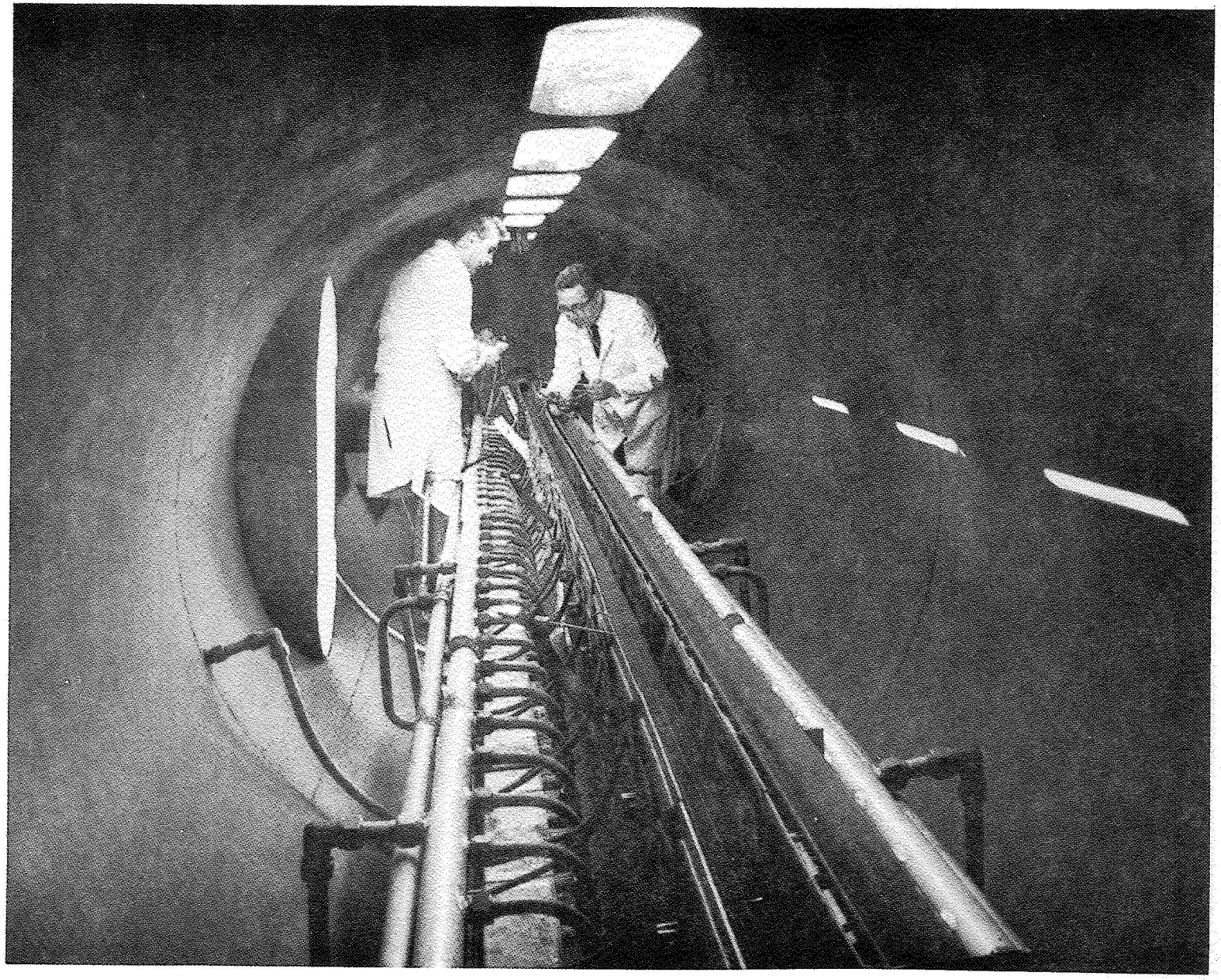

Fig. 1. Photograph of twenty burner sections installed inside the tank.

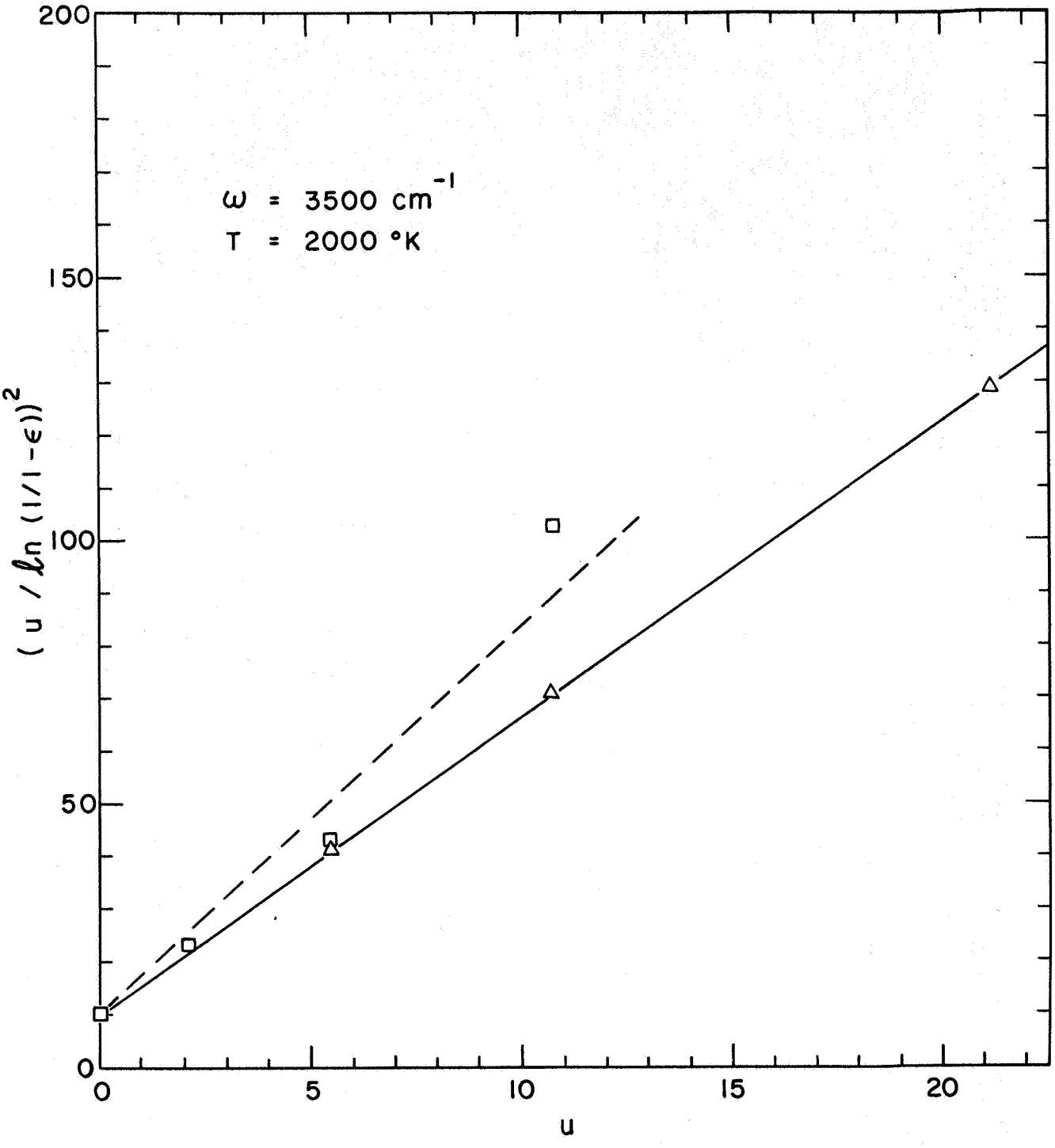

Fig. 2. Curve of growth at 2000°K for ω = 3500 cm^{-1} in terms of $\left(u/\ell n\ (1/1-\epsilon)\right)^2$ versus u. Previous data are indicated by (□), the present data by (Δ).

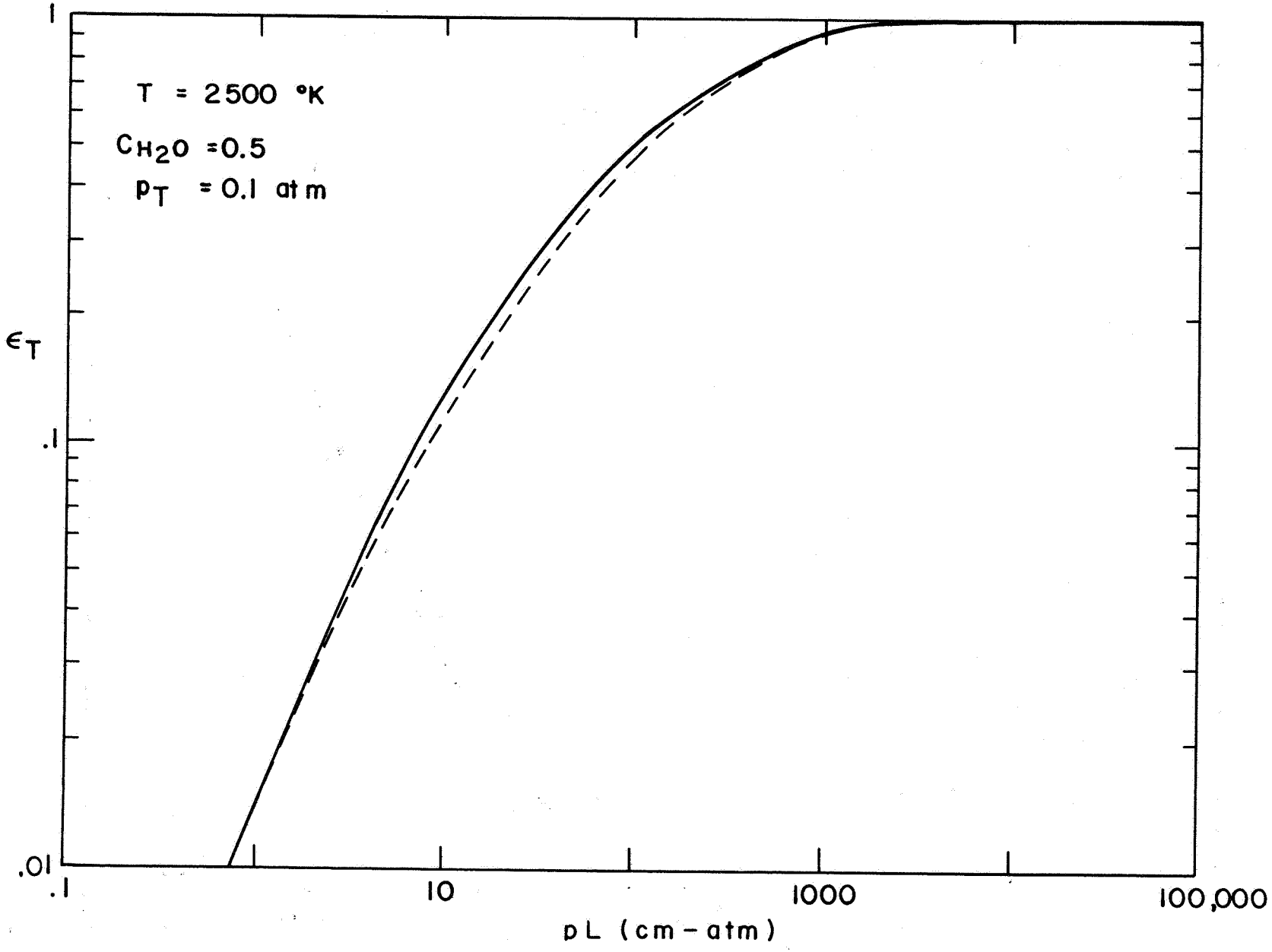

Fig. 3. Comparison of the total emissivity between 1150 and 5900 cm^{-1} at 2500°K based on previous k and a (solid line) and based on present k and (1/d) (dashed line) at p_T = 0.1 atm as a function of pL(cm-atm) for 50% H_2O and 50% N_2.

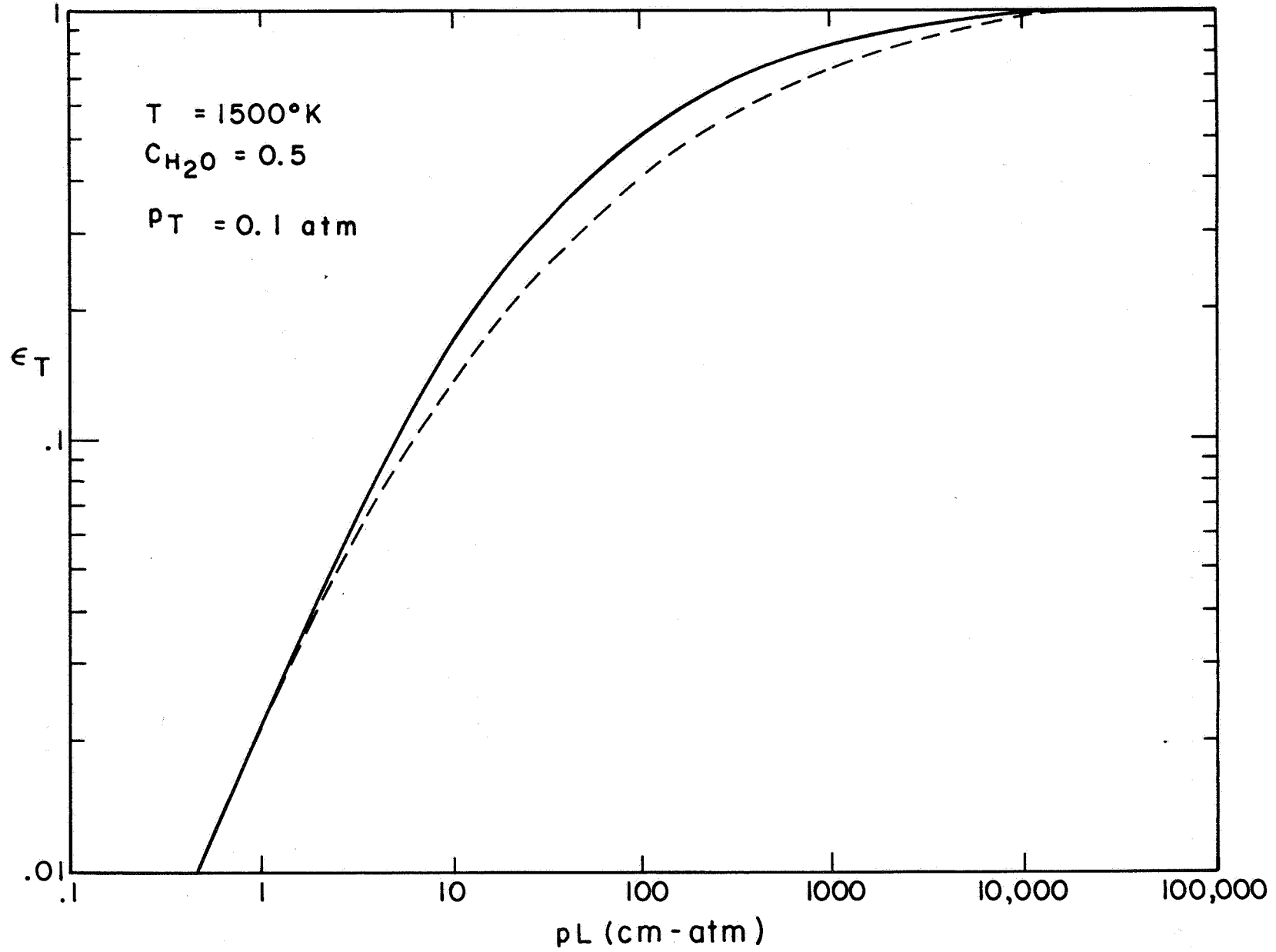

Fig. 3a. Comparison of the total emissivity between 1150 and 5900 cm^{-1} at 1500°K, based on previous k and a (solid line) and based on present k and (1/d) (dashed line) at p_T = 0.1 atm as a function of pL(cm-atm) for 50% H_2O and 50% N_2.

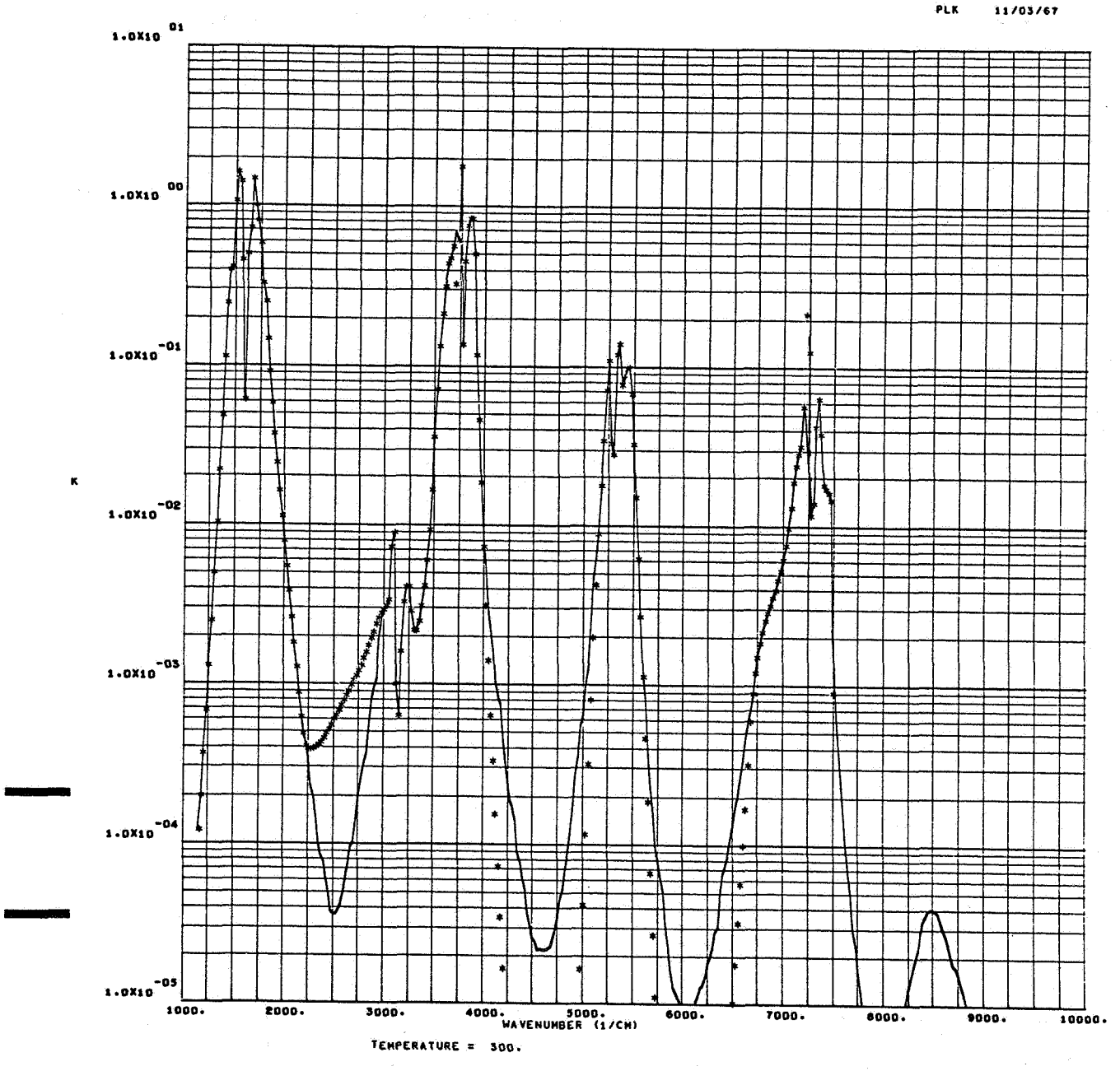

Fig. 4. Comparison of previous k (*) and present k (solid line) at 300°K.

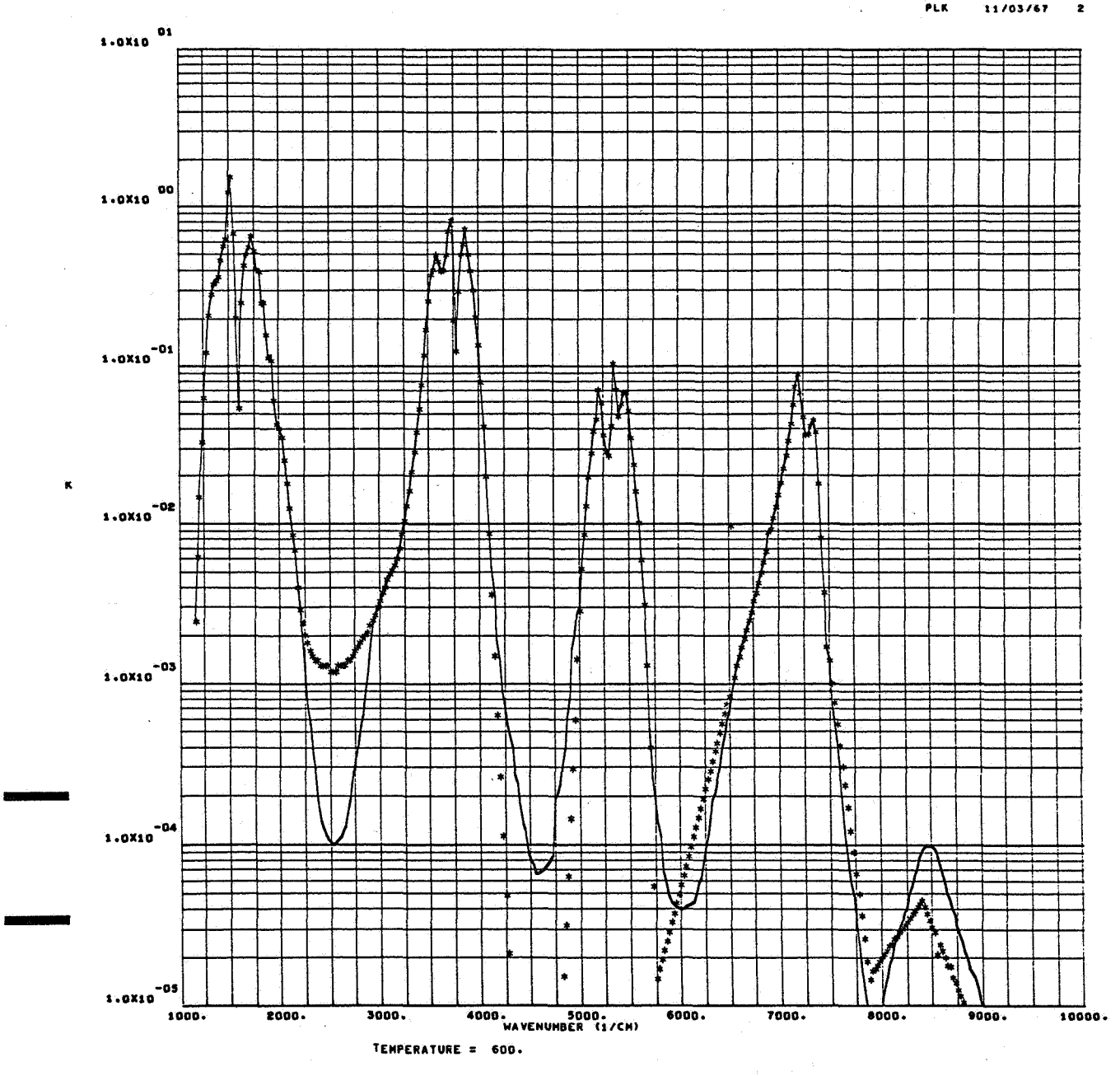

Fig. 5. Comparison of previous k (*) and present k (solid line) at 600°K.

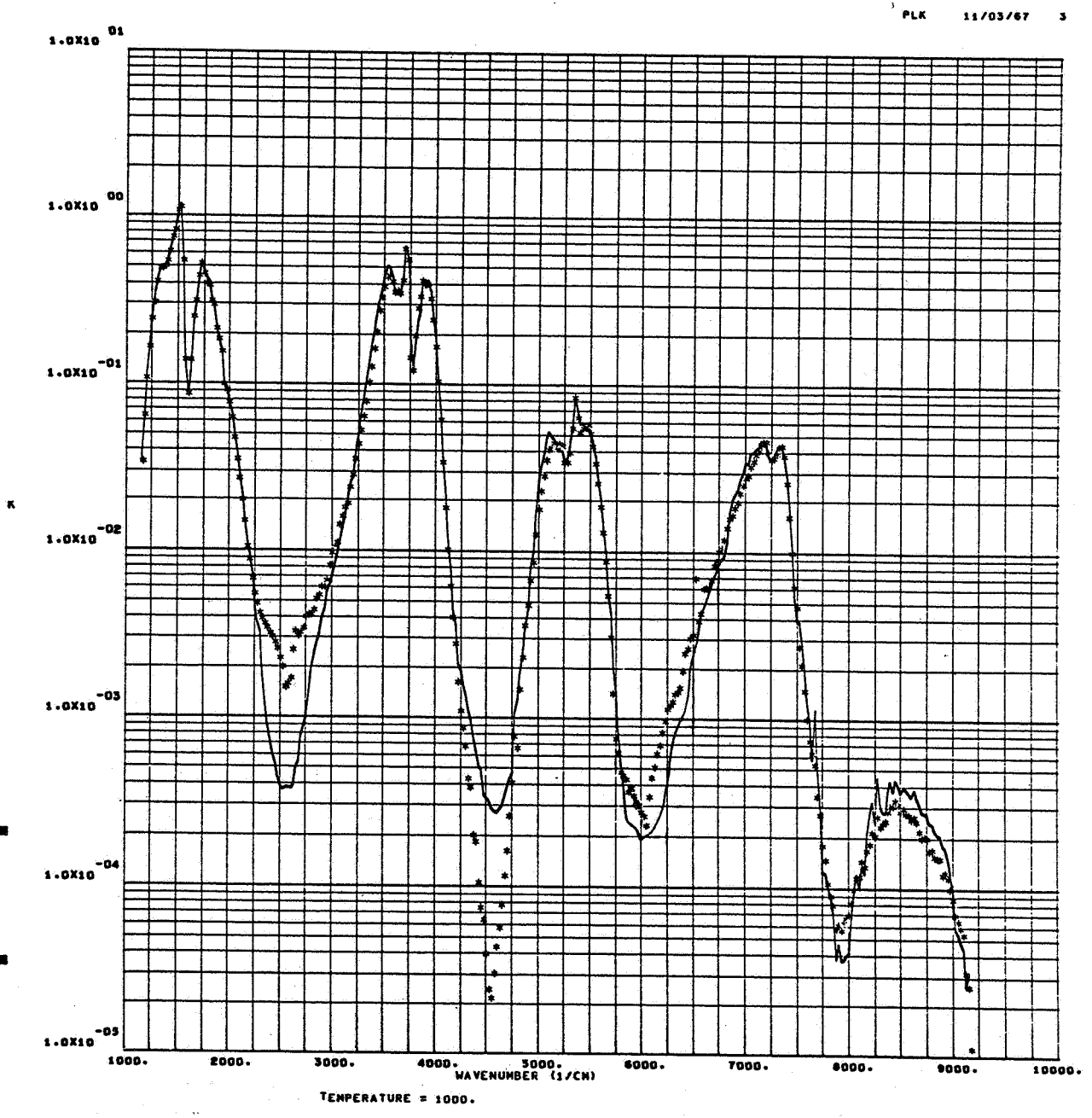

Fig. 6. Comparison of previous k (*) and present k (solid line) at 1000°K.

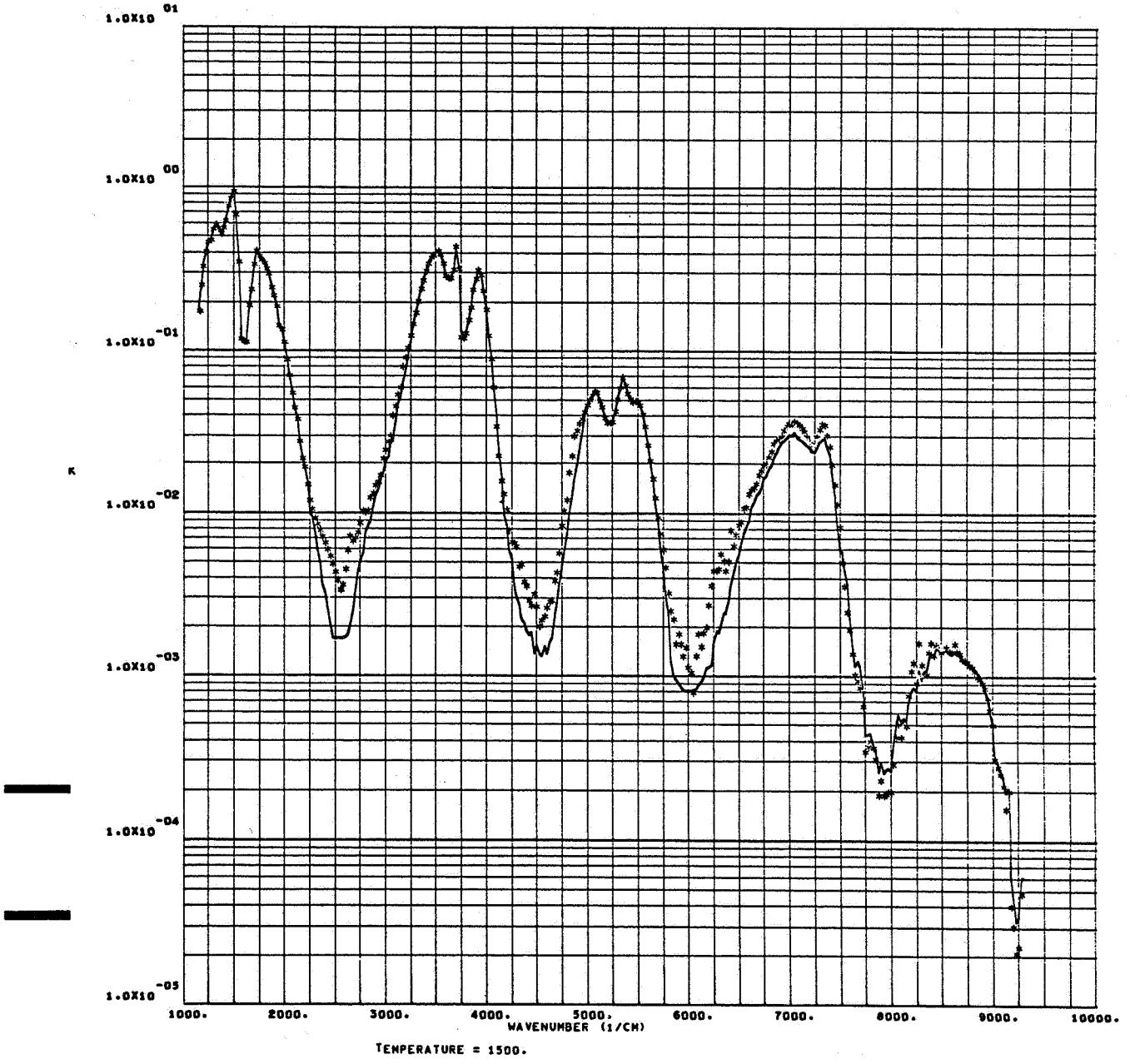

Fig. 7. Comparison of previous k (*) and present k (solid line) at 1500°K.

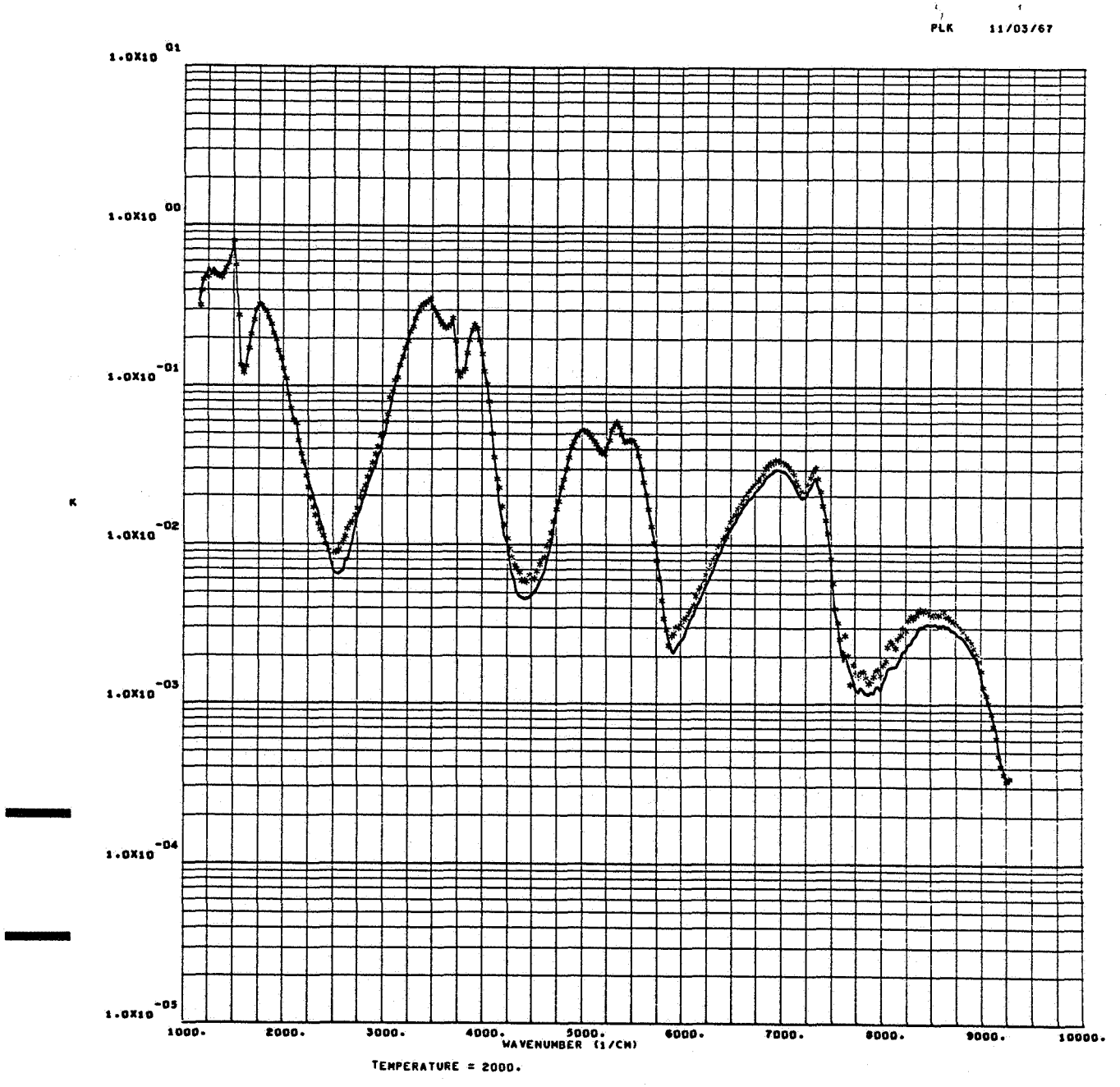

Fig. 8. Comparison of previous k (*) and present k (solid line) at 2000°K.

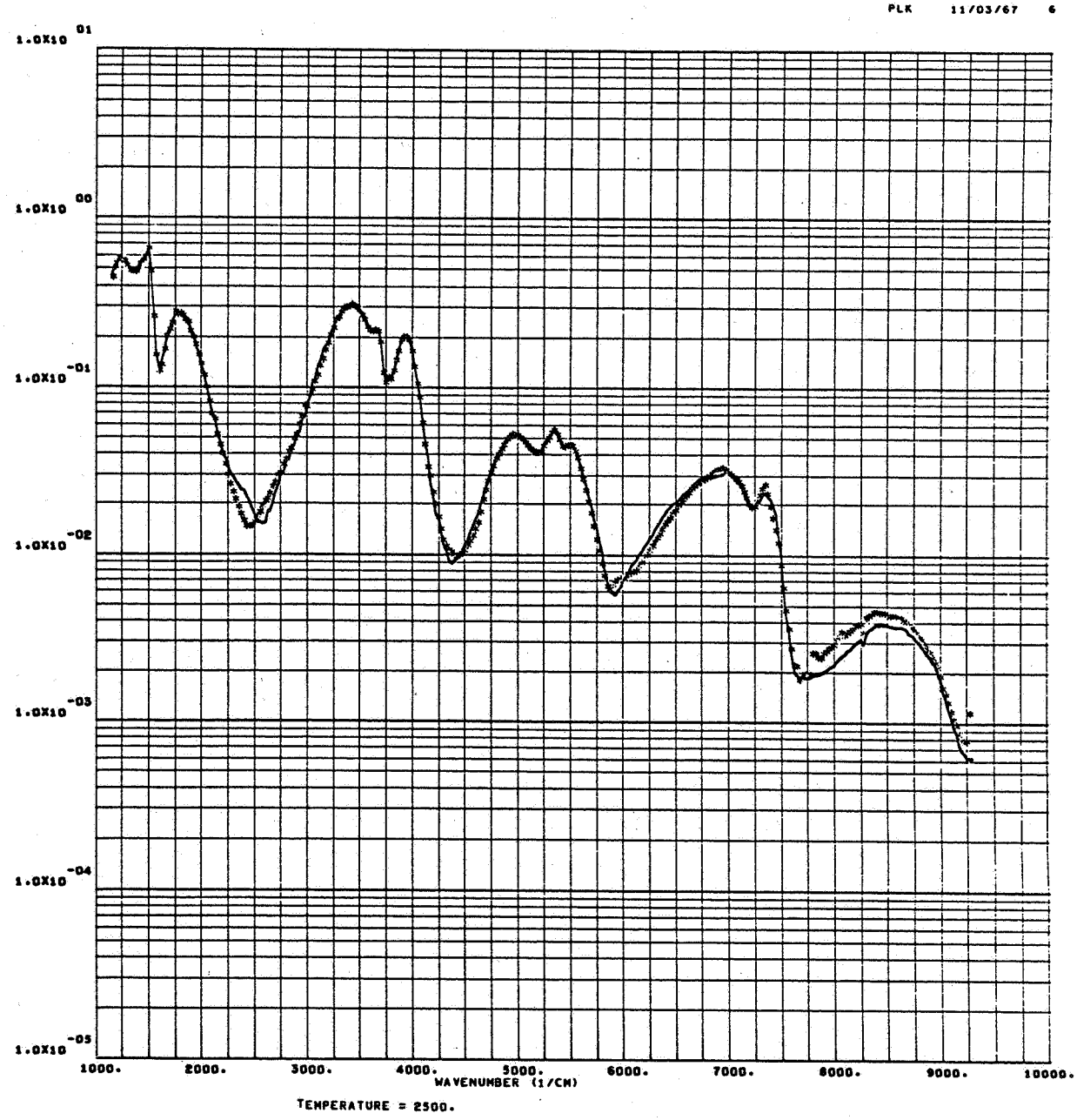

Fig. 9. Comparison of previous k (*) and present k (solid line) at 2500°K.

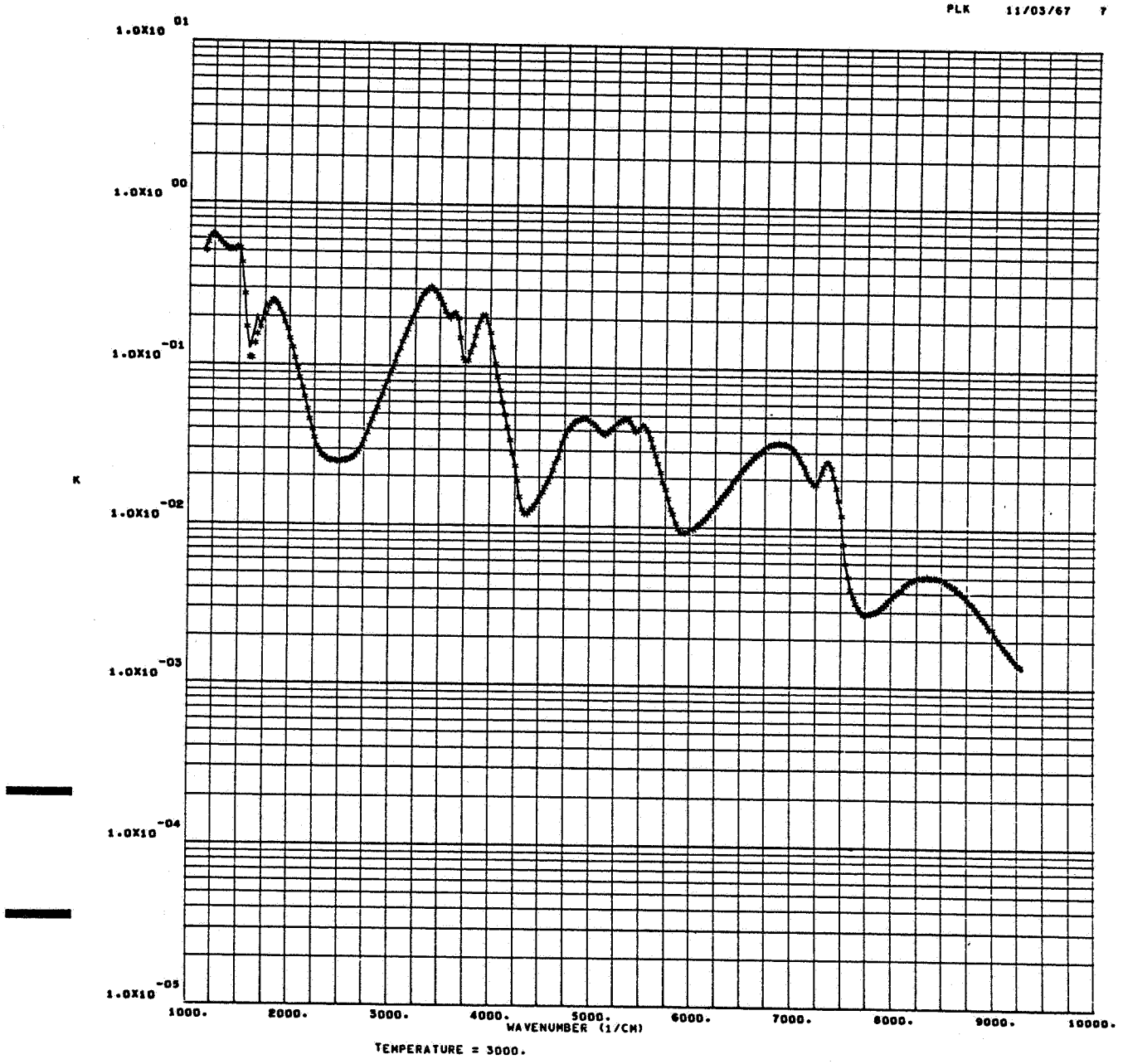

Fig. 10. Comparison of previous k (*) and present k (solid line) at 3000°K.

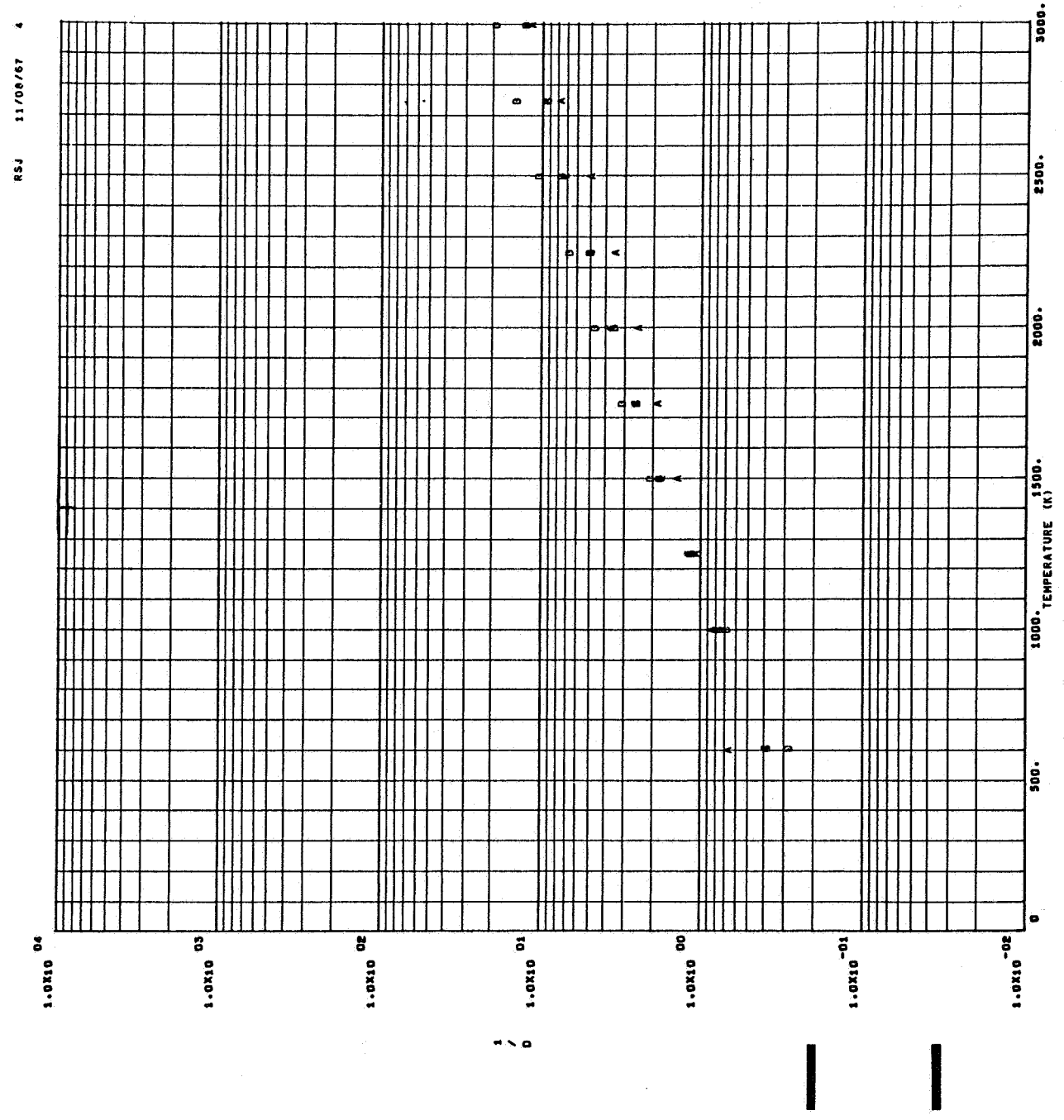

Fig. 11. Plot of $(1/d_{LR})$ versus T at 1500 cm^{-1} (A), 1525 (B), 1550 (C), and 1575 cm^{-1} (D).

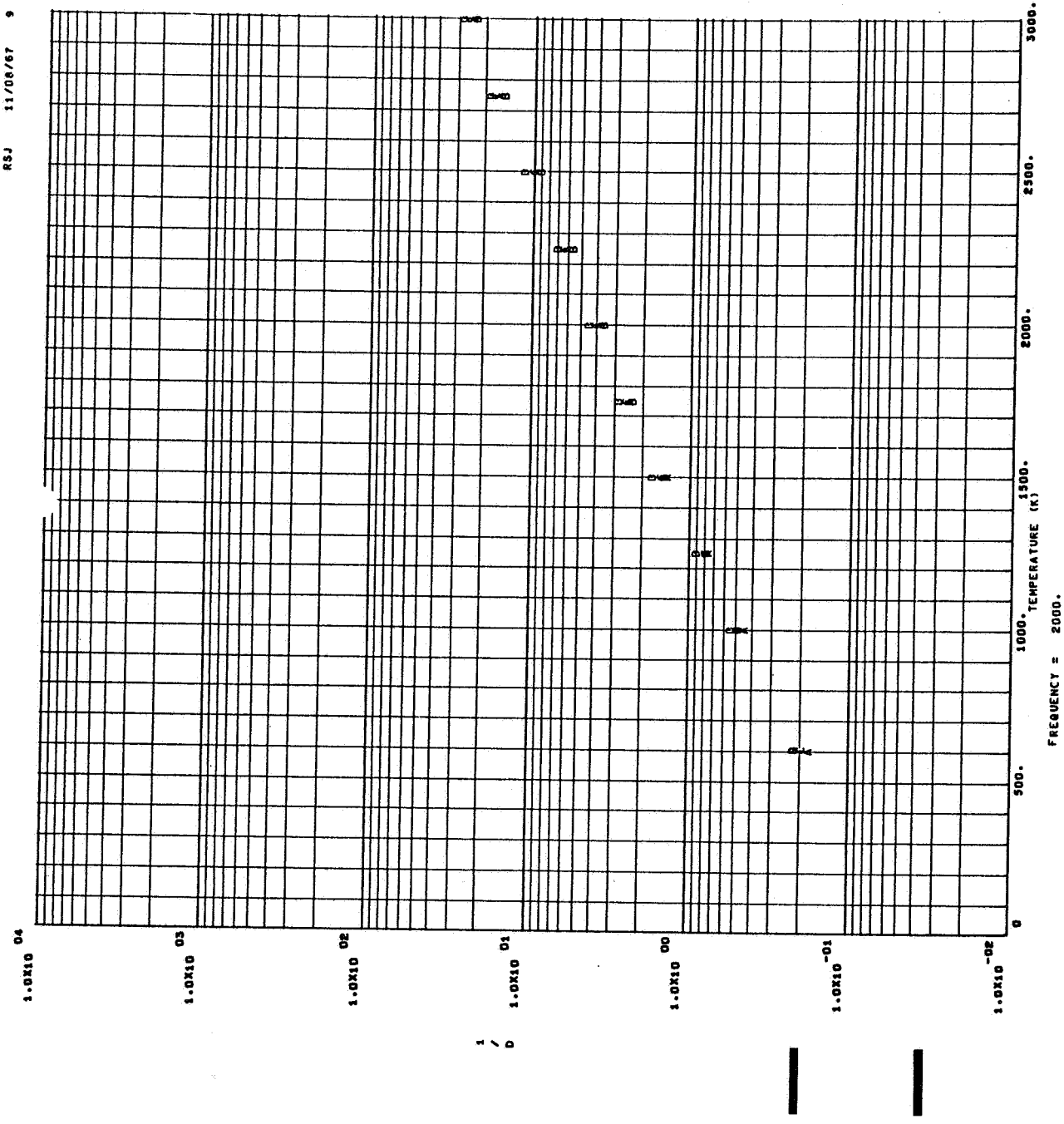

Fig. 12. Plot of $(1/d_{IR})$ versus T at 2000 cm^{-1} (A), 2025 (B), 2050 (C), and 2075 cm^{-1} (D).

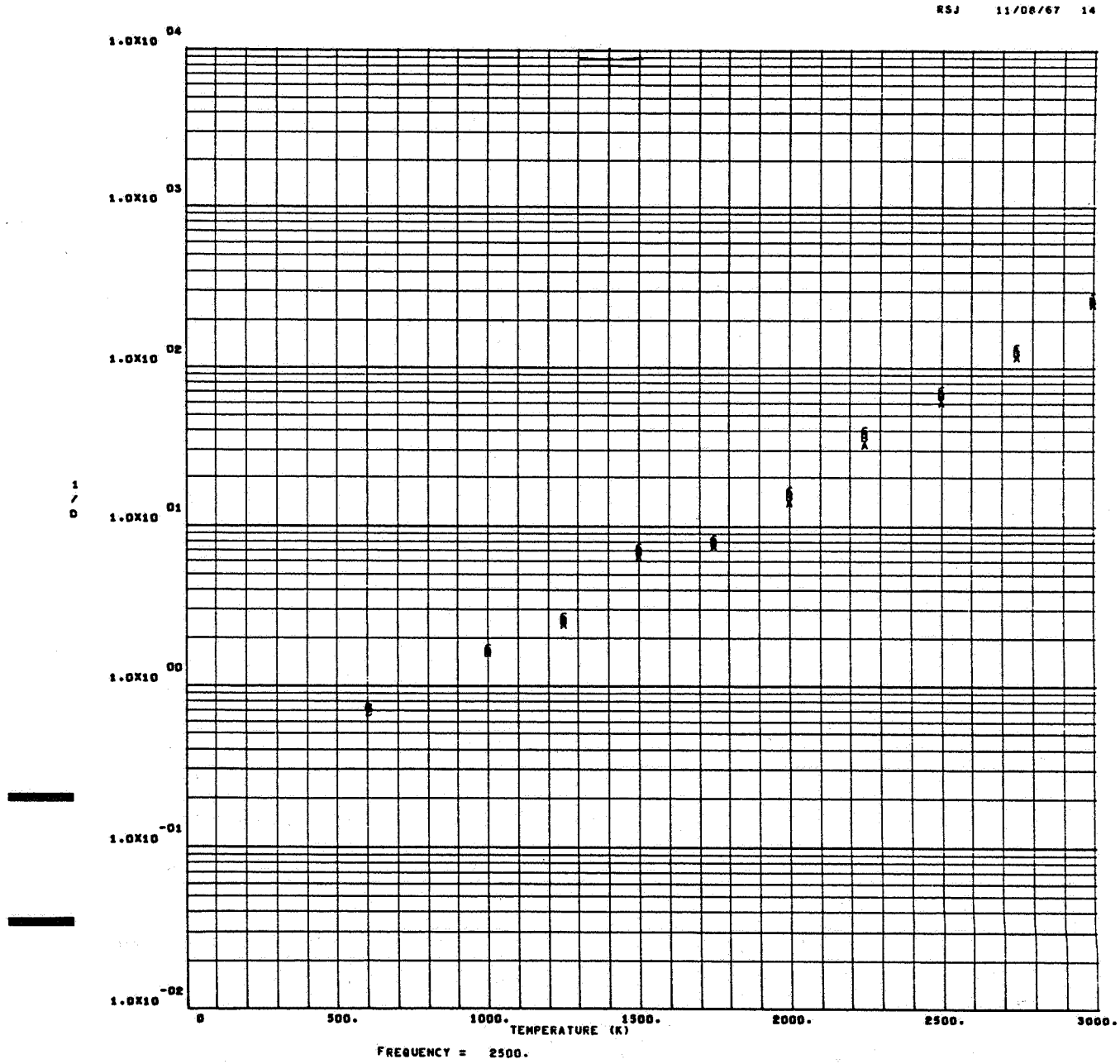

Fig. 13. Plot of $(1/d_{LR})$ versus T at 2500 cm^{-1} (A), 2525 (B), 2550 (C), and 2575 cm^{-1} (D).

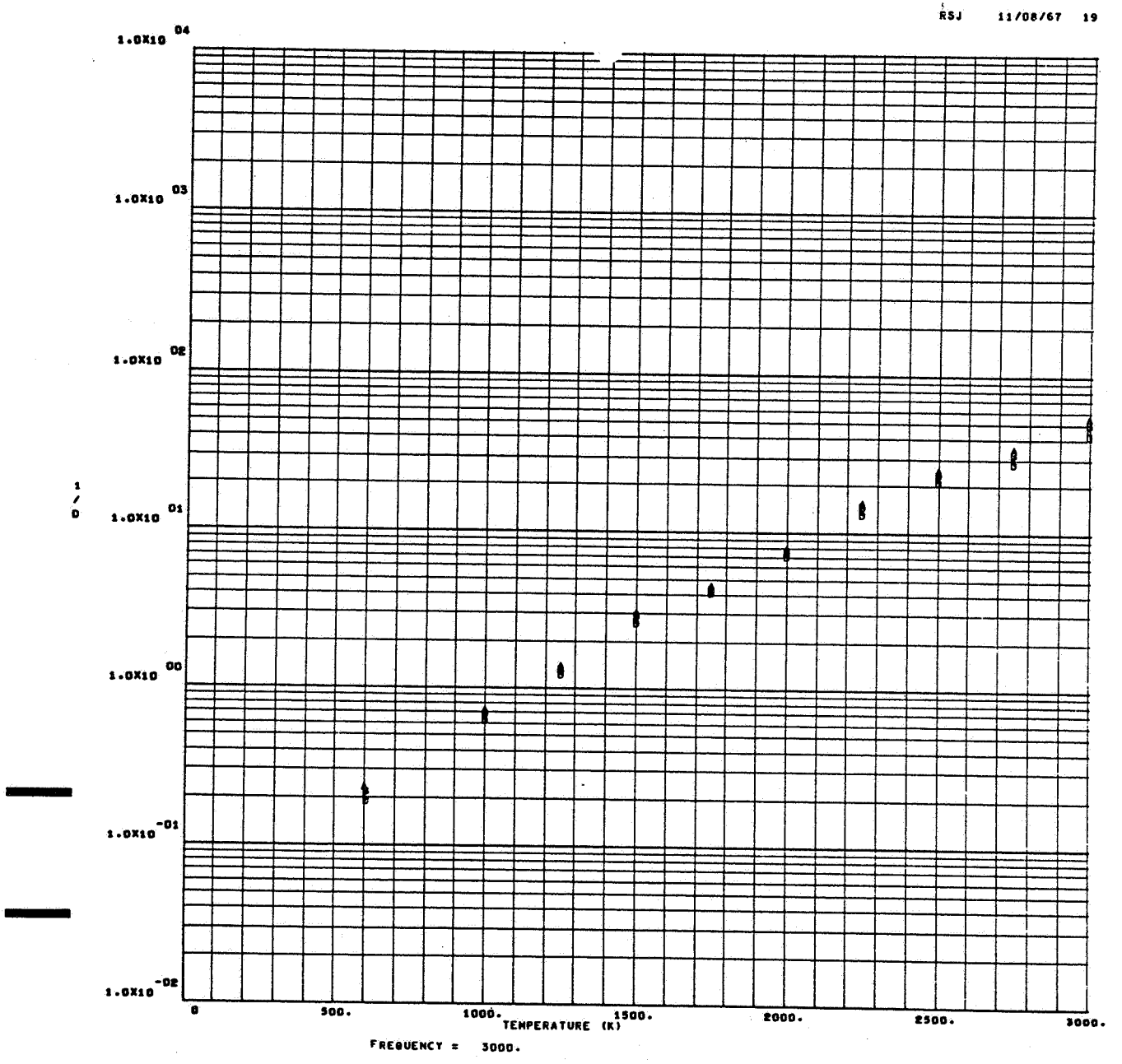

Fig. 14. Plot of $(1/d_{LR})$ versus T at 3000 cm^{-1} (A), 3025 (B), 3050 (C), and 3075 cm^{-1} (D).

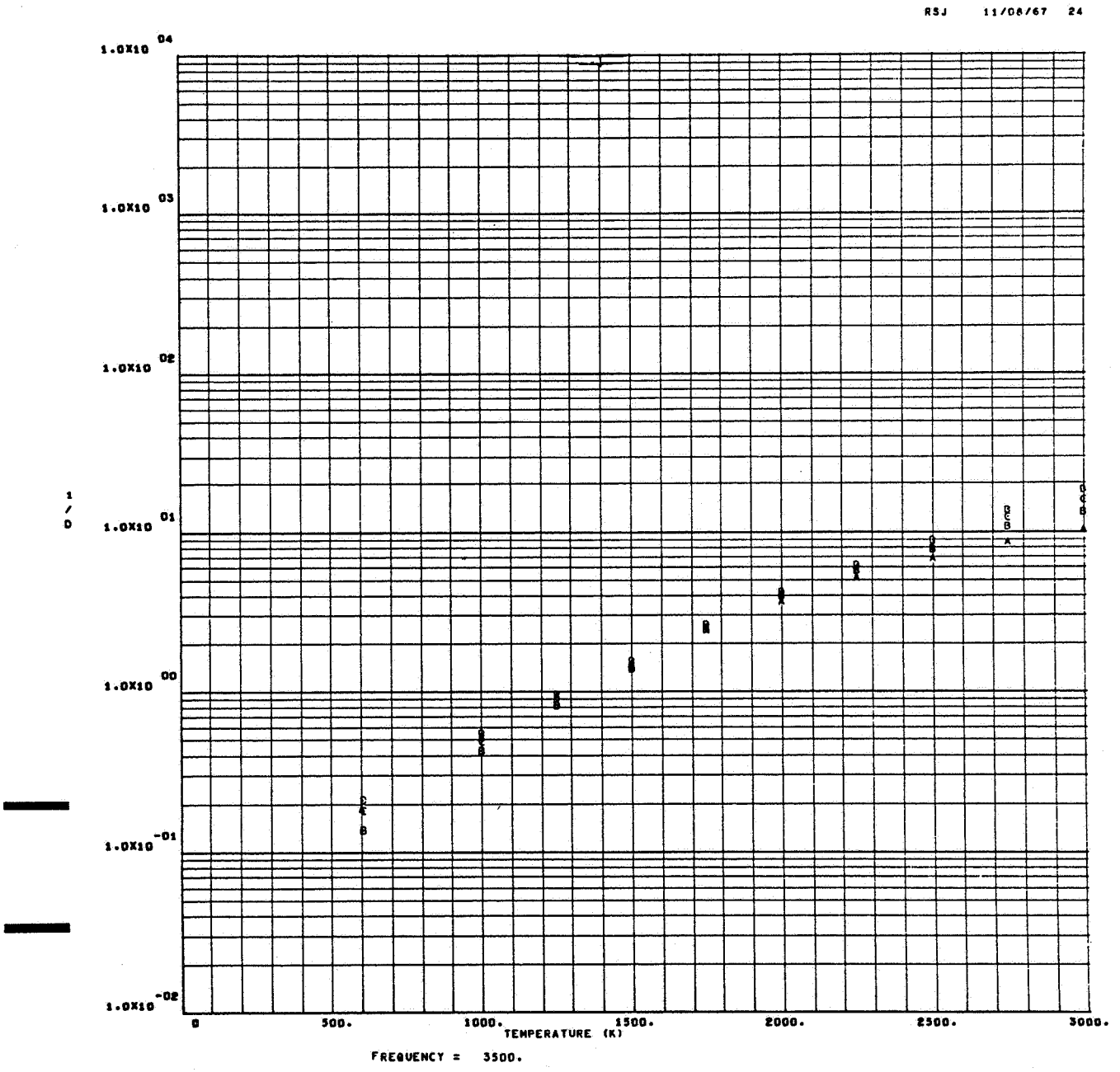

Fig. 15. Plot of $(1/d_{LR})$ versus T at 3500 cm^{-1} (A), 3525 (B), 3550 (C), and 3575 cm^{-1} (D).

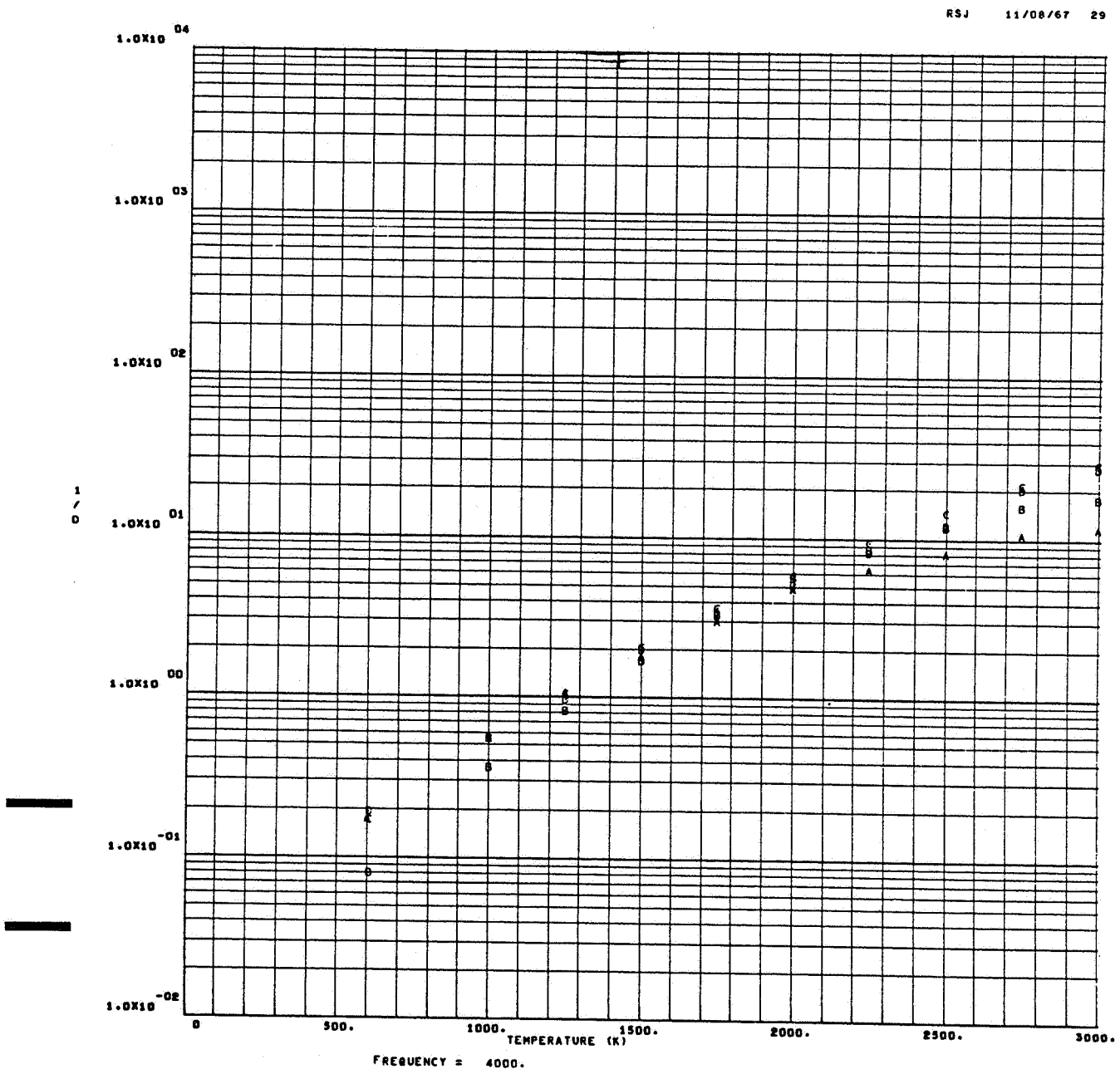

Fig. 16. Plot of $(1/d_{LR})$ versus T at 4000 cm^{-1} (A), 4025 (B), 4050 (C), and 4075 cm^{-1} (D).

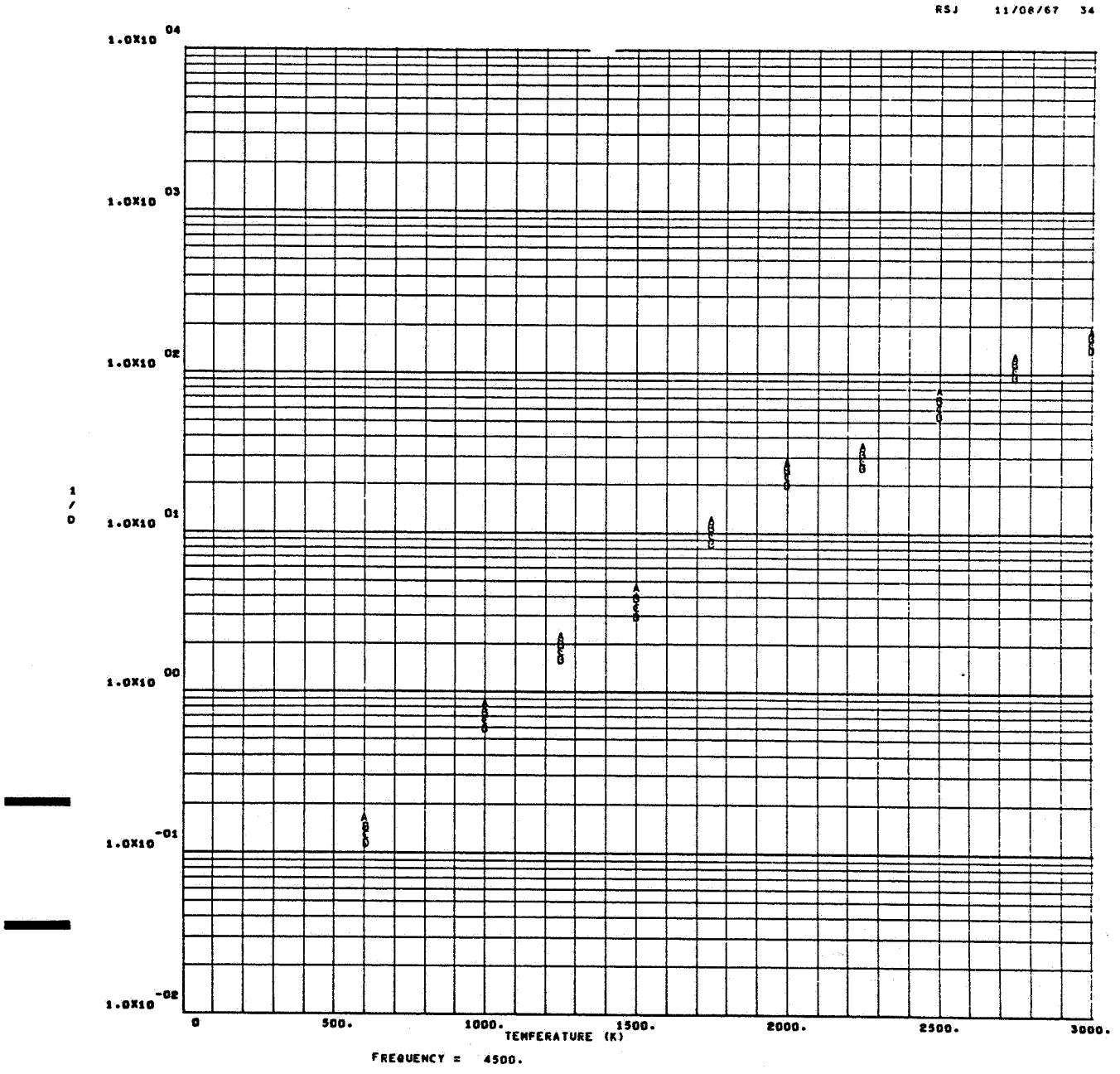

Fig. 17. Plot of $(1/d_{LR})$ versus T at 4500 cm^{-1} (A), 4525 (B), 4550 (C), and 4575 cm^{-1} (D).

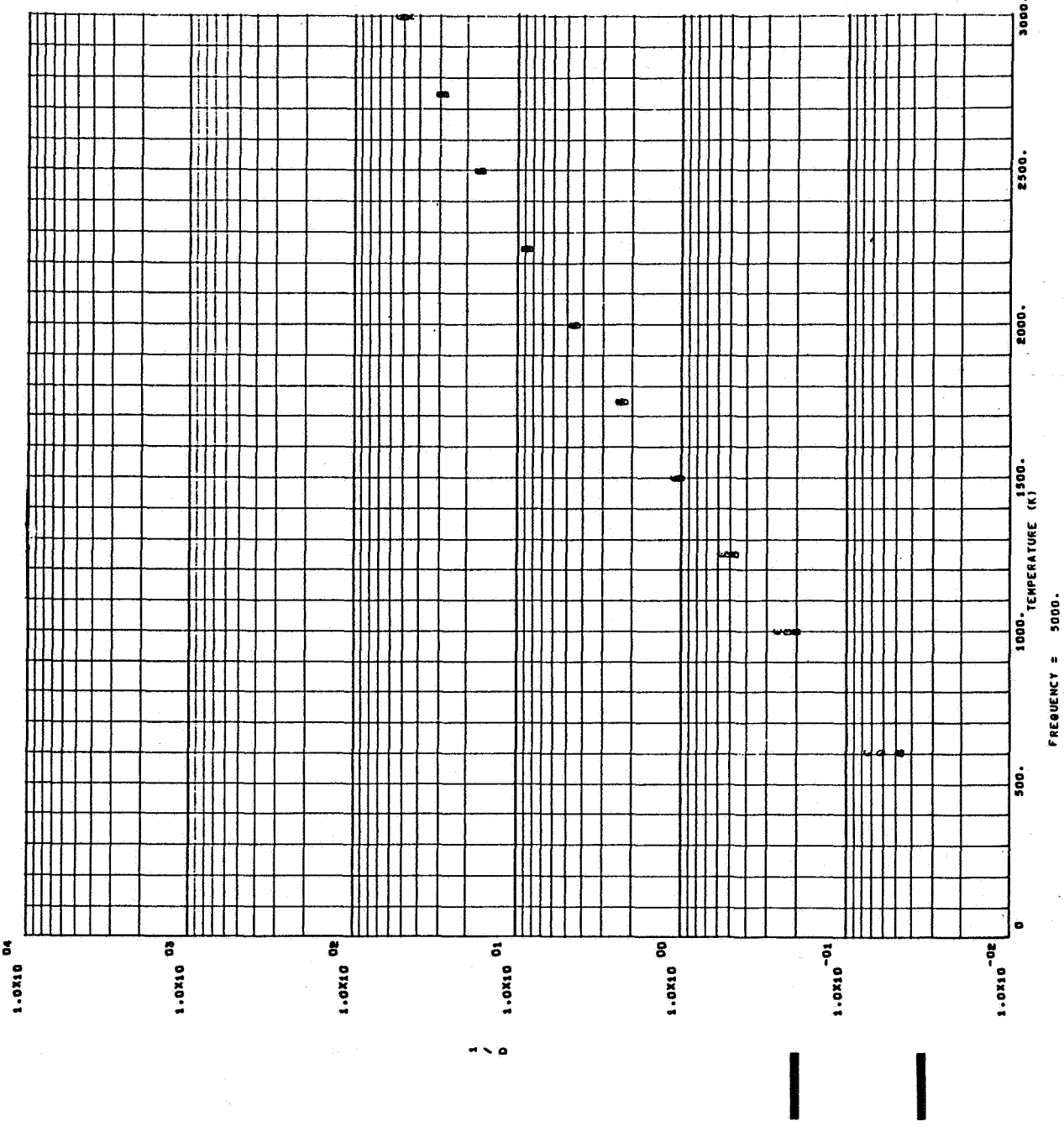

Fig. 18. Plot of $(1/d_{LR})$ versus T at 5000 cm^{-1} (A), 5025 (B), 5050 (C), and 5075 cm^{-1} (D).

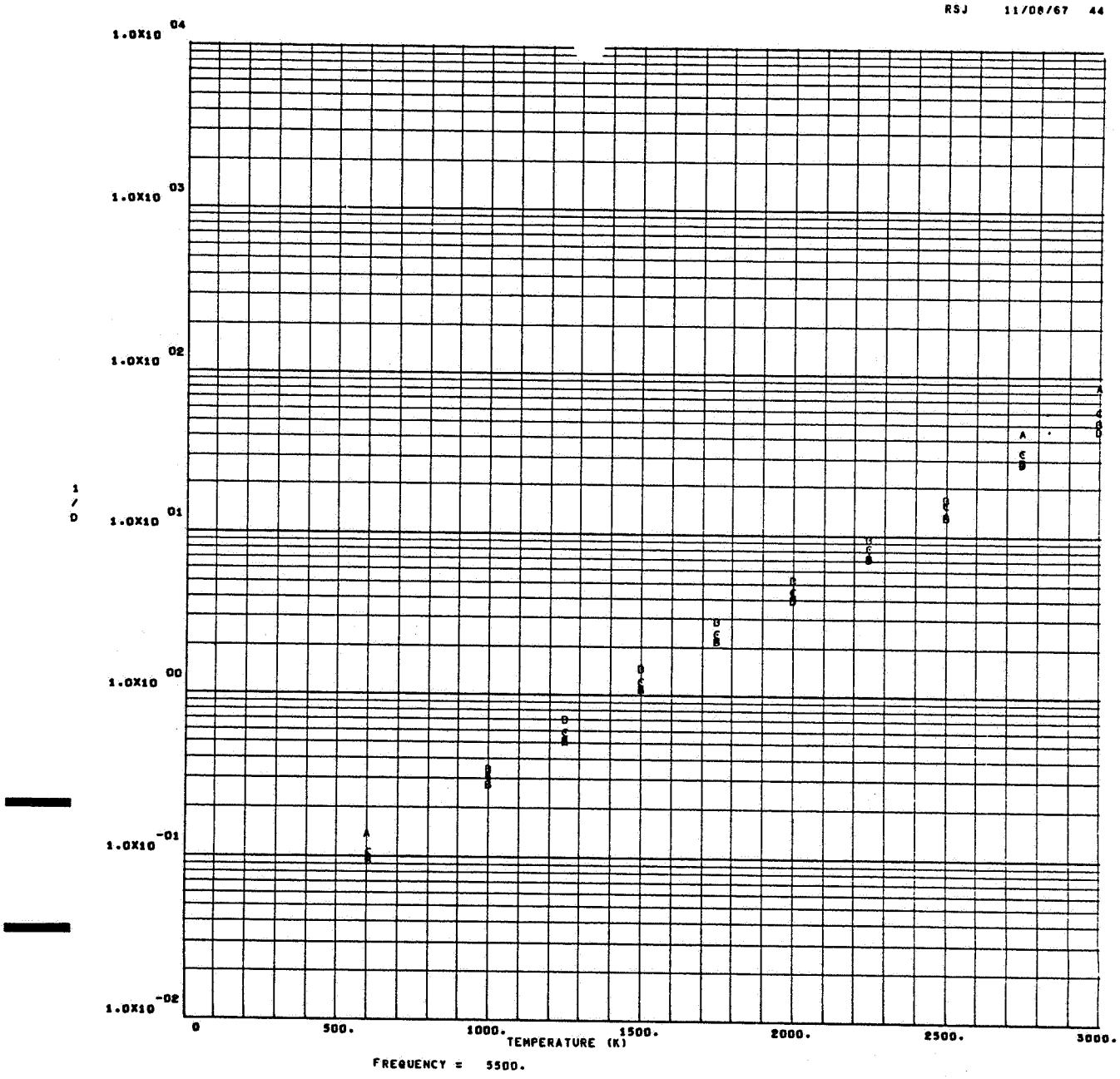

Fig. 19. Plot of $(1/d_{LR})$ versus T at 5500 cm^{-1} (A), 5525 (B), 5550 (C), and 5575 cm^{-1} (D).

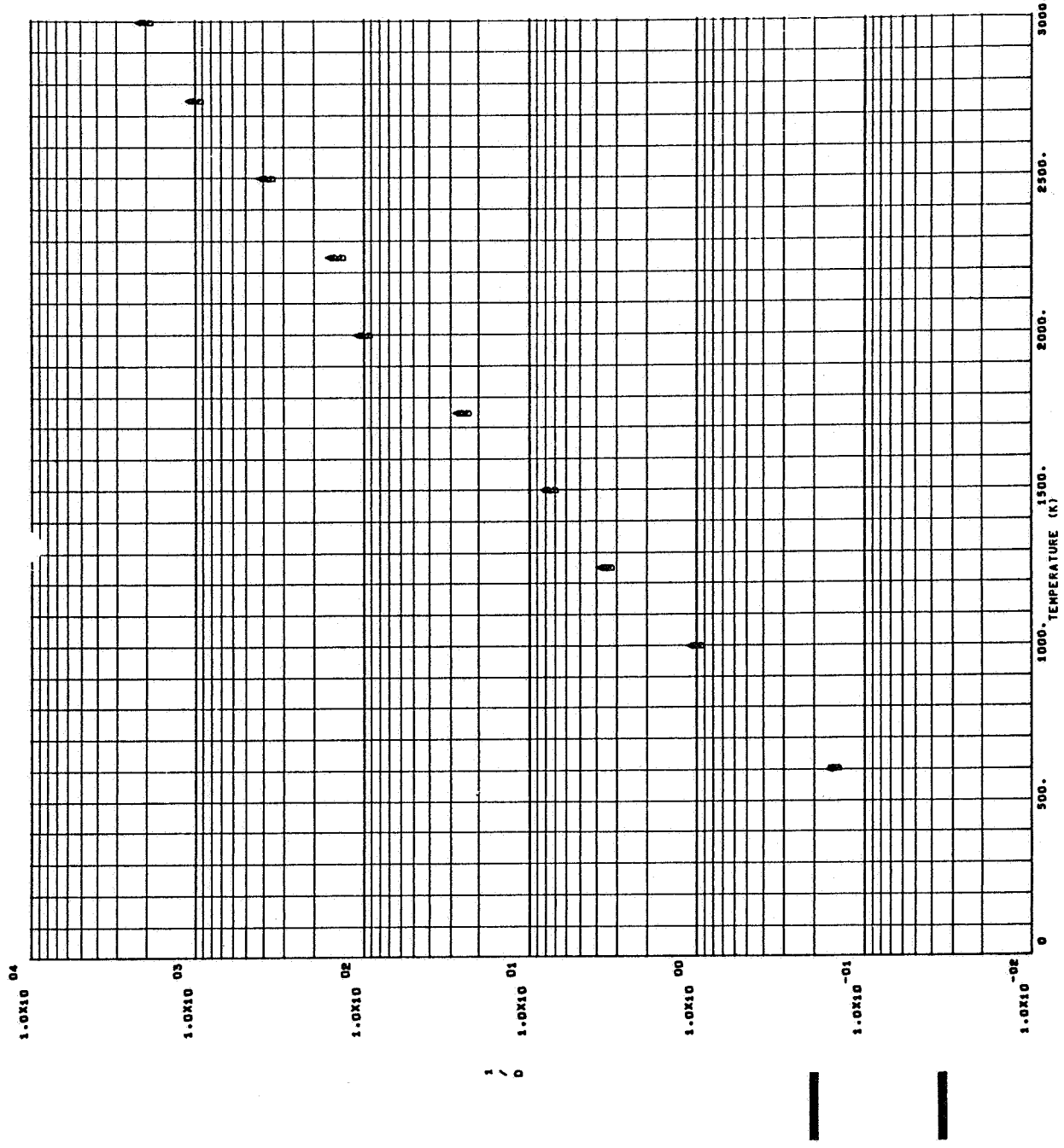

Fig. 20. Plot of $(1/d_{LR})$ versus T at 6000 cm^{-1} (A), 6025 (B), 6050 (C), and 6075 cm^{-1} (D).

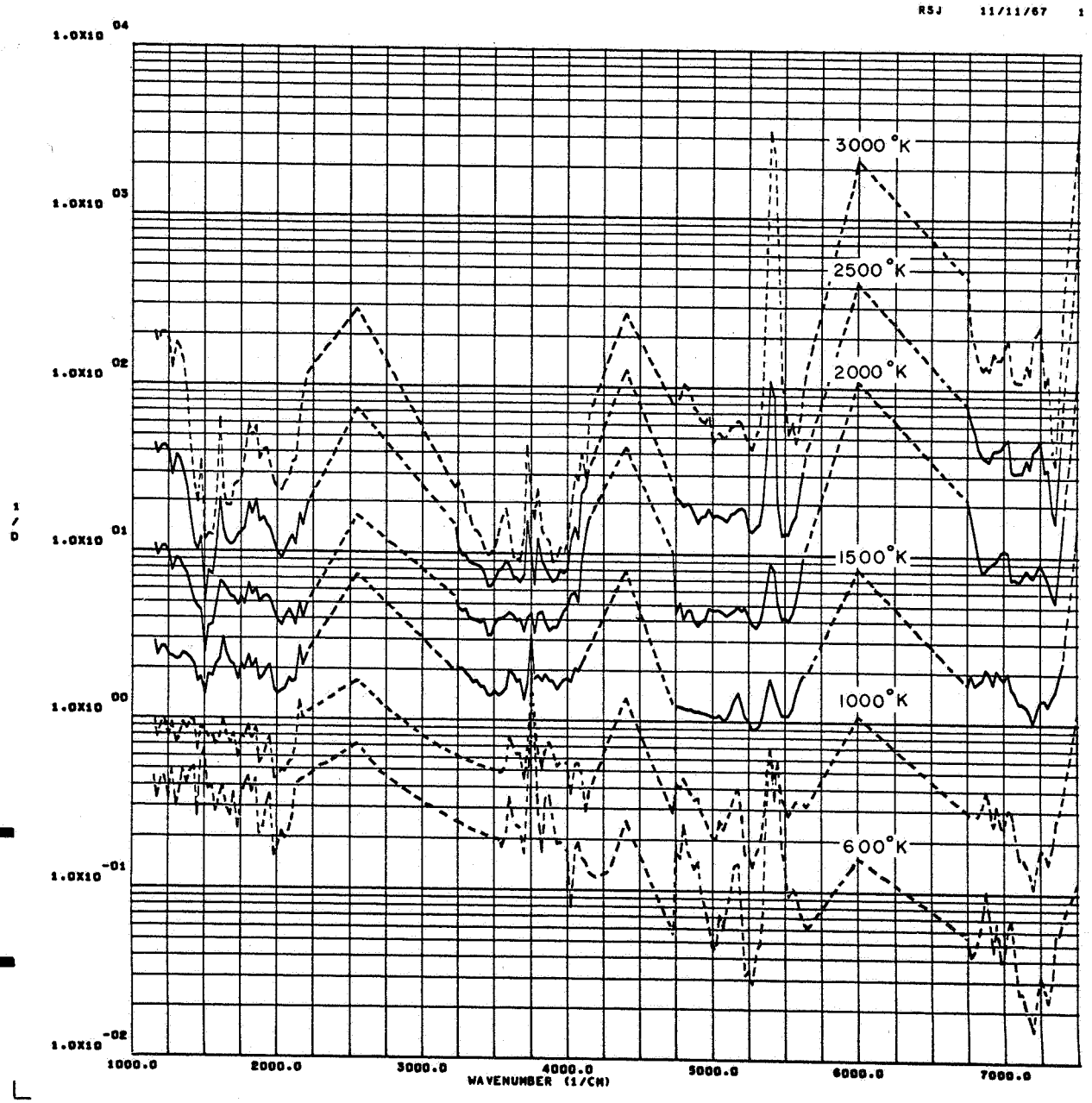

Fig. 21. Plot of $(1/d_{LR})$ versus ω between 1150 cm^{-1} and 7500 cm^{-1} for T = 600°, 1000°, 1500°, 2000°, 2500°, and 3000°K. The extrapolated regions are indicated by dashed lines.

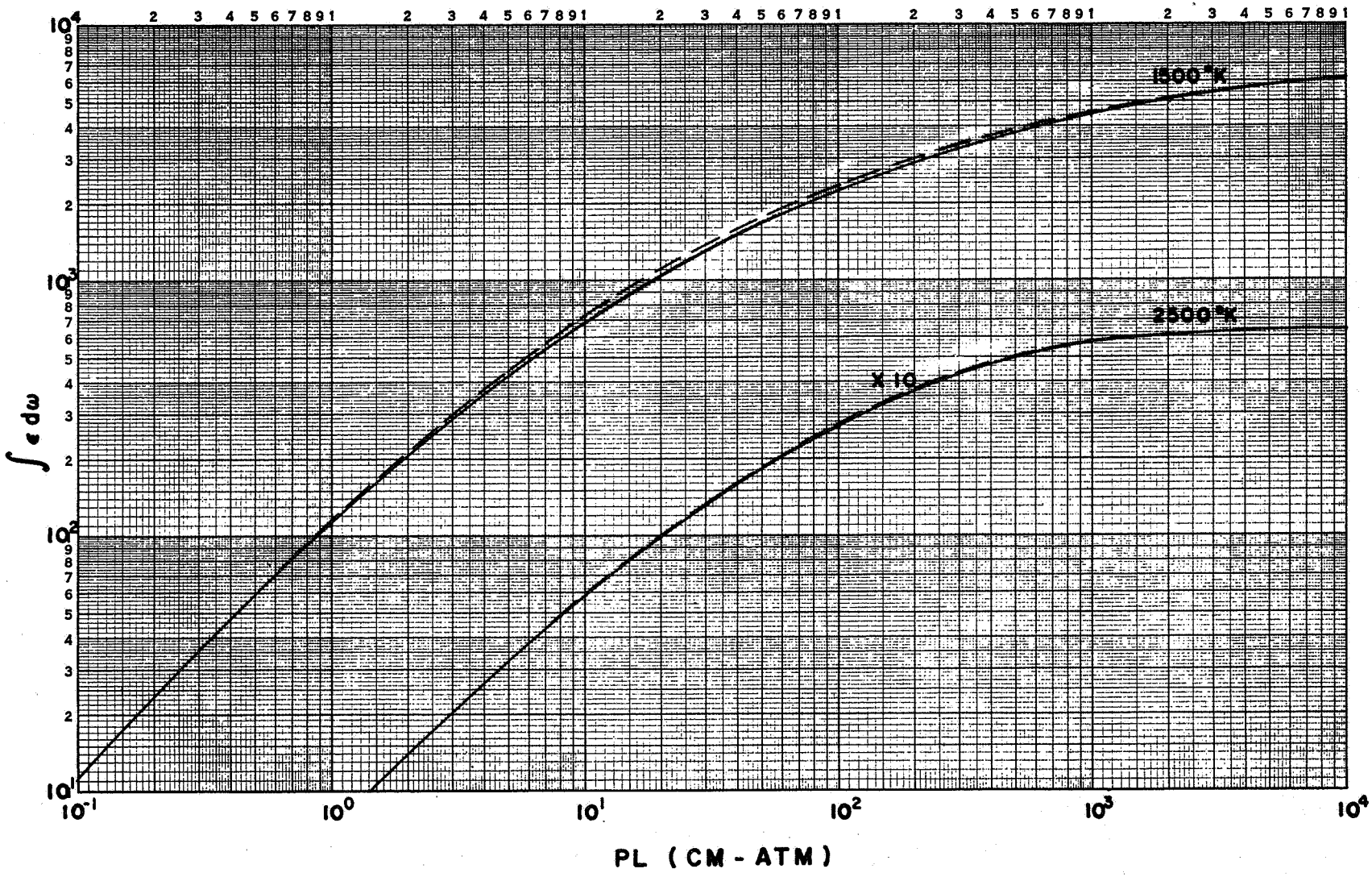

Fig. 22. Integrated emissivity between 1150 and 7500 cm^{-1} versus pL, based on (1/d) from Table II (solid line) and (1/d) as a sinusoidal function of ω (dashed line) for 1500° and 2500°K. Total pressure is 0.1 atm, 50% H_2O and 50% N_2. Note: The values for the 2500°K case must be multiplied by 10.

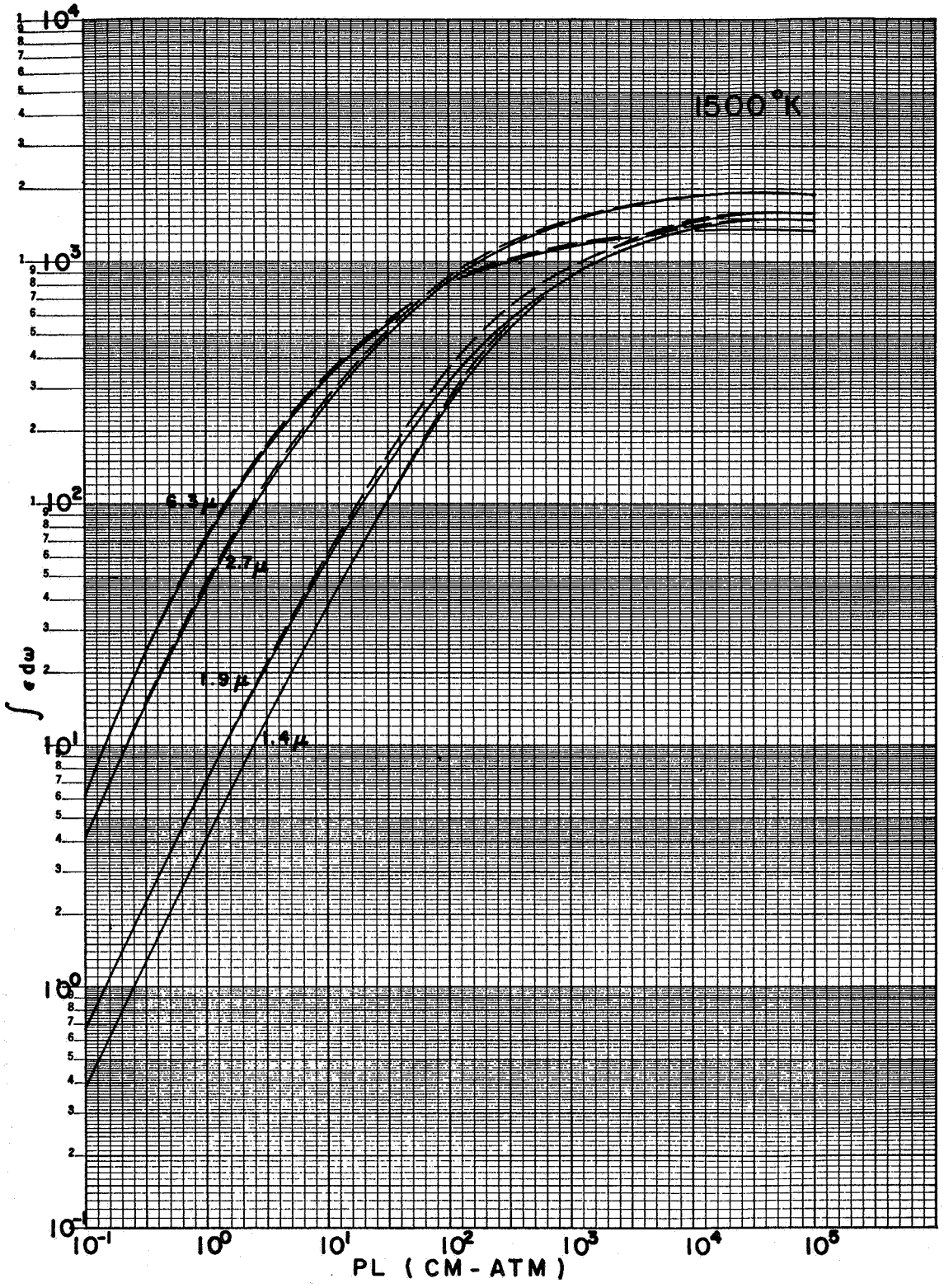

Fig. 23. Integrated band emissivities at 1500°K versus pL, based on (1/d) from Table II (solid line) and on (1/d) as a sinusoidal function of ω (dashed line). Total pressure is 0.1 atm, 50% H_2O and 50% N_2.

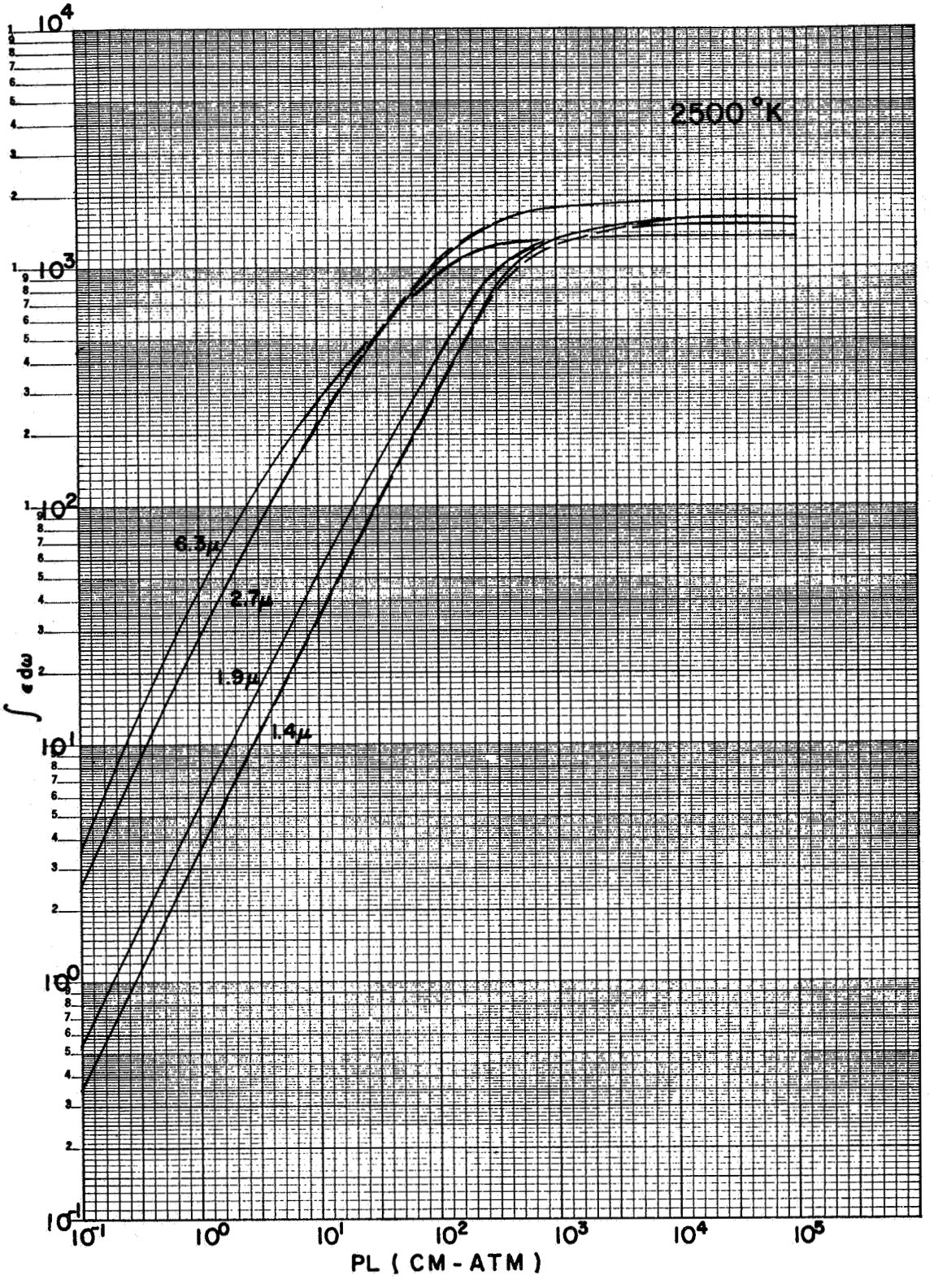

Fig. 24. Integrated band emissivities at 2500°K versus pL, based on (1/d) from Table II (solid line) and on (1/d) as a sinusoidal function of ω (dashed line). Total pressure is 0.1 atm, 50% H_2O and 50% N_2.

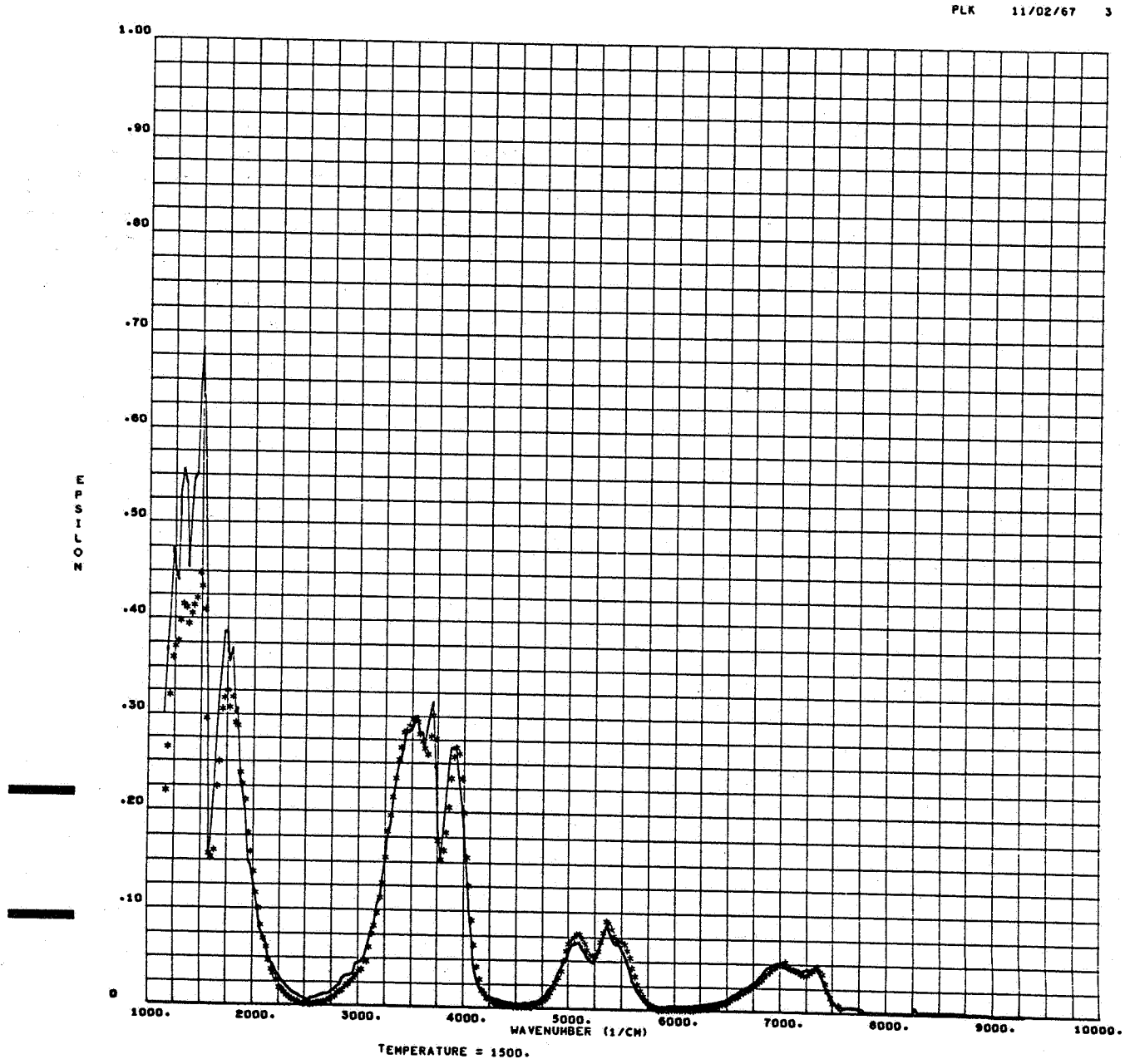

Fig. 25. Comparison between experimental (solid line) and computed spectra (*) at 1500°K and 2' pathlength.

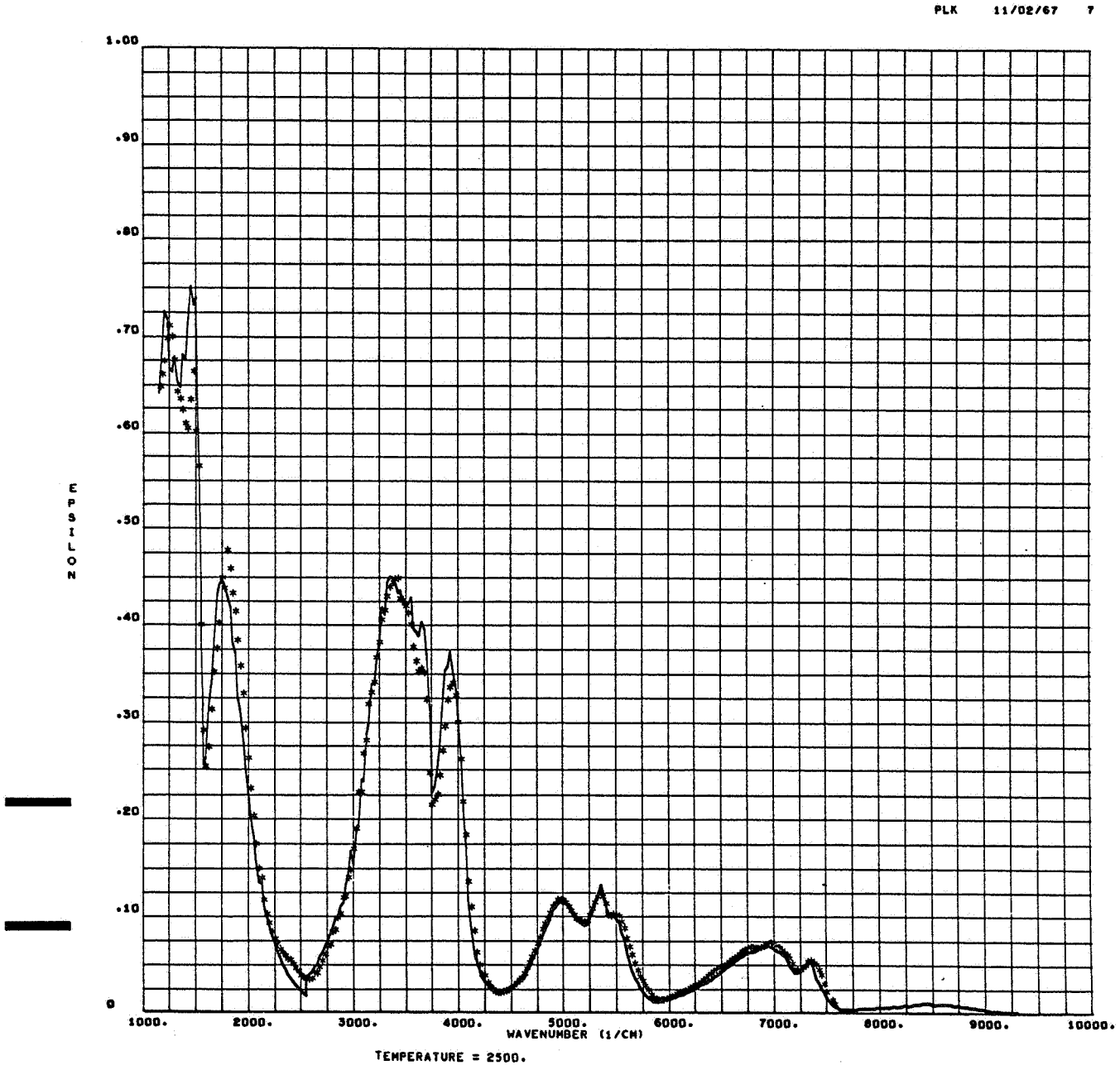

Fig. 26. Comparison between experimental (solid line) and computed spectra (*) at 2500°K and 2' pathlength.

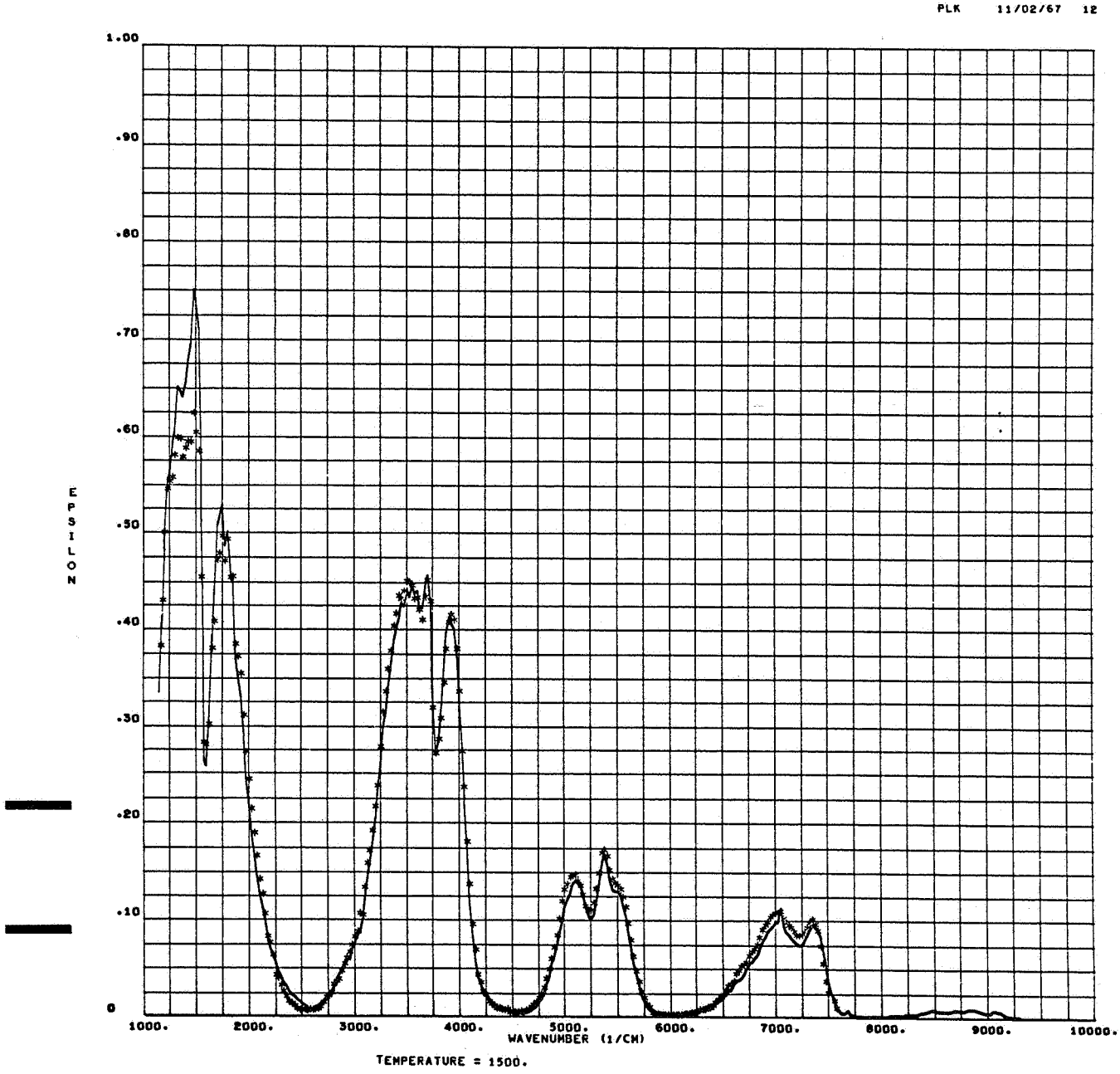

Fig. 27. Comparison between experimental (solid line) and computed spectra (*) at 1500°K and 5' pathlength.

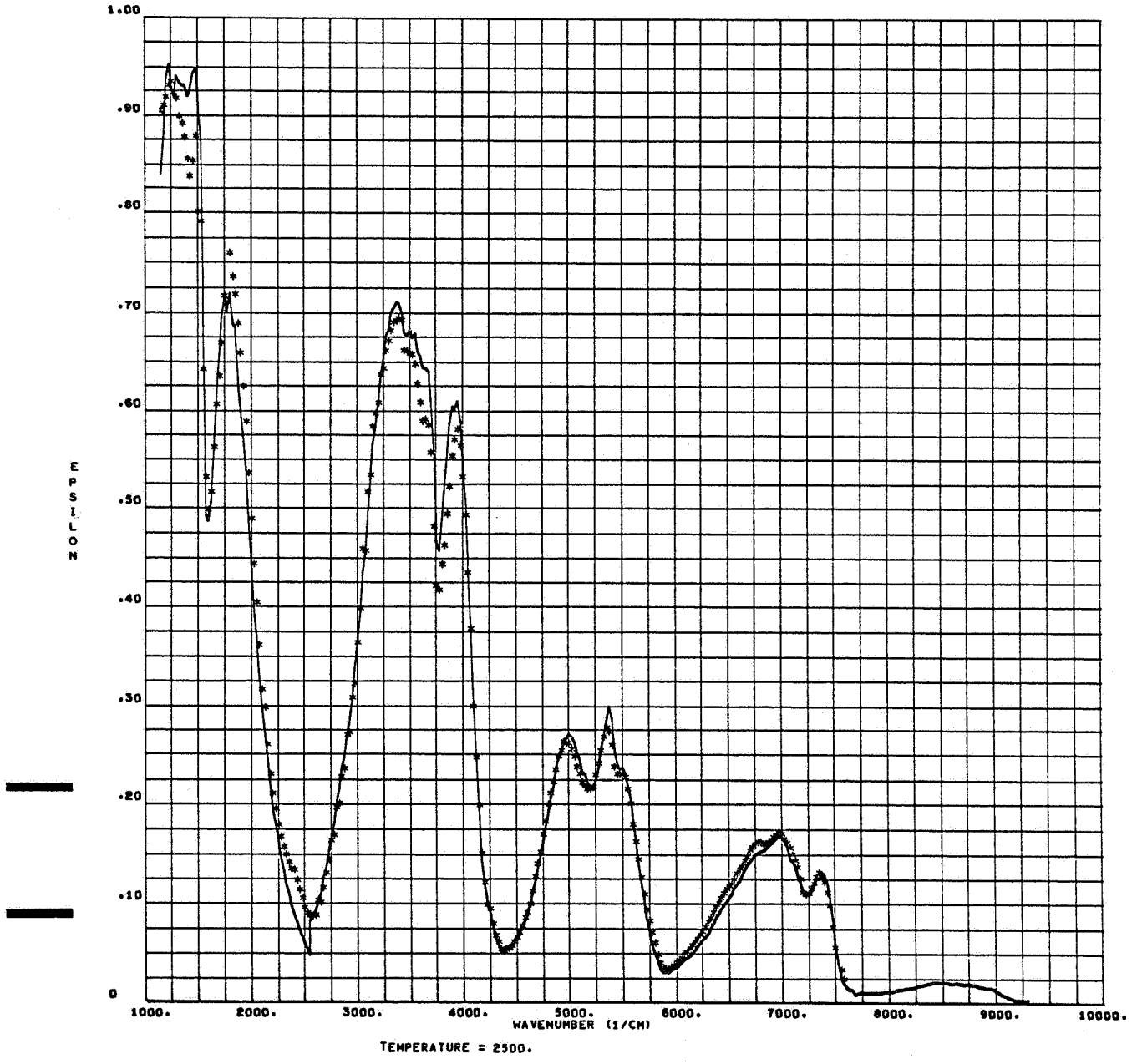

Fig. 28. Comparison between experimental (solid line) and computed spectra (*) at 2500°K and 5' pathlength.

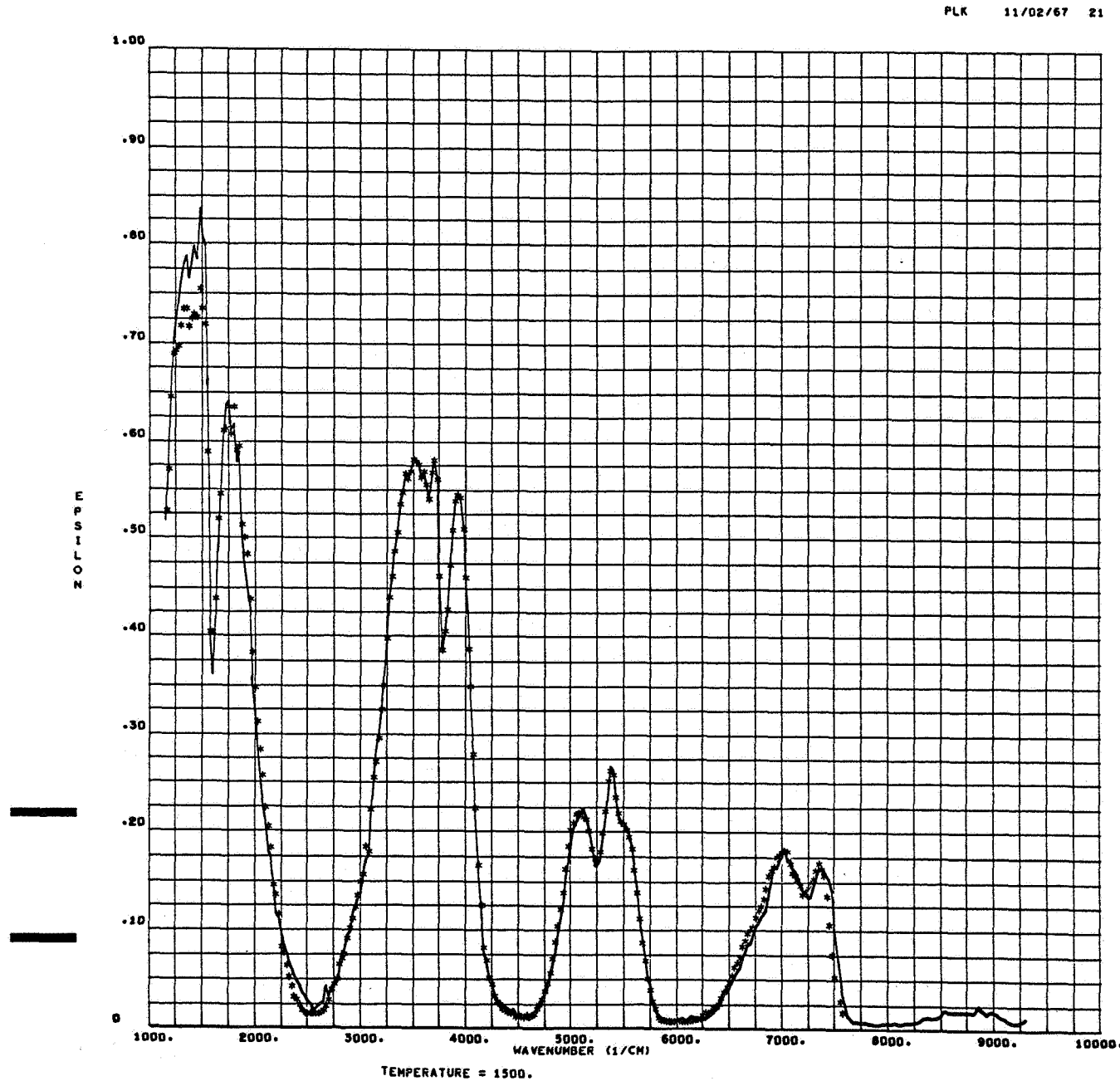

Fig. 29. Comparison between experimental (solid line) and computed spectra (*) at 1500°K and 10' pathlength.

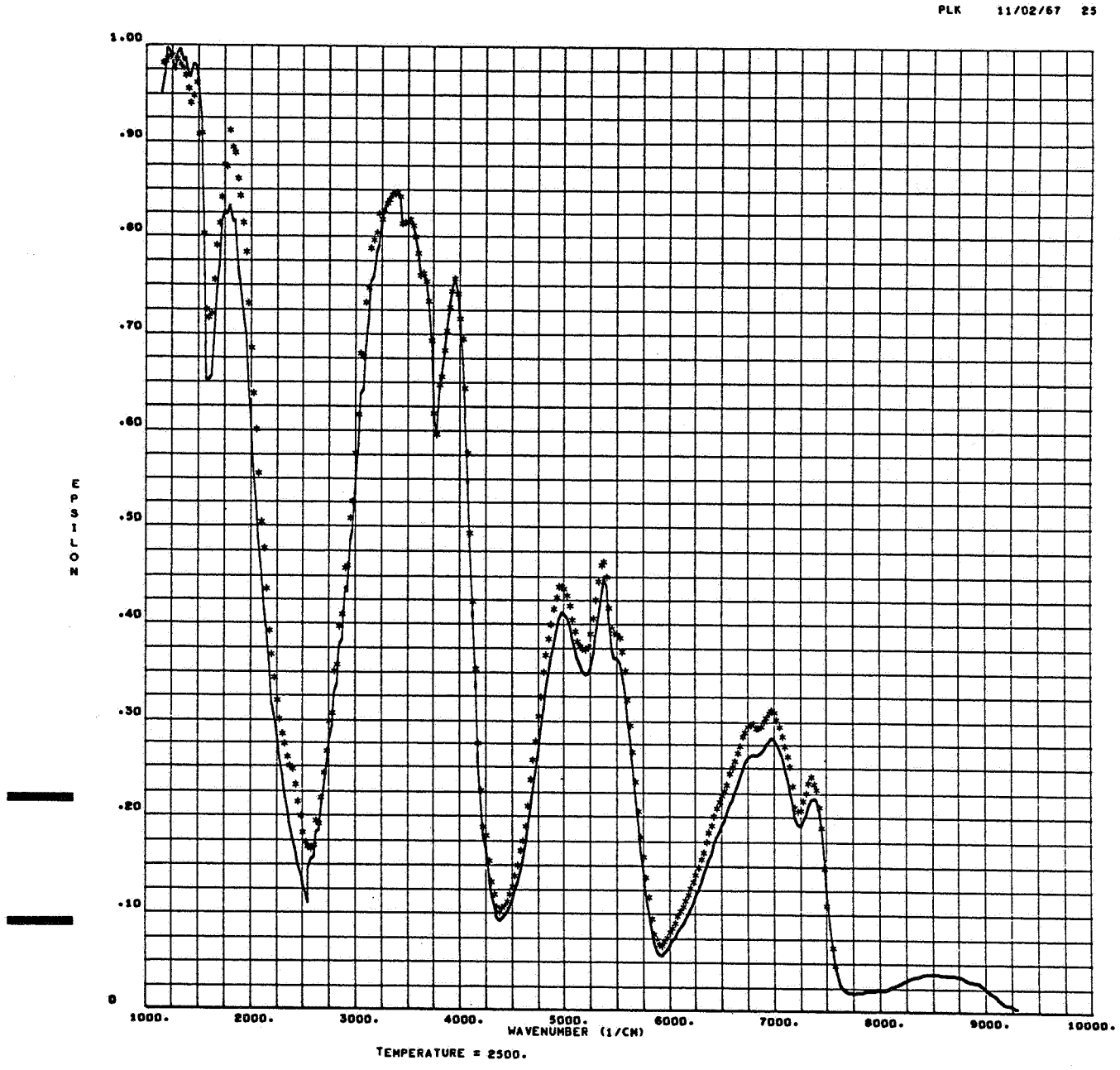

Fig. 30. Comparison between experimental (solid line) and computed spectra (*) at 2500°K and 10' pathlength.

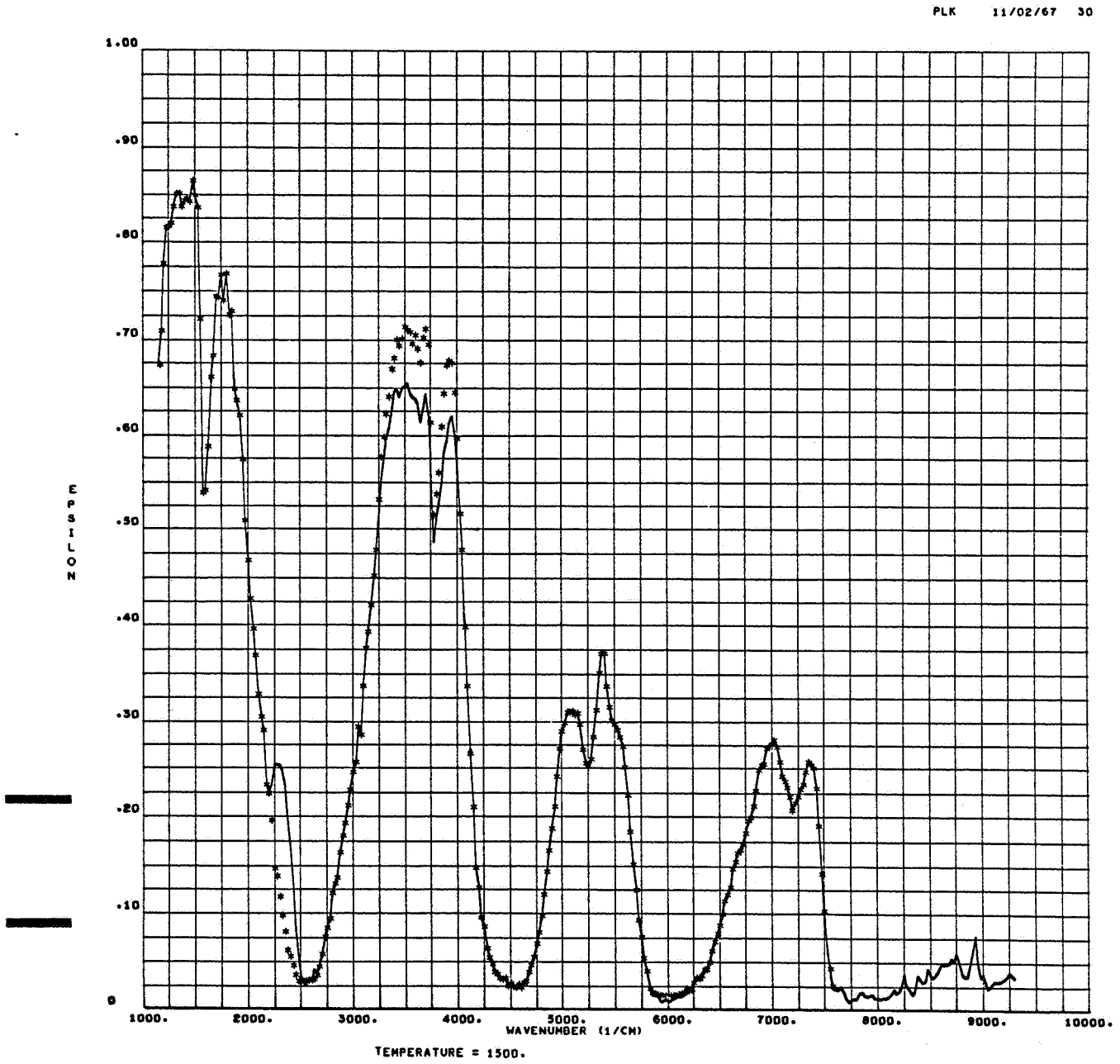

Fig. 31. Comparison between experimental (solid line) and computed spectra (*) at 1500°K and 20' pathlength.

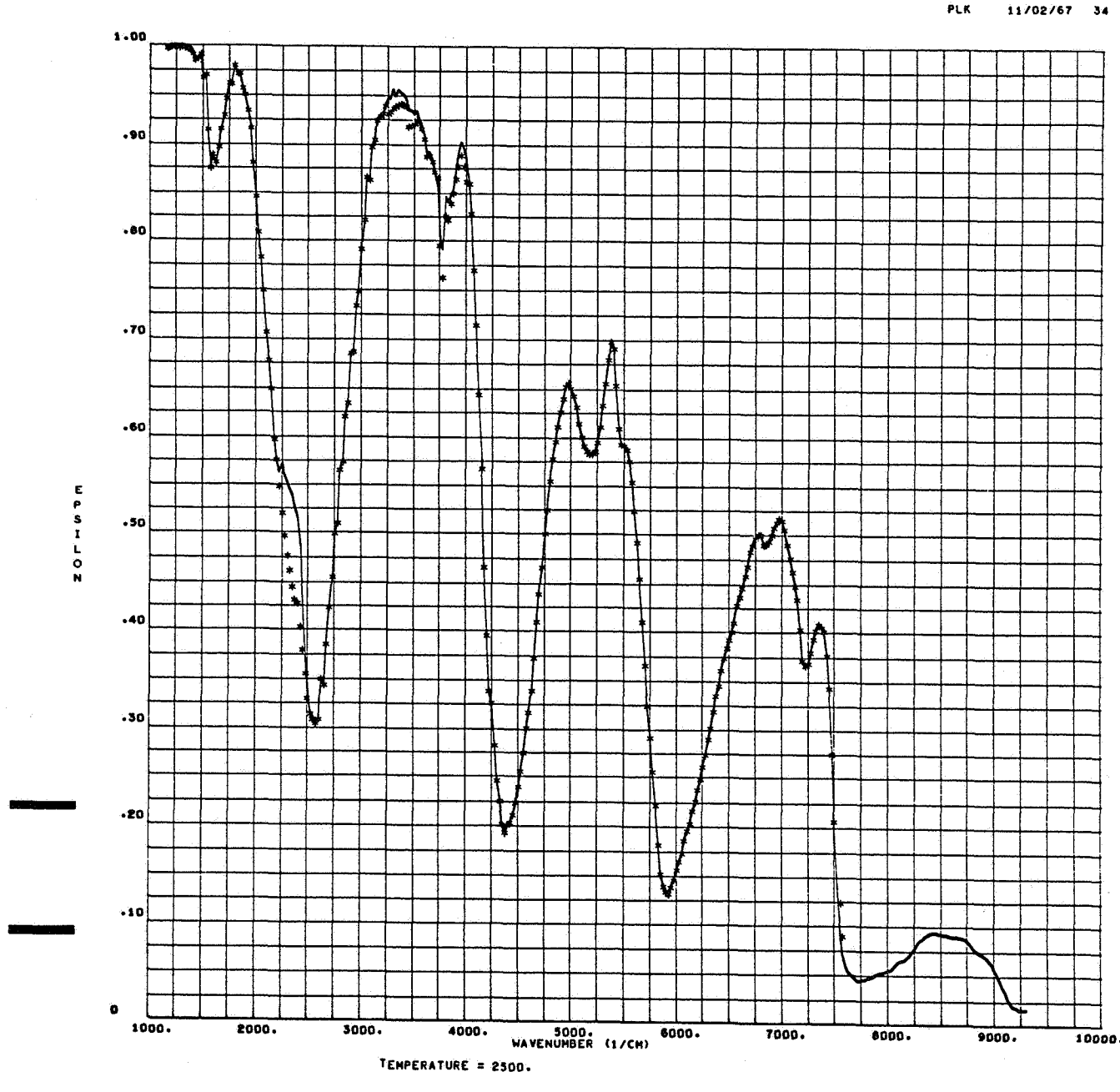

Fig. 32. Comparison between experimental (solid line) and computed spectra (*) at 2500°K and 20' pathlength.

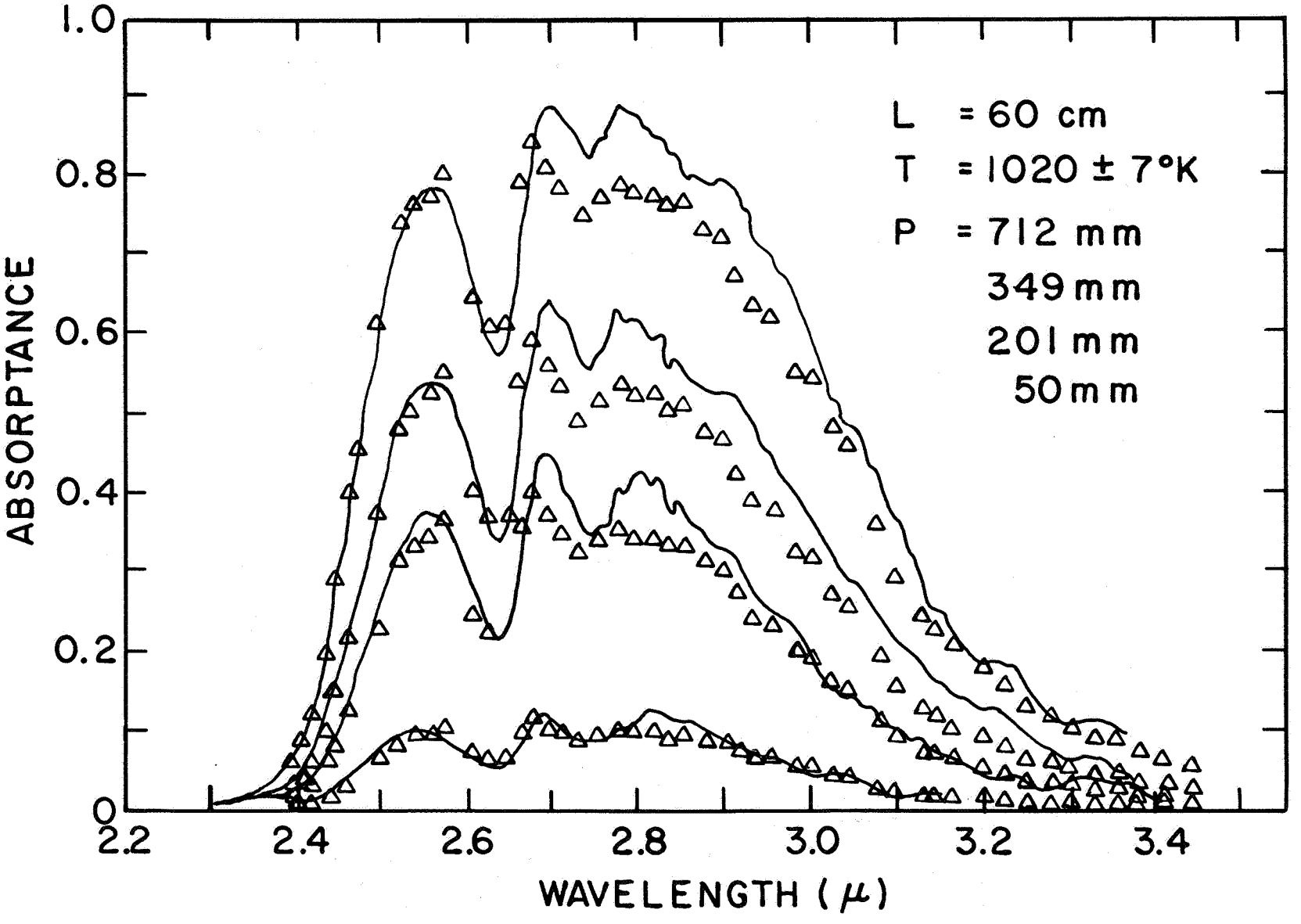

Fig. 33. Comparison with experimental results obtained by Simmons (solid line) at 1020 ± 7°K for different pressures of H_2O at a pathlength of 60 cm.

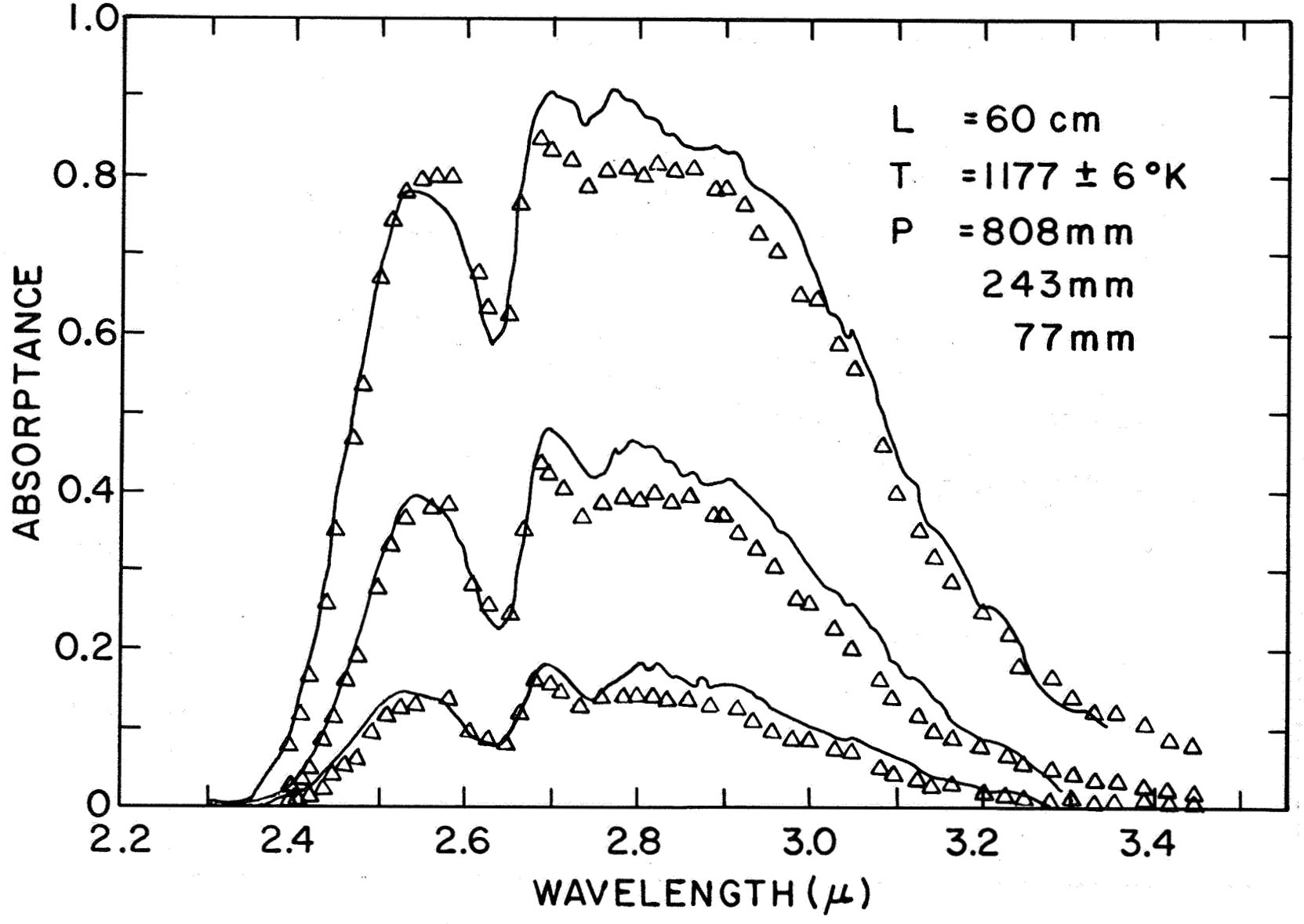

Fig. 34. Comparisons with experimental results obtained by Simmons (solid line) at 1177 ± 6°K for different pressures of H_2O at a pathlength of 60 cm.

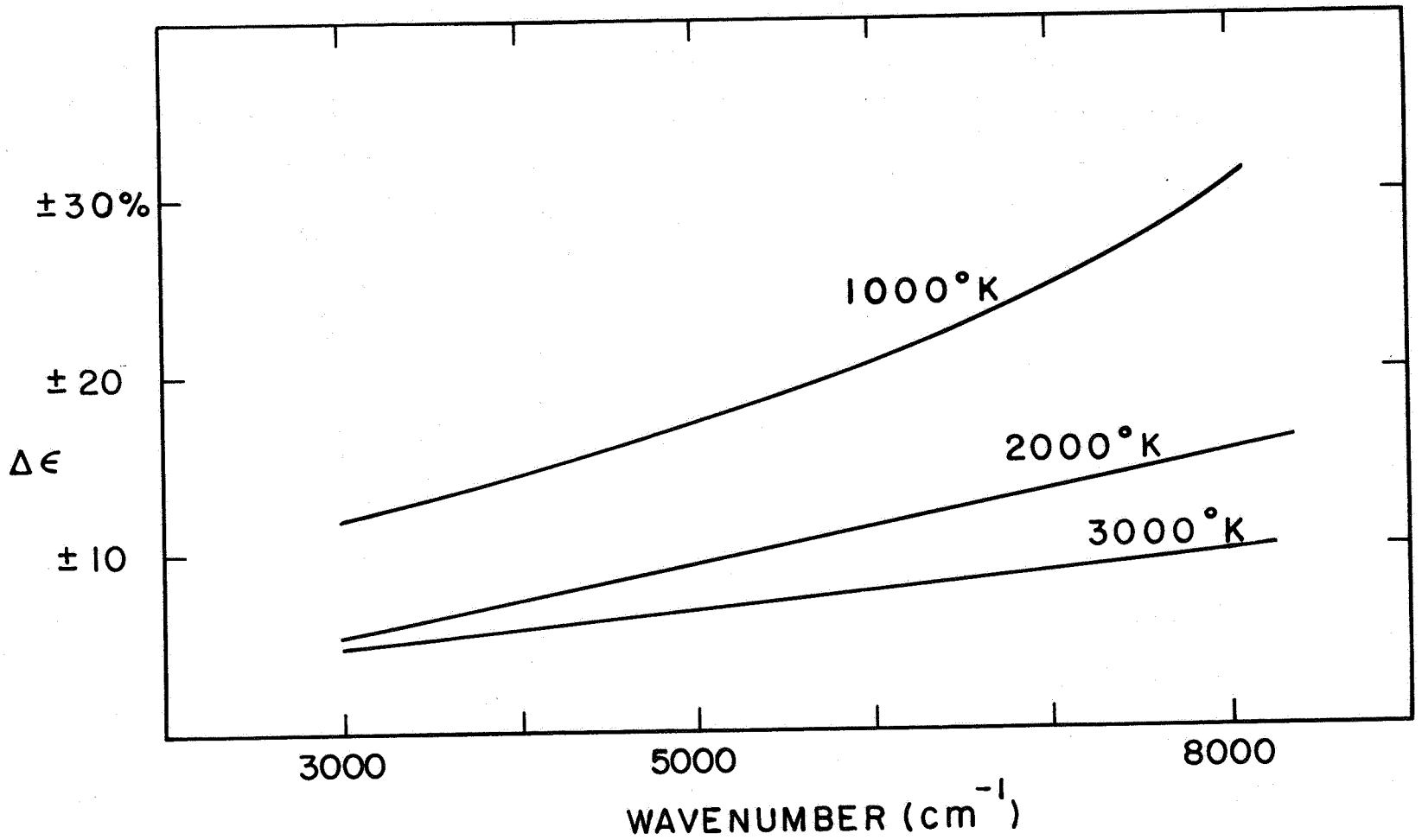

Fig. 35. Error in ε due to uncertainty of ± 3% in T versus ω for three different temperatures.

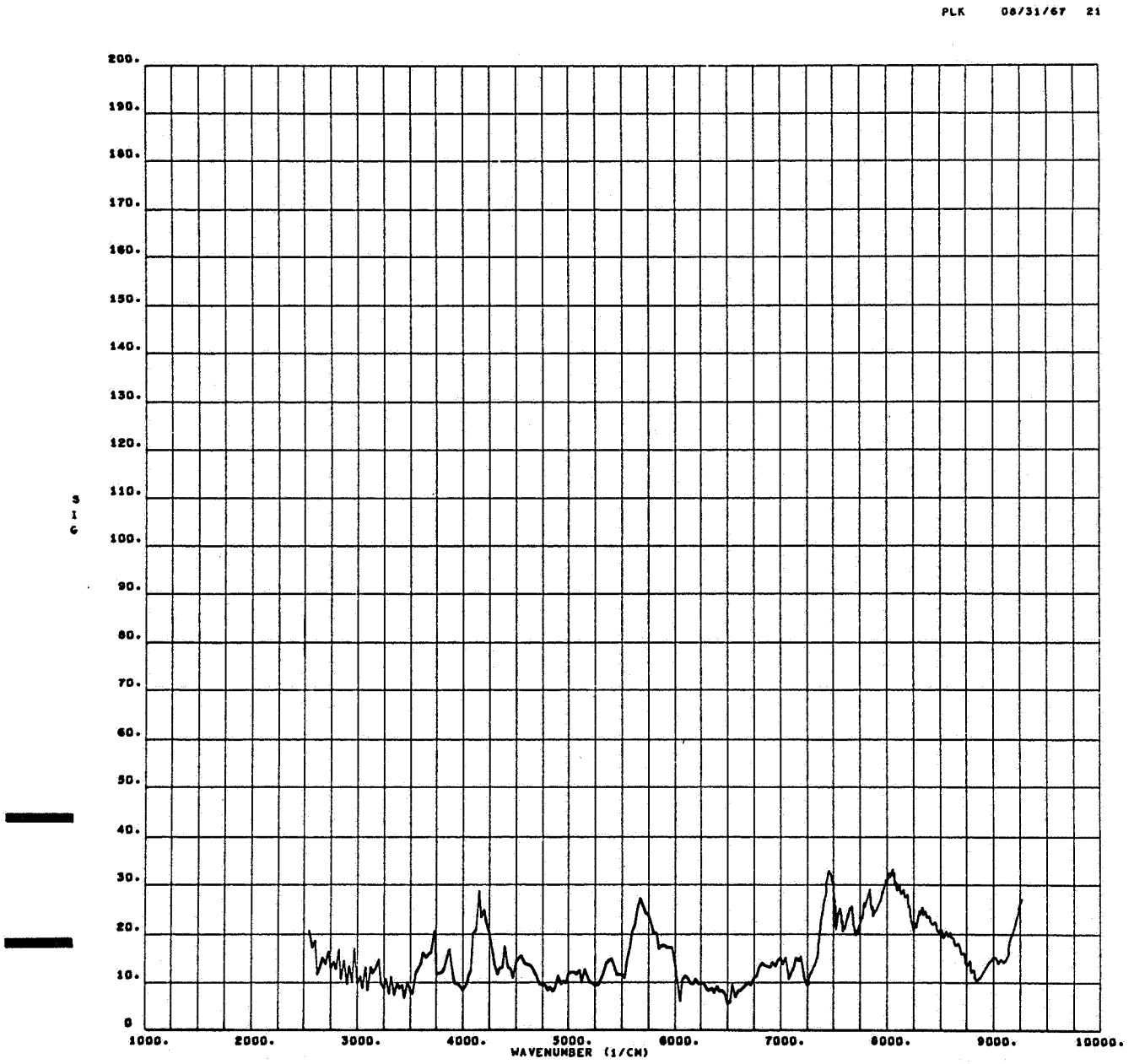

Fig. 36. RMS scatter of experimental values to curve of growth at T = 2750°K.

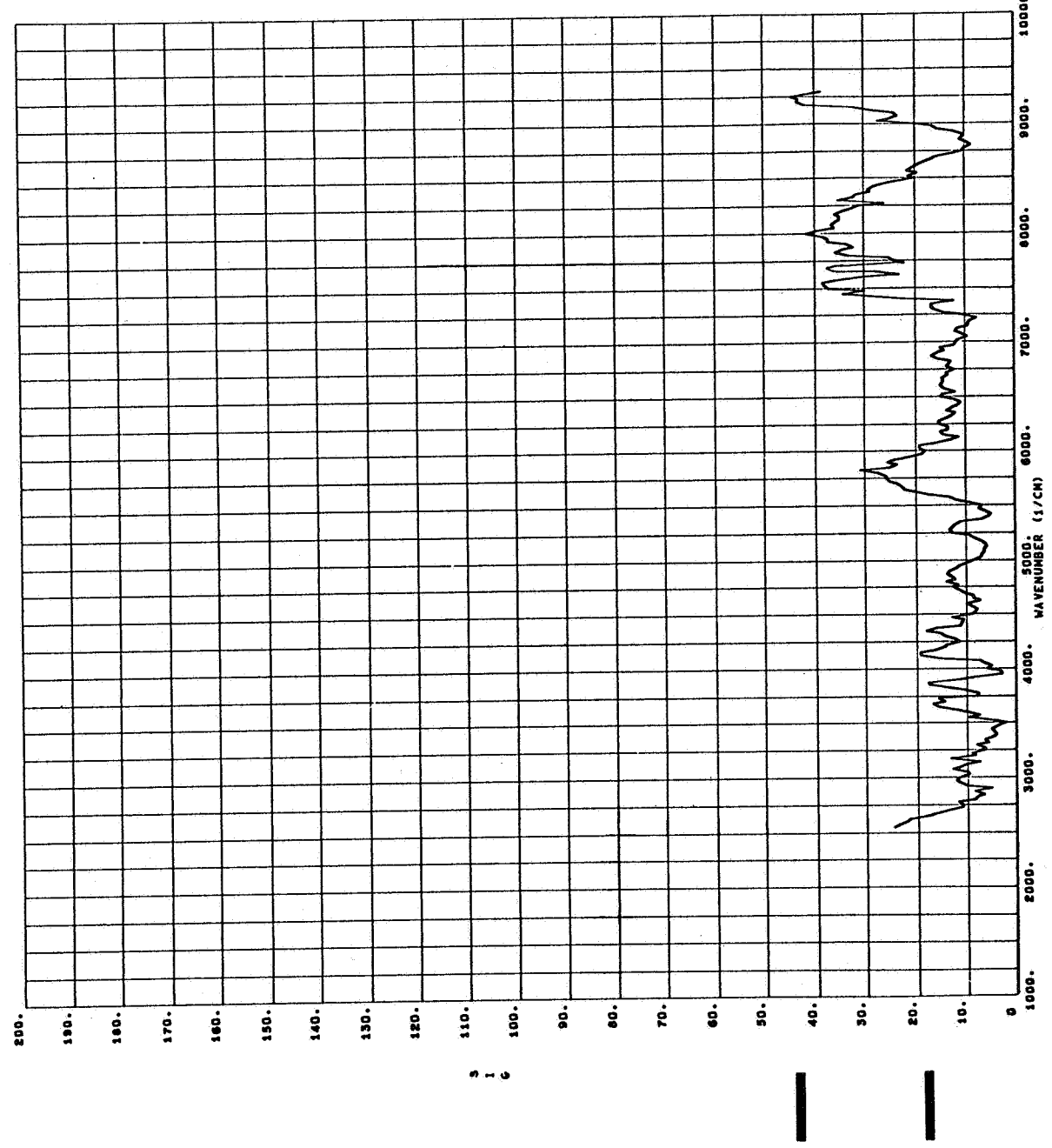

Fig. 37. RMS scatter of experimental values to curve of growth at T = 2000°K.

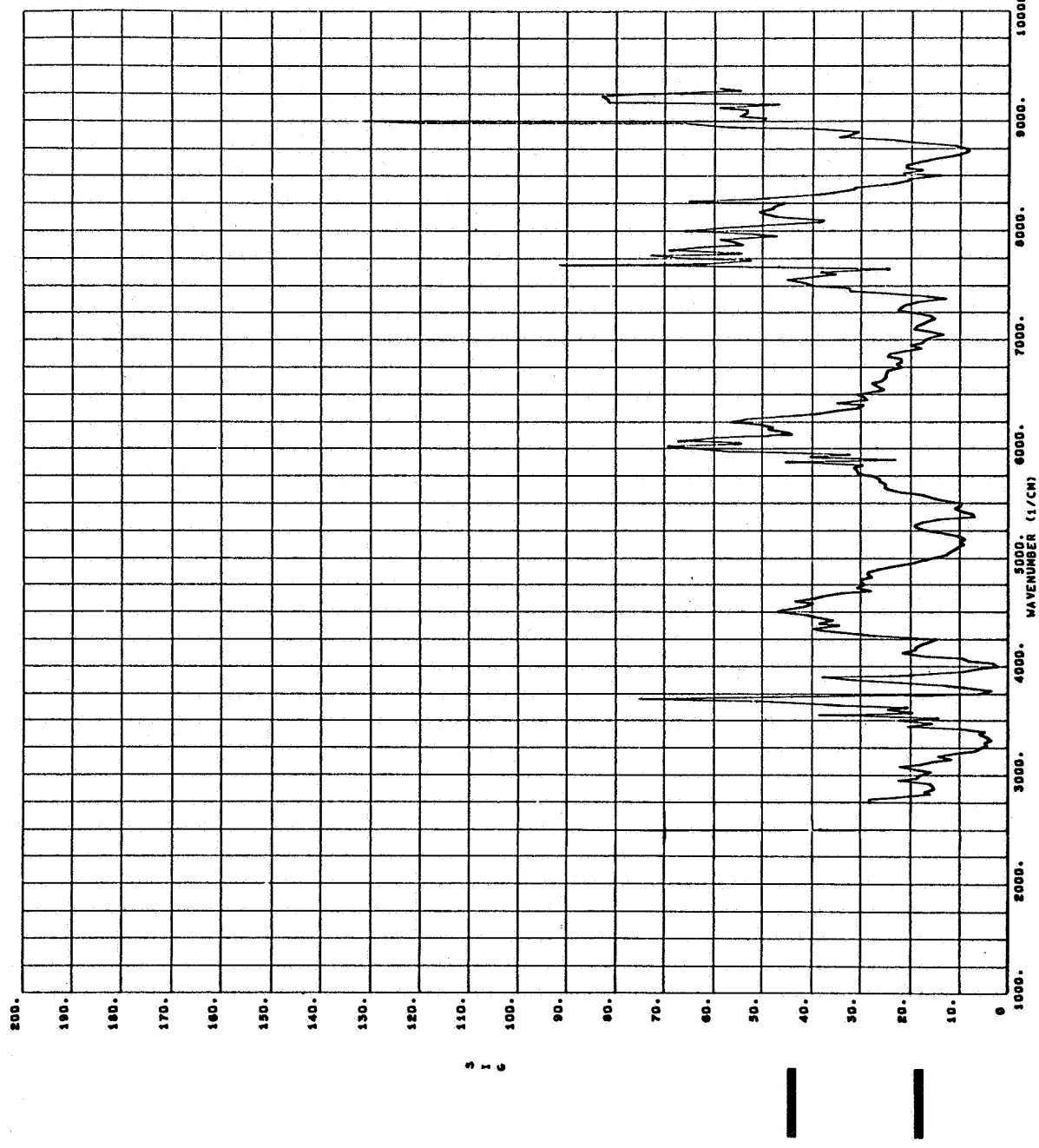

Fig. 38. RMS scatter of experimental values to curve of growth at T = 1250°K.

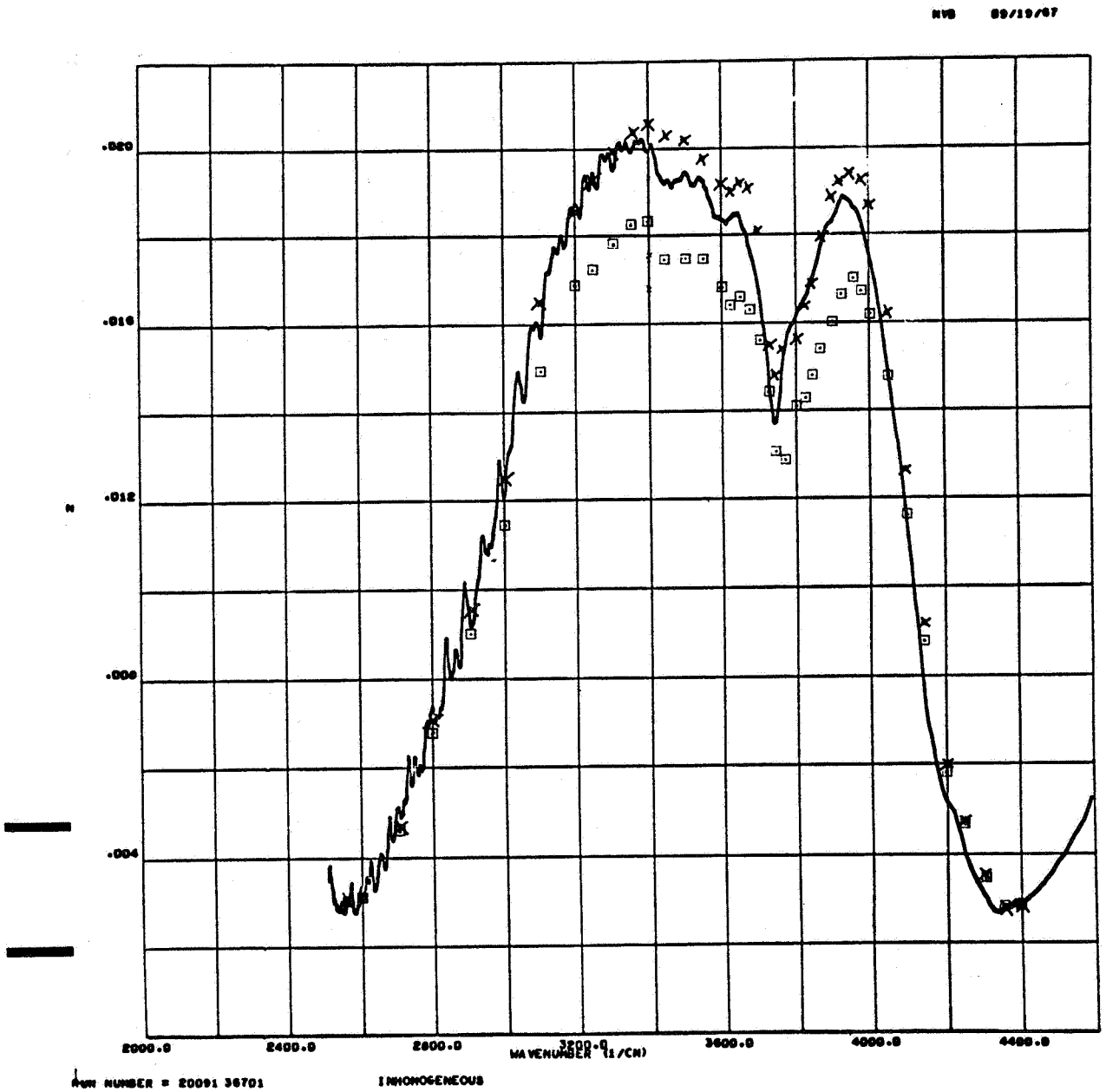

Fig. 39. Radiance from four slabs (ℓ = 150 cm each) in watts/cm^2 cm^{-1}. Solid line is the experimental curve. Calculated values from Model 3 are given by (□), from Model 3a are given by (X). Conditions for T and c are given in Section 4.5.

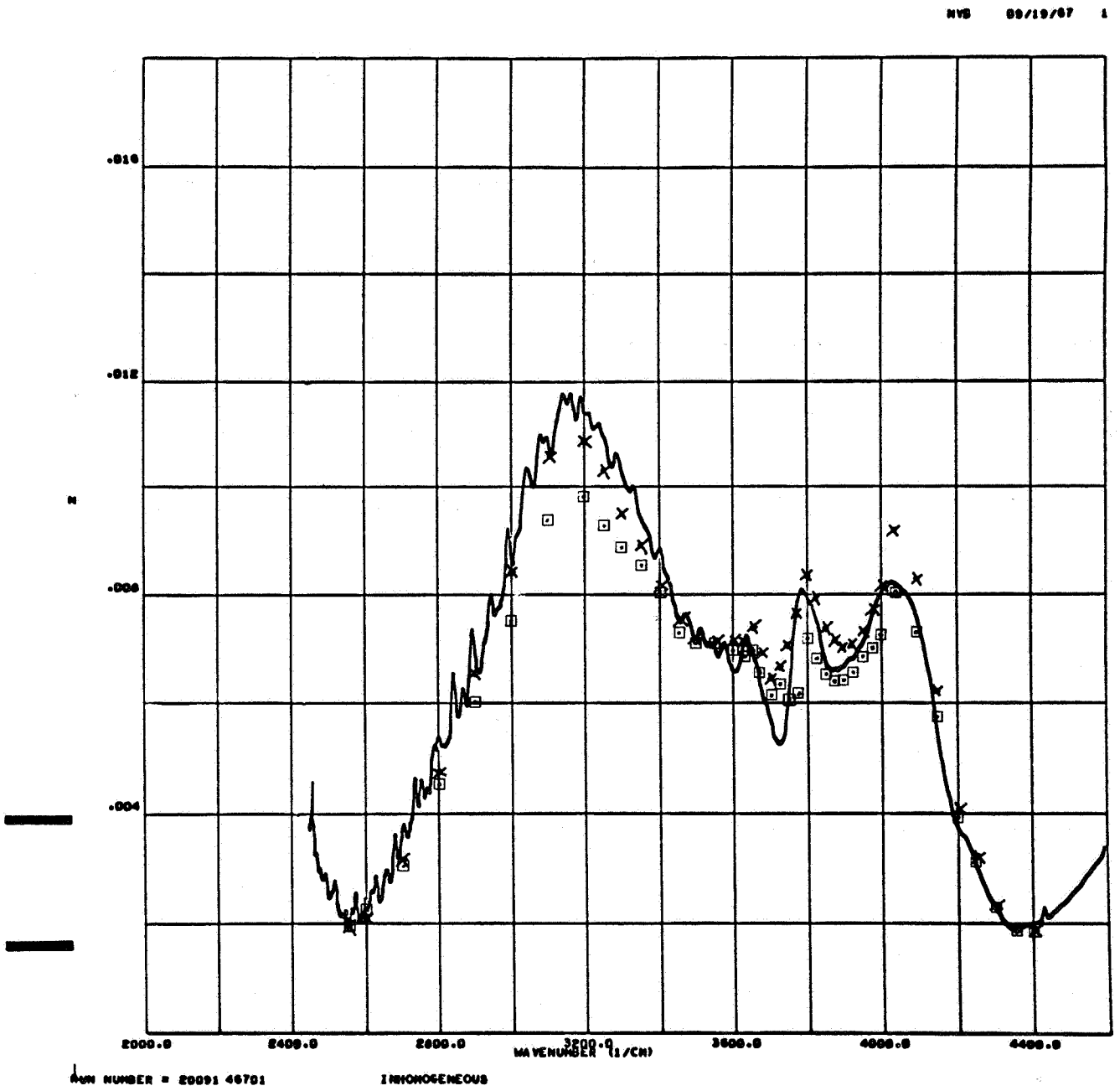

Fig. 40. Radiance from four slabs (ℓ = 150 cm each) in watts/cm^2 cm^{-1}. Solid line is the experimental curve. Calculated values from Model 3 are given by (□), from Model 3a are given by (X). Conditions for T and c are given in Section 4.5.

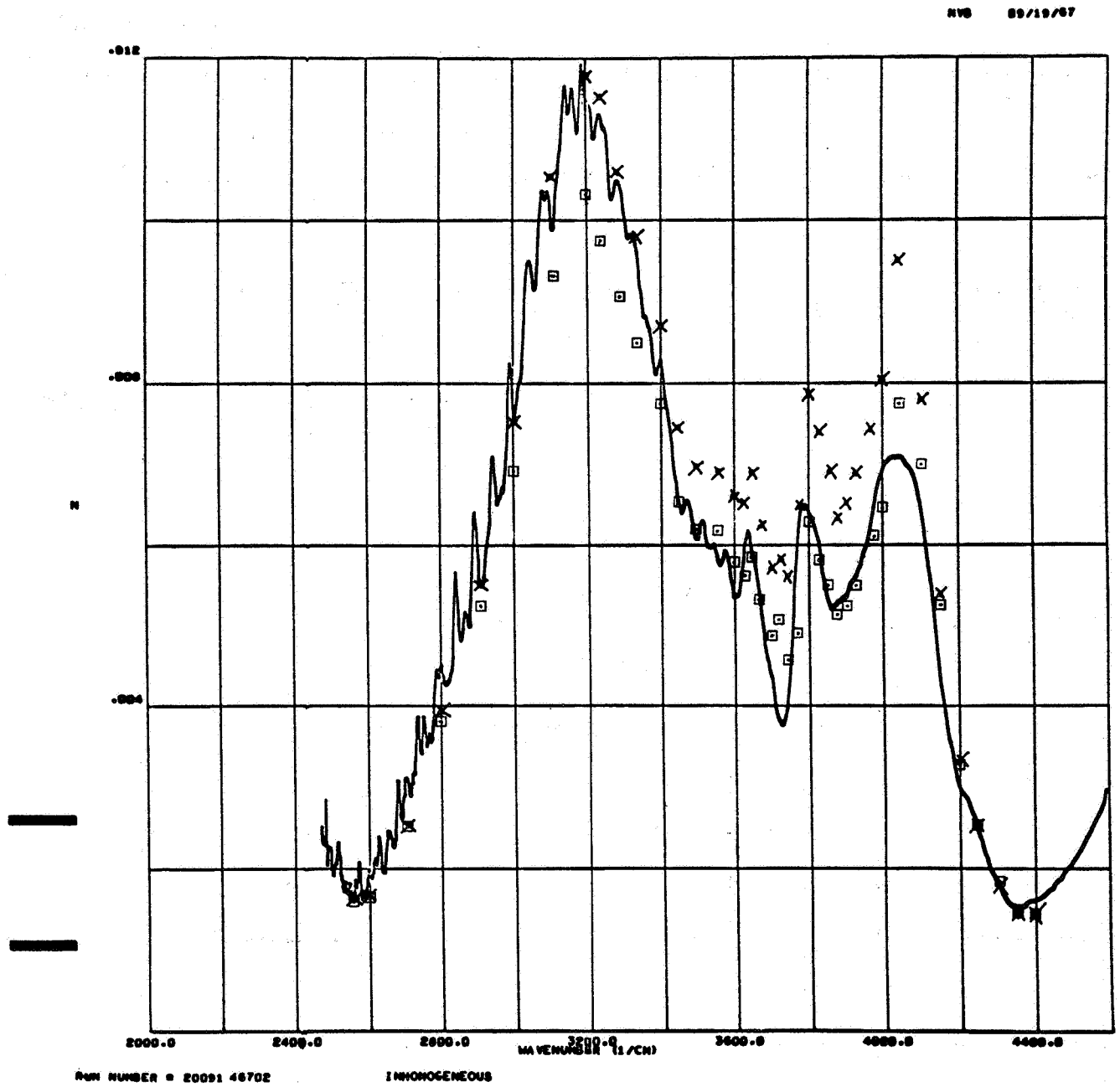

Fig. 41. Radiance from four slabs (ℓ = 150 cm each) in watts/cm^2 cm^{-1}. Solid line is the experimental curve. Calculated values from Model 3 are given by (□), from Model 3a are given by (X). Conditions for T and c are given in Section 4.5.

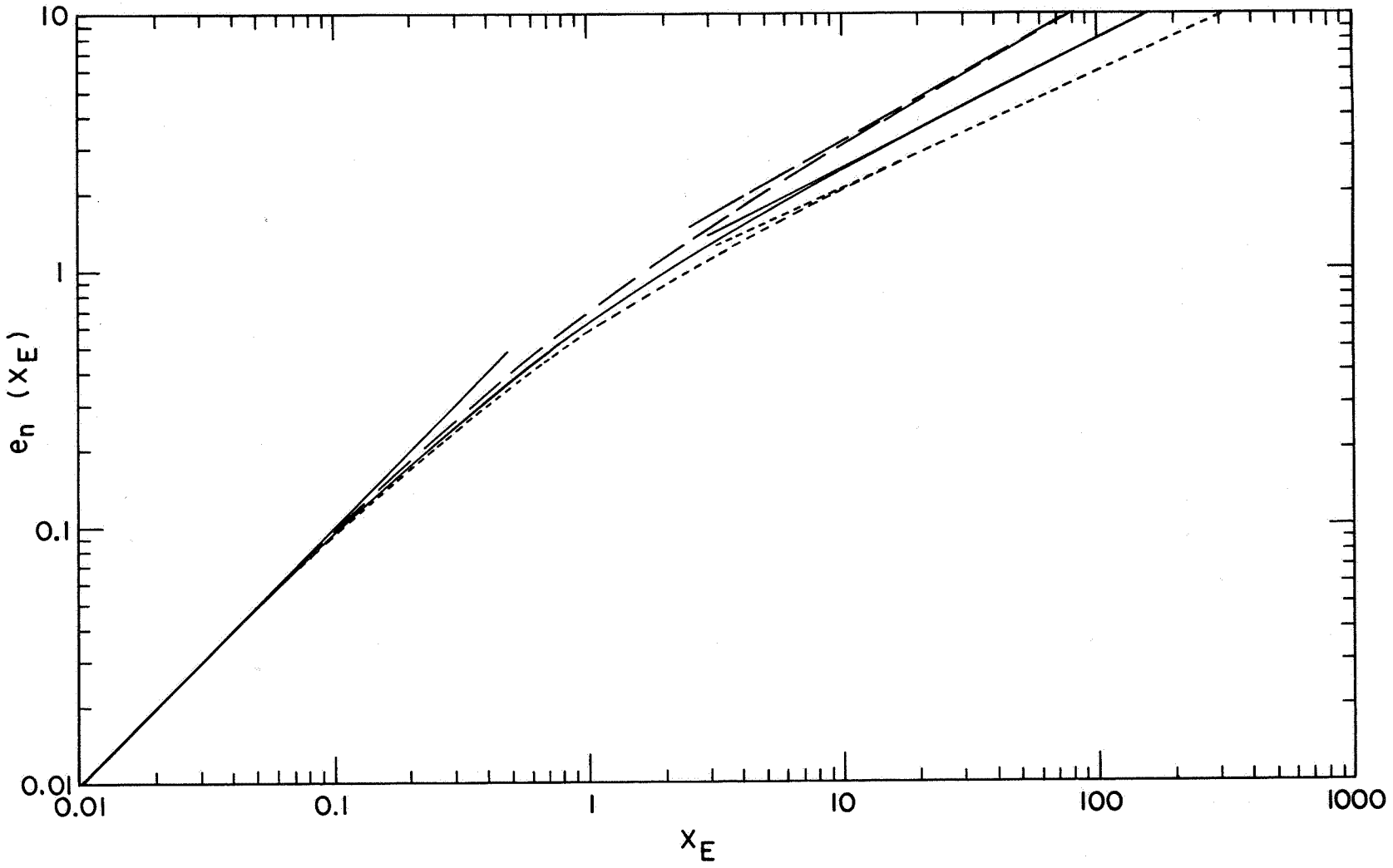

Fig. 42. Graph of $e_n(x_E)$ vs x_E for n = 1.8 (dashed), n = 2.0 (solid), and n = 2.2 (dotted). For a Lorentz shape n = 2; a line with n < 2 has above-Lorentzian wings; a line with n > 2 has below-Lorentzian wings.

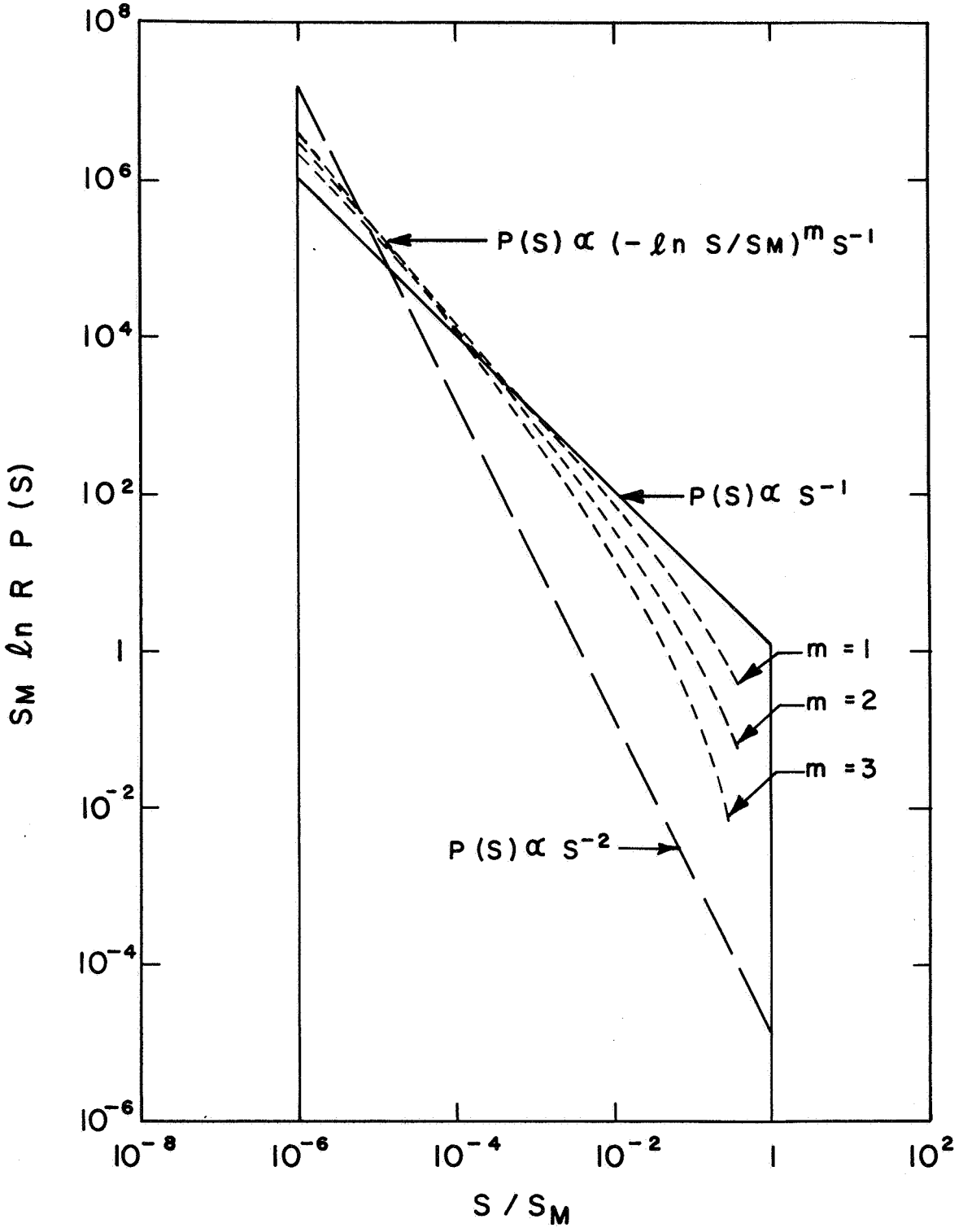

Fig. 43. Line intensity probability distribution functions. Solid line: $P(S) \propto S^{-1}$. Dotted lines: $P(S) \propto [\ell n\ (S_M/S)]^m S^{-1}$, for m = 1, 2, 3. Dashed line: $P(S) \propto S^{-2}$. All P(S) = 0 outside of region $(S_M/R \leq S \leq S_M)$.

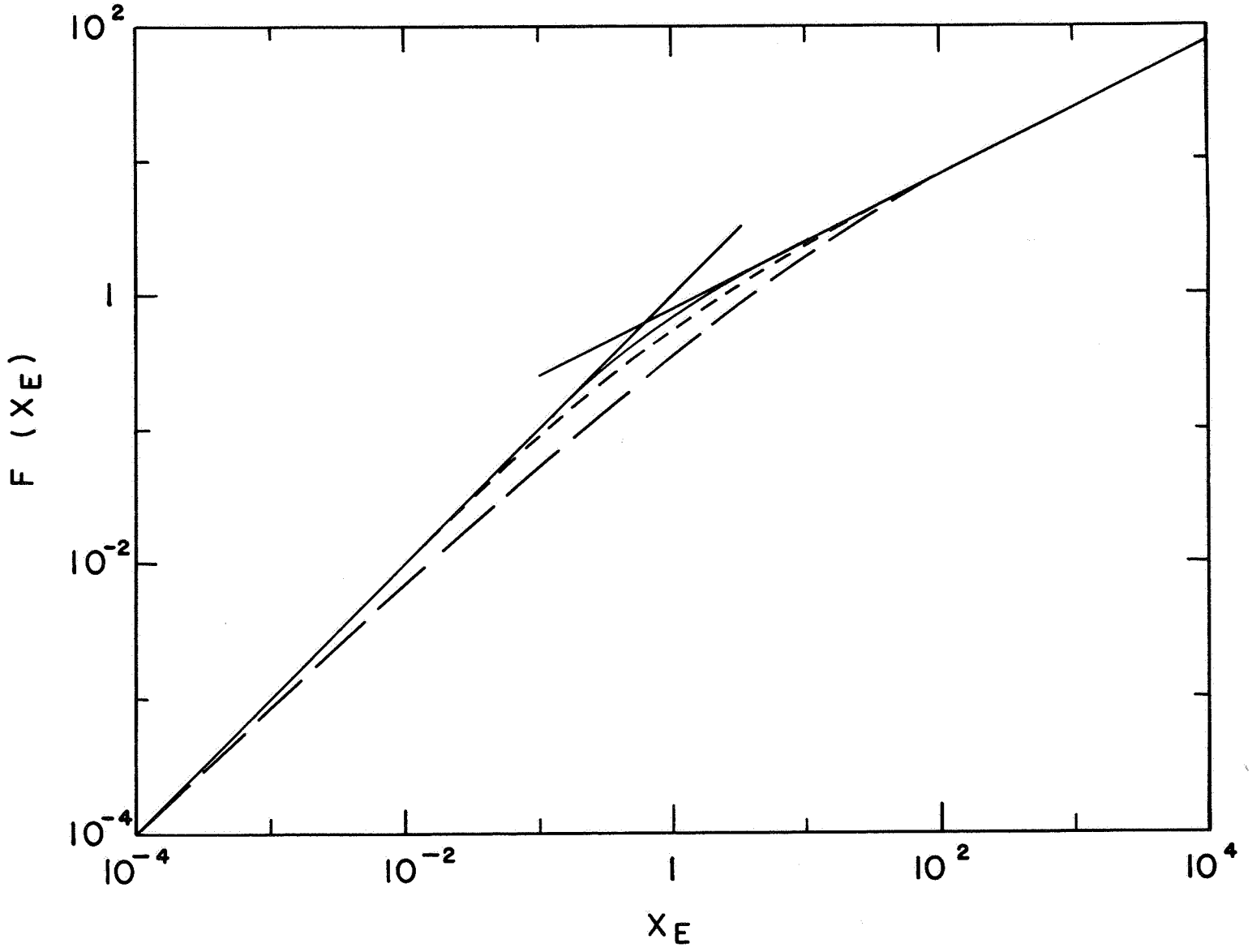

Fig. 44. Curves of growth for random Lorentz band models. Solid line: $P(S) = \delta(S-S_E)$. Dotted line: $P(S) \propto S^{-1} \exp(-S/\pi S_E)$. Dashed line: $P(S) \propto S^{-2} [(S_M+S) \exp(-S/S_M)-(S_M-RS) \exp(-RS/S_M)]$ for $R = 10^6$.

TABLE. I

ABSORPTION COEFFICIENTS OF H2O

K (PER CM AT STP)

1/CM	300 K	600 K	1000 K	1500 K	2000 K	2500 K	3000 K
50.	.950E 00	.103E 00	.420E-01	.114E-01	.450E-02	.300E-02	.190E-02
75.	.208E 01	.365E 00	.113E 00	.375E-01	.195E-01	.134E-01	.670E-02
100.	.386E 01	.990E 00	.300E 00	.104E 00	.577E-01	.365E-01	.211E-01
125.	.650E 01	.201E 01	.650E 00	.214E 00	.128E 00	.845E-01	.529E-01
150.	.825E 01	.325E 01	.121E 01	.415E 00	.260E 00	.168E 00	.109E 00
175.	.870E 01	.452E 01	.189E 01	.765E 00	.450E 00	.289E 00	.193E 00
200.	.810E 01	.540E 01	.261E 01	.126E 01	.695E 00	.460E 00	.309E 00
225.	.682E 01	.600E 01	.337E 01	.179E 01	.101E 01	.679E 00	.454E 00
250.	.493E 01	.622E 01	.407E 01	.230E 01	.135E 01	.935E 00	.620E 00
275.	.316E 01	.592E 01	.456E 01	.281E 01	.172E 01	.122E 01	.822E 00
300.	.199E 01	.528E 01	.479E 01	.328E 01	.213E 01	.149E 01	.104E 01
325.	.113E 01	.450E 01	.484E 01	.361E 01	.249E 01	.179E 01	.128E 01
350.	.585E 00	.370E 01	.471E 01	.383E 01	.284E 01	.208E 01	.154E 01
375.	.293E 00	.289E 01	.443E 01	.394E 01	.312E 01	.237E 01	.182E 01
400.	.138E 00	.205E 01	.400E 01	.396E 01	.330E 01	.260E 01	.207E 01
425.	.620E-01	.143E 01	.347E 01	.388E 01	.341E 01	.280E 01	.229E 01
450.	.255E-01	.950E 00	.292E 01	.370E 01	.345E 01	.295E 01	.248E 01
475.	.940E-02	.610E 00	.236E 01	.343E 01	.342E 01	.304E 01	.262E 01
500.	.340E-02	.386E 00	.188E 01	.310E 01	.334E 01	.309E 01	.273E 01
525.	.105E-02	.236E 00	.145E 01	.274E 01	.319E 01	.307E 01	.280E 01
550.	.350E-03	.144E 00	.110E 01	.238E 01	.300E 01	.301E 01	.283E 01
575.	.126E-03	.820E-01	.818E 00	.204E 01	.276E 01	.289E 01	.282E 01
600.	.430E-04	.445E-01	.598E 00	.174E 01	.248E 01	.275E 01	.277E 01
625.	.150E-04	.242E-01	.427E 00	.145E 01	.222E 01	.260E 01	.269E 01
650.	.510E-05	.127E-01	.294E 00	.118E 01	.195E 01	.241E 01	.258E 01
675.	.170E-05	.630E-02	.200E 00	.950E 00	.169E 01	.221E 01	.245E 01
700.	.570E-06	.300E-02	.134E 00	.748E 00	.146E 01	.200E 01	.229E 01
725.	.195E-06	.140E-02	.902E-01	.580E 00	.124E 01	.178E 01	.213E 01

TABLE I (CONT.D)

ABSORPTION COEFFICIENTS OF H2O
K (PER CM AT STP)

1/CM	300 K	600 K	1000 K	1500 K	2000 K	2500 K	3000 K
750.	.680E-07	.620E-03	.590E-01	.443E 00	.103E 01	.156E 01	.196E 01
775.	.385E-07	.275E-03	.450E-01	.330E 00	.845E 00	.136E 01	.177E 01
800.	.670E-07	.113E-03	.355E-01	.242E 00	.695E 00	.117E 01	.159E 01
825.	.113E-06	.500E-04	.289E-01	.174E 00	.560E 00	.100E 01	.143E 01
850.	.195E-06	.230E-04	.245E-01	.123E 00	.450E 00	.855E 00	.126E 01
875.	.328E-06	.103E-04	.214E-01	.100E 00	.357E 00	.718E 00	.111E 01
900.	.560E-06	.460E-05	.189E-01	.830E-01	.278E 00	.595E 00	.955E 00
925.	.950E-06	.205E-05	.174E-01	.730E-01	.239E 00	.492E 00	.825E 00
950.	.160E-05	.140E-05	.166E-01	.665E-01	.211E 00	.405E 00	.705E 00
975.	.275E-05	.350E-05	.165E-01	.630E-01	.195E 00	.352E 00	.600E 00
1000.	.470E-05	.850E-05	.167E-01	.620E-01	.190E 00	.312E 00	.510E 00
1025.	.810E-05	.215E-04	.175E-01	.630E-01	.191E 00	.289E 00	.425E 00
1050.	.136E-04	.570E-04	.188E-01	.675E-01	.194E 00	.281E 00	.358E 00
1075.	.235E-04	.150E-03	.208E-01	.745E-01	.202E 00	.283E 00	.329E 00
1100.	.400E-04	.380E-03	.233E-01	.865E-01	.223E 00	.314E 00	.357E 00
1125.	.680E-04	.950E-03	.268E-01	.122E 00	.260E 00	.380E 00	.449E 00
1150.	.120E-03	.245E-02	.343E-01	.176E 00	.328E 00	.461E 00	.507E 00
1175.	.200E-03	.620E-02	.638E-01	.251E 00	.411E 00	.511E 00	.5685 00
1200.	.365E-03	.148E-01	.107E 00	.330E 00	.458E 00	.542E 00	.604E 00
1225.	.680E-03	.330E-01	.166E 00	.405E 00	.487E 00	.571E 00	.632E 00
1250.	.130E-02	.635E-01	.244E 00	.459E 00	.535E 00	.557E 00	.637E 00
1275.	.250E-02	.123E 00	.341E 00	.477E 00	.502E 00	.562E 00	.608E 00
1300.	.500E-02	.212E 00	.407E 00	.547E 00	.531E 00	.514E 00	.578E 00
1325.	.103E-01	.285E 00	.489E 00	.592E 00	.497E 00	.486E 00	.554E 00
1350.	.219E-01	.328E 00	.491E 00	.558E 00	.489E 00	.485E 00	.537E 00
1375.	.485E-01	.345E 00	.505E 00	.521E 00	.477E 00	.484E 00	.520E 00
1400.	.114E 00	.361E 00	.538E 00	.563E 00	.503E 00	.502E 00	.516E 00
1425.	.249E 00	.460E 00	.621E 00	.624E 00	.538E 00	.538E 00	.514E 00
1450.	.397E 00	.569E 00	.749E 00	.768E 00	.581E 00	.565E 00	.518E 00
1475.	.418E 00	.627E 00	.824E 00	.849E 00	.640E 00	.594E 00	.530E 00

TABLE I (CONT.D)

ABSORPTION COEFFICIENTS OF H2O
K (PER CM AT STP)

1/CM	300 K	600 K	1000 K	1500 K	2000 K	2500 K	3000 K
1500.	.108E 01	.125E 01	.113E 01	.940E 00	.807E 00	.663E 00	.525E 00
1525.	.165E 01	.155E 01	.118E 01	.670E 00	.562E 00	.483E 00	.430E 00
1550.	.142E 01	.675E 00	.557E 00	.349E 00	.276E 00	.263E 00	.277E 00
1575.	.451E 00	.202E 00	.132E 00	.118E 00	.134E 00	.156E 00	.173E 00
1600.	.603E-01	.538E-01	.863E-01	.112E 00	.120E 00	.125E 00	.125E 00
1625.	.501E 00	.252E 00	.118E 00	.112E 00	.131E 00	.140E 00	.140E 00
1650.	.730E 00	.430E 00	.237E 00	.191E 00	.171E 00	.170E 00	.170E 00
1675.	.149E 01	.506E 00	.294E 00	.238E 00	.210E 00	.201E 00	.202E 00
1700.	.100E 01	.553E 00	.434E 00	.340E 00	.260E 00	.220E 00	.173E 00
1725.	.802E 00	.658E 00	.528E 00	.411E 00	.300E 00	.240E 00	.191E 00
1750.	.580E 00	.527E 00	.460E 00	.378E 00	.322E 00	.283E 00	.240E 00
1775.	.330E 00	.403E 00	.430E 00	.356E 00	.318E 00	.270E 00	.226E 00
1800.	.250E 00	.393E 00	.405E 00	.342E 00	.301E 00	.275E 00	.242E 00
1825.	.147E 00	.249E 00	.313E 00	.318E 00	.291E 00	.268E 00	.250E 00
1850.	.910E-01	.252E 00	.298E 00	.295E 00	.269E 00	.253E 00	.247E 00
1875.	.580E-01	.158E 00	.214E 00	.244E 00	.244E 00	.245E 00	.238E 00
1900.	.370E-01	.113E 00	.184E 00	.218E 00	.214E 00	.218E 00	.222E 00
1925.	.244E-01	.118E 00	.156E 00	.188E 00	.195E 00	.200E 00	.206E 00
1950.	.162E-01	.606E-01	.976E-01	.141E 00	.166E 00	.179E 00	.185E 00
1975.	.112E-01	.425E-01	.903E-01	.133E 00	.148E 00	.156E 00	.166E 00
2000.	.780E-02	.400E-01	.765E-01	.112E 00	.129E 00	.137E 00	.147E 00
2025.	.540E-02	.352E-01	.647E-01	.876E-01	.110E 00	.118E 00	.129E 00
2050.	.380E-02	.252E-01	.507E-01	.705E-01	.888E-01	.100E 00	.111E 00
2075.	.260E-02	.179E-01	.377E-01	.546E-01	.724E-01	.828E-01	.960E-01
2100.	.180E-02	.123E-01	.294E-01	.443E-01	.608E-01	.686E-01	.840E-01
2125.	.127E-02	.850E-02	.212E-01	.378E-01	.579E-01	.640E-01	.725E-01
2150.	.880E-03	.680E-02	.152E-01	.275E-01	.449E-01	.521E-01	.628E-01
2175.	.620E-03	.400E-02	.107E-01	.214E-01	.374E-01	.453E-01	.530E-01
2200.	.480E-03	.298E-02	.931E-02	.189E-01	.329E-01	.403E-01	.455E-01
2225.	.405E-03	.175E-02	.696E-02	.152E-01	.295E-01	.365E-01	.398E-01

TABLE I '(CONT.D)

ABSORPTION COEFFICIENTS OF H2O
K (PER CM AT STP)

1/CM	300 K	600 K	1000 K	1500 K	2000 K	2500 K	3000 K
2250.	.321E-03	.120E-02	.452E-02	.101E-01	.252E-01	.331E-01	.350E-01
2275.	.229E-03	.721E-03	.364E-02	.930E-02	.225E-01	.305E-01	.312E-01
2300.	.195E-03	.544E-03	.318E-02	.750E-02	.202E-01	.284E-01	.290E-01
2325.	.154E-03	.375E-03	.185E-02	.603E-02	.175E-01	.269E-01	.275E-01
2350.	.101E-03	.263E-03	.119E-02	.480E-02	.156E-01	.253E-01	.267E-01
2375.	.852E-04	.185E-03	.909E-03	.360E-02	.133E-01	.241E-01	.259E-01
2400.	.763E-04	.137E-03	.711E-03	.316E-02	.122E-01	.237E-01	.252E-01
2425.	.615E-04	.126E-03	.610E-03	.257E-02	.101E-01	.218E-01	.251E-01
2450.	.480E-04	.113E-03	.518E-03	.201E-02	.920E-02	.200E-01	.249E-01
2475.	.372E-04	.106E-03	.435E-03	.168E-02	.785E-02	.183E-01	.247E-01
2500.	.355E-04	.101E-03	.376E-03	.168E-02	.669E-02	.166E-01	.248E-01
2525.	.358E-04	.990E-04	.366E-03	.167E-02	.651E-02	.156E-01	.249E-01
2550.	.389E-04	.102E-03	.376E-03	.167E-02	.641E-02	.152E-01	.251E-01
2575.	.422E-04	.106E-03	.373E-03	.168E-02	.656E-02	.150E-01	.253E-01
2600.	.521E-04	.111E-03	.371E-03	.170E-02	.673E-02	.152E-01	.258E-01
2625.	.646E-04	.121E-03	.384E-03	.179E-02	.798E-02	.179E-01	.263E-01
2650.	.742E-04	.129E-03	.479E-03	.201E-02	.788E-02	.175E-01	.270E-01
2675.	.953E-04	.165E-03	.544E-03	.249E-02	.945E-02	.204E-01	.280E-01
2700.	.101E-03	.190E-03	.761E-03	.324E-02	.106E-01	.231E-01	.295E-01
2725.	.147E-03	.272E-03	.892E-03	.441E-02	.125E-01	.257E-01	.318E-01
2750.	.195E-03	.326E-03	.100E-02	.499E-02	.147E-01	.295E-01	.343E-01
2775.	.261E-03	.421E-03	.145E-02	.568E-02	.161E-01	.306E-01	.378E-01
2800.	.305E-03	.515E-03	.195E-02	.754E-02	.185E-01	.363E-01	.417E-01
2825.	.362E-03	.645E-03	.237E-02	.830E-02	.205E-01	.373E-01	.459E-01
2850.	.507E-03	.850E-03	.274E-02	.888E-02	.234E-01	.431E-01	.500E-01
2875.	.799E-03	.118E-02	.322E-02	.110E-01	.262E-01	.451E-01	.550E-01
2900.	.935E-03	.160E-02	.386E-02	.126E-01	.292E-01	.530E-01	.602E-01
2925.	.108E-02	.231E-02	.451E-02	.140E-01	.306E-01	.536E-01	.665E-01
2950.	.192E-02	.271E-02	.563E-02	.159E-01	.357E-01	.629E-01	.735E-01
2975.	.263E-02	.300E-02	.625E-02	.179E-01	.385E-01	.666E-01	.801E-01

TABLE I (CONT.D)

ABSORPTION COEFFICIENTS OF H2O
K (PER CM AT STP)

1/CM	300 K	600 K	1000 K	1500 K	2000 K	2500 K	3000 K
3000.	.295E-02	.330E-02	.701E-02	.203E-01	.460E-01	.782E-01	.885E-01
3025.	.310E-02	.370E-02	.846E-02	.220E-01	.519E-01	.889E-01	.970E-01
3050.	.340E-02	.400E-02	.969E-02	.279E-01	.662E-01	.109E 00	.106E 00
3075.	.730E-02	.450E-02	.111E-01	.272E-01	.676E-01	.109E 00	.117E 00
3100.	.900E-02	.480E-02	.137E-01	.372E-01	.864E-01	.133E 00	.129E 00
3125.	.100E-02	.510E-02	.162E-01	.471E-01	.100E 00	.142E 00	.142E 00
3150.	.640E-03	.550E-02	.205E-01	.530E-01	.122E 00	.168E 00	.155E 00
3175.	.160E-02	.600E-02	.247E-01	.633E-01	.135E 00	.177E 00	.170E 00
3200.	.330E-02	.700E-02	.283E-01	.770E-01	.153E 00	.185E 00	.187E 00
3225.	.410E-02	.860E-02	.376E-01	.914E-01	.166E 00	.206E 00	.202E 00
3250.	.410E-02	.103E-01	.514E-01	.117E 00	.194E 00	.228E 00	.220E 00
3275.	.290E-02	.129E-01	.664E-01	.147E 00	.220E 00	.254E 00	.241E 00
3300.	.220E-02	.161E-01	.834E-01	.171E 00	.237E 00	.263E 00	.262E 00
3325.	.220E-02	.212E-01	.103E 00	.201E 00	.268E 00	.283E 00	.280E 00
3350.	.250E-02	.285E-01	.135E 00	.240E 00	.295E 00	.295E 00	.293E 00
3375.	.310E-02	.385E-01	.169E 00	.272E 00	.312E 00	.301E 00	.302E 00
3400.	.420E-02	.540E-01	.214E 00	.309E 00	.329E 00	.307E 00	.308E 00
3425.	.600E-02	.770E-01	.267E 00	.343E 00	.332E 00	.314E 00	.300E 00
3450.	.940E-02	.117E 00	.333E 00	.372E 00	.344E 00	.303E 00	.290E 00
3475.	.165E-01	.173E 00	.365E 00	.385E 00	.353E 00	.300E 00	.272E 00
3500.	.360E-01	.258E 00	.438E 00	.393E 00	.315E 00	.288E 00	.265E 00
3525.	.720E-01	.375E 00	.510E 00	.409E 00	.294E 00	.271E 00	.241E 00
3550.	.133E 00	.401E 00	.499E 00	.390E 00	.281E 00	.257E 00	.222E 00
3575.	.215E 00	.500E 00	.443E 00	.341E 00	.254E 00	.230E 00	.208E 00
3600.	.318E 00	.450E 00	.346E 00	.286E 00	.245E 00	.219E 00	.201E 00
3625.	.442E 00	.400E 00	.354E 00	.279E 00	.233E 00	.216E 00	.210E 00
3650.	.473E 00	.405E 00	.347E 00	.281E 00	.238E 00	.219E 00	.213E 00
3675.	.568E 00	.501E 00	.423E 00	.315E 00	.243E 00	.218E 00	.200E 00
3700.	.690E 00	.708E 00	.673E 00	.432E 00	.268E 00	.189E 00	.150E 00
3725.	.617E 00	.831E 00	.566E 00	.320E 00	.194E 00	.123E 00	.113E 00

TABLE I (CONT.D)

ABSORPTION COEFFICIENTS OF H2O
K (PER CM AT STP)

1/CM	300 K	600 K	1000 K	1500 K	2000 K	2500 K	3000 K
3750.	.181E 01	.520E 00	.200E 00	.131E 00	.124E 00	.107E 00	.108E 00
3775.	.136E 00	.124E 00	.120E 00	.119E 00	.115E 00	.115E 00	.109E 00
3800.	.455E 00	.298E 00	.167E 00	.129E 00	.123E 00	.112E 00	.122E 00
3825.	.760E 00	.503E 00	.242E 00	.154E 00	.129E 00	.127E 00	.136E 00
3850.	.836E 00	.584E 00	.277E 00	.184E 00	.161E 00	.145E 00	.154E 00
3875.	.840E 00	.728E 00	.422E 00	.236E 00	.197E 00	.167E 00	.177E 00
3900.	.505E 00	.500E 00	.379E 00	.276E 00	.227E 00	.192E 00	.197E 00
3925.	.117E 00	.400E 00	.423E 00	.315E 00	.243E 00	.202E 00	.209E 00
3950.	.460E-01	.300E 00	.358E 00	.290E 00	.230E 00	.202E 00	.207E 00
3975.	.183E-01	.205E 00	.269E 00	.235E 00	.195E 00	.192E 00	.190E 00
4000.	.730E-02	.135E 00	.186E 00	.179E 00	.159E 00	.168E 00	.161E 00
4025.	.557E-02	.790E-01	.113E 00	.124E 00	.124E 00	.134E 00	.132E 00
4050.	.283E-02	.415E-01	.662E-01	.886E-01	.103E 00	.106E 00	.104E 00
4075.	.226E-02	.197E-01	.367E-01	.594E-01	.801E-01	.879E-01	.860E-01
4100.	.155E-02	.860E-02	.211E-01	.395E-01	.503E-01	.610E-01	.710E-01
4125.	.103E-02	.521E-02	.119E-01	.246E-01	.354E-01	.480E-01	.598E-01
4150.	.821E-03	.365E-02	.759E-02	.166E-01	.258E-01	.370E-01	.499E-01
4175.	.752E-03	.183E-02	.445E-02	.100E-01	.179E-01	.268E-01	.418E-01
4200.	.429E-03	.141E-02	.354E-02	.821E-02	.142E-01	.212E-01	.348E-01
4225.	.327E-03	.902E-03	.209E-02	.588E-02	.112E-01	.172E-01	.287E-01
4250.	.225E-03	.685E-03	.189E-02	.512E-02	.101E-01	.164E-01	.236E-01
4275.	.186E-03	.551E-03	.156E-02	.366E-02	.812E-02	.136E-01	.189E-01
4300.	.173E-03	.472E-03	.139E-02	.306E-02	.661E-02	.115E-01	.150E-01
4325.	.138E-03	.395E-03	.110E-02	.272E-02	.587E-02	.104E-01	.126E-01
4350.	.900E-04	.270E-03	.968E-03	.222E-02	.497E-02	.921E-02	.119E-01
4375.	.752E-04	.233E-03	.744E-03	.208E-02	.466E-02	.876E-02	.118E-01
4400.	.618E-04	.175E-03	.638E-03	.185E-02	.465E-02	.914E-02	.123E-01
4425.	.504E-04	.134E-03	.499E-03	.174E-02	.455E-02	.935E-02	.128E-01
4450.	.375E-04	.123E-03	.485E-03	.182E-02	.456E-02	.971E-02	.134E-01
4475.	.305E-04	.892E-04	.338E-03	.134E-02	.460E-02	.104E-01	.142E-01

TABLE I (CONT.D)

ABSORPTION COEFFICIENTS OF H2O
K (PER CM AT STP)

1/CM	300 K	600 K	1000 K	1500 K	2000 K	2500 K	3000 K
4500.	.257E-04	.790E-04	.329E-03	.154E-02	.477E-02	.112E-01	.151E-01
4525.	.242E-04	.740E-04	.308E-03	.135E-02	.497E-02	.122E-01	.162E-01
4550.	.215E-04	.653E-04	.282E-03	.131E-02	.521E-02	.133E-01	.173E-01
4575.	.218E-04	.660E-04	.272E-03	.152E-02	.573E-02	.148E-01	.187E-01
4600.	.215E-04	.671E-04	.268E-03	.134E-02	.607E-02	.159E-01	.202E-01
4625.	.217E-04	.695E-04	.285E-03	.161E-02	.677E-02	.173E-01	.223E-01
4650.	.219E-04	.722E-04	.297E-03	.169E-02	.783E-02	.197E-01	.246E-01
4675.	.226E-04	.771E-04	.341E-03	.236E-02	.925E-02	.226E-01	.270E-01
4700.	.250E-04	.815E-04	.387E-03	.286E-02	.106E-01	.250E-01	.300E-01
4725.	.280E-04	.845E-04	.420E-03	.357E-02	.124E-01	.276E-01	.338E-01
4750.	.351E-04	.192E-03	.470E-03	.467E-02	.166E-01	.313E-01	.370E-01
4775.	.435E-04	.200E-03	.105E-02	.566E-02	.185E-01	.341E-01	.399E-01
4800.	.522E-04	.233E-03	.129E-02	.736E-02	.229E-01	.378E-01	.422E-01
4825.	.673E-04	.306E-03	.183E-02	.982E-02	.258E-01	.404E-01	.440E-01
4850.	.886E-04	.399E-03	.246E-02	.128E-01	.302E-01	.430E-01	.458E-01
4875.	.113E-03	.618E-03	.346E-02	.161E-01	.358E-01	.459E-01	.465E-01
4900.	.174E-03	.825E-03	.441E-02	.200E-01	.417E-01	.493E-01	.473E-01
4925.	.265E-03	.163E-02	.777E-02	.245E-01	.450E-01	.507E-01	.478E-01
4950.	.355E-03	.200E-02	.978E-02	.317E-01	.492E-01	.527E-01	.478E-01
4975.	.538E-03	.271E-02	.167E-01	.401E-01	.503E-01	.523E-01	.473E-01
5000.	.651E-03	.301E-02	.264E-01	.467E-01	.520E-01	.526E-01	.460E-01
5025.	.987E-03	.530E-02	.321E-01	.499E-01	.523E-01	.510E-01	.447E-01
5050.	.135E-02	.860E-02	.389E-01	.528E-01	.513E-01	.492E-01	.430E-01
5075.	.226E-02	.130E-01	.472E-01	.559E-01	.500E-01	.469E-01	.415E-01
5100.	.431E-02	.198E-01	.526E-01	.557E-01	.480E-01	.452E-01	.400E-01
5125.	.628E-02	.282E-01	.488E-01	.495E-01	.451E-01	.430E-01	.390E-01
5150.	.900E-02	.390E-01	.471E-01	.449E-01	.430E-01	.423E-01	.385E-01
5175.	.180E-01	.462E-01	.412E-01	.391E-01	.403E-01	.415E-01	.393E-01
5200.	.348E-01	.710E-01	.402E-01	.360E-01	.384E-01	.414E-01	.405E-01
5225.	.718E-01	.590E-01	.399E-01	.360E-01	.376E-01	.420E-01	.418E-01

TABLE I (CONT.D)

ABSORPTION COEFFICIENTS OF H2O
K (PER CM AT STP)

1/CM	300 K	600 K	1000 K	1500 K	2000 K	2500 K	3000 K
5250.	.111E 00	.368E-01	.340E-01	.369E-01	.409E-01	.454E-01	.434E-01
5275.	.329E-01	.285E-01	.365E-01	.423E-01	.461E-01	.482E-01	.450E-01
5300.	.281E-01	.270E-01	.432E-01	.505E-01	.529E-01	.511E-01	.462E-01
5325.	.121E 00	.422E-01	.589E-01	.598E-01	.572E-01	.544E-01	.470E-01
5350.	.139E 00	.105E 00	.844E-01	.687E-01	.593E-01	.560E-01	.480E-01
5375.	.774E-01	.710E-01	.683E-01	.618E-01	.556E-01	.534E-01	.478E-01
5400.	.858E-01	.483E-01	.579E-01	.547E-01	.503E-01	.495E-01	.460E-01
5425.	.985E-01	.575E-01	.589E-01	.510E-01	.451E-01	.449E-01	.425E-01
5450.	.996E-01	.682E-01	.539E-01	.489E-01	.454E-01	.446E-01	.400E-01
5475.	.680E-01	.680E-01	.548E-01	.495E-01	.460E-01	.458E-01	.405E-01
5500.	.325E-01	.520E-01	.515E-01	.483E-01	.449E-01	.454E-01	.418E-01
5525.	.150E-01	.350E-01	.451E-01	.464E-01	.452E-01	.449E-01	.438E-01
5550.	.620E-02	.238E-01	.369E-01	.408E-01	.414E-01	.417E-01	.420E-01
5575.	.270E-02	.158E-01	.282E-01	.339E-01	.366E-01	.384E-01	.400E-01
5600.	.113E-02	.101E-01	.203E-01	.263E-01	.303E-01	.333E-01	.360E-01
5625.	.829E-03	.590E-02	.148E-01	.206E-01	.247E-01	.295E-01	.320E-01
5650.	.365E-03	.310E-02	.969E-02	.154E-01	.203E-01	.258E-01	.280E-01
5675.	.240E-03	.130E-02	.589E-02	.112E-01	.164E-01	.222E-01	.250E-01
5700.	.158E-03	.400E-03	.417E-02	.850E-02	.134E-01	.190E-01	.220E-01
5725.	.103E-03	.262E-03	.208E-02	.594E-02	.109E-01	.162E-01	.190E-01
5750.	.741E-04	.181E-03	.142E-02	.455E-02	.907E-02	.141E-01	.170E-01
5775.	.625E-04	.135E-03	.816E-03	.316E-02	.698E-02	.121E-01	.150E-01
5800.	.499E-04	.111E-03	.624E-03	.230E-02	.551E-02	.102E-01	.130E-01
5825.	.325E-04	.677E-04	.425E-03	.124E-02	.385E-02	.818E-02	.120E-01
5850.	.231E-04	.563E-04	.278E-03	.986E-03	.290E-02	.672E-02	.105E-01
5875.	.165E-04	.481E-04	.247E-03	.944E-03	.253E-02	.612E-02	.980E-02
5900.	.126E-04	.432E-04	.241E-03	.886E-03	.220E-02	.582E-02	.940E-02
5925.	.118E-04	.420E-04	.235E-03	.847E-03	.209E-02	.571E-02	.930E-02
5950.	.110E-04	.408E-04	.226E-03	.812E-03	.221E-02	.604E-02	.925E-02
5975.	.101E-04	.400E-04	.213E-03	.805E-03	.239E-02	.641E-02	.930E-02

TABLE I (CONT.D)

ABSORPTION COEFFICIENTS OF H2O
K (PER CM AT STP)

1/CM	300 K	600 K	1000 K	1500 K	2000 K	2500 K	3000 K
6000.	.983E-05	.395E-04	.186E-03	.801E-03	.247E-02	.691E-02	.950E-02
6025.	.979E-05	.401E-04	.193E-03	.805E-03	.260E-02	.732E-02	.970E-02
6050.	.976E-05	.410E-04	.201E-03	.814E-03	.285E-02	.776E-02	.100E-01
6075.	.988E-05	.420E-04	.210E-03	.832E-03	.317E-02	.842E-02	.103E-01
6100.	.991E-05	.425E-04	.219E-03	.877E-03	.340E-02	.888E-02	.105E-01
6125.	.102E-04	.435E-04	.231E-03	.937E-03	.361E-02	.929E-02	.110E-01
6150.	.110E-04	.486E-04	.244E-03	.971E-03	.402E-02	.994E-02	.113E-01
6175.	.127E-04	.579E-04	.257E-03	.111E-02	.437E-02	.104E-01	.119E-01
6200.	.131E-04	.612E-04	.277E-03	.113E-02	.465E-02	.110E-01	.125E-01
6225.	.150E-04	.783E-04	.353E-03	.116E-02	.510E-02	.116E-01	.130E-01
6250.	.178E-04	.922E-04	.394E-03	.157E-02	.555E-02	.123E-01	.135E-01
6275.	.203E-04	.115E-03	.481E-03	.188E-02	.601E-02	.131E-01	.143E-01
6300.	.230E-04	.145E-03	.617E-03	.183E-02	.644E-02	.139E-01	.150E-01
6325.	.280E-04	.187E-03	.723E-03	.202E-02	.686E-02	.146E-01	.157E-01
6350.	.305E-04	.209E-03	.811E-03	.243E-02	.779E-02	.157E-01	.164E-01
6375.	.455E-04	.244E-03	.935E-03	.243E-02	.844E-02	.166E-01	.172E-01
6400.	.661E-04	.320E-03	.989E-03	.288E-02	.902E-02	.173E-01	.180E-01
6425.	.723E-04	.397E-03	.122E-02	.359E-02	.100E-01	.184E-01	.191E-01
6450.	.847E-04	.481E-03	.143E-02	.429E-02	.108E-01	.192E-01	.200E-01
6475.	.103E-03	.591E-03	.174E-02	.488E-02	.116E-01	.200E-01	.211E-01
6500.	.131E-03	.703E-03	.217E-02	.549E-02	.124E-01	.205E-01	.222E-01
6525.	.165E-03	.872E-03	.265E-02	.641E-02	.131E-01	.211E-01	.233E-01
6550.	.205E-03	.110E-02	.298E-02	.749E-02	.140E-01	.218E-01	.244E-01
6575.	.253E-03	.130E-02	.346E-02	.811E-02	.150E-01	.230E-01	.255E-01
6600.	.338E-03	.150E-02	.445E-02	.890E-02	.159E-01	.237E-01	.267E-01
6625.	.437E-03	.170E-02	.491E-02	.107E-01	.170E-01	.245E-01	.276E-01
6650.	.581E-03	.190E-02	.537E-02	.116E-01	.179E-01	.254E-01	.287E-01
6675.	.685E-03	.220E-02	.578E-02	.128E-01	.189E-01	.263E-01	.296E-01
6700.	.900E-03	.250E-02	.649E-02	.134E-01	.195E-01	.275E-01	.305E-01
6725.	.121E-02	.280E-02	.722E-02	.142E-01	.202E-01	.281E-01	.313E-01

TABLE I (CONT.D)

ABSORPTION COEFFICIENTS OF H2O
K (PER CM AT STP)

1/CM	300 K	600 K	1000 K	1500 K	2000 K	2500 K	3000 K
6750.	.152E-02	.330E-02	.813E-02	.161E-01	.212E-01	.288E-01	.320E-01
6775.	.185E-02	.370E-02	.907E-02	.168E-01	.222E-01	.292E-01	.329E-01
6800.	.220E-02	.430E-02	.929E-02	.183E-01	.233E-01	.294E-01	.335E-01
6825.	.255E-02	.500E-02	.114E-01	.195E-01	.245E-01	.289E-01	.339E-01
6850.	.290E-02	.580E-02	.167E-01	.215E-01	.260E-01	.291E-01	.343E-01
6875.	.320E-02	.670E-02	.208E-01	.237E-01	.274E-01	.293E-01	.345E-01
6900.	.360E-02	.880E-02	.220E-01	.253E-01	.282E-01	.300E-01	.343E-01
6925.	.400E-02	.920E-02	.238E-01	.273E-01	.290E-01	.304E-01	.341E-01
6950.	.460E-02	.108E-01	.272E-01	.279E-01	.298E-01	.310E-01	.339E-01
6975.	.530E-02	.128E-01	.304E-01	.292E-01	.297E-01	.312E-01	.333E-01
7000.	.620E-02	.152E-01	.344E-01	.303E-01	.293E-01	.310E-01	.325E-01
7025.	.760E-02	.182E-01	.341E-01	.297E-01	.290E-01	.300E-01	.313E-01
7050.	.980E-02	.222E-01	.398E-01	.318E-01	.291E-01	.294E-01	.299E-01
7075.	.132E-01	.271E-01	.402E-01	.294E-01	.274E-01	.282E-01	.283E-01
7100.	.190E-01	.335E-01	.421E-01	.286E-01	.262E-01	.269E-01	.263E-01
7125.	.240E-01	.432E-01	.431E-01	.276E-01	.245E-01	.257E-01	.243E-01
7150.	.288E-01	.570E-01	.458E-01	.270E-01	.228E-01	.243E-01	.223E-01
7175.	.323E-01	.740E-01	.449E-01	.261E-01	.214E-01	.221E-01	.208E-01
7200.	.570E-01	.890E-01	.435E-01	.255E-01	.199E-01	.196E-01	.199E-01
7225.	.216E-01	.680E-01	.378E-01	.239E-01	.195E-01	.192E-01	.190E-01
7250.	.126E-01	.475E-01	.364E-01	.238E-01	.197E-01	.192E-01	.187E-01
7275.	.117E-01	.369E-01	.385E-01	.249E-01	.212E-01	.204E-01	.200E-01
7300.	.140E-01	.370E-01	.419E-01	.272E-01	.228E-01	.213E-01	.224E-01
7325.	.425E-01	.418E-01	.440E-01	.280E-01	.248E-01	.229E-01	.243E-01
7350.	.640E-01	.460E-01	.427E-01	.290E-01	.263E-01	.238E-01	.260E-01
7375.	.385E-01	.385E-01	.374E-01	.259E-01	.235E-01	.224E-01	.260E-01
7400.	.182E-01	.179E-01	.282E-01	.231E-01	.211E-01	.214E-01	.240E-01
7425.	.170E-01	.810E-02	.191E-01	.175E-01	.181E-01	.194E-01	.210E-01
7450.	.161E-01	.370E-02	.105E-01	.127E-01	.152E-01	.171E-01	.180E-01
7475.	.145E-01	.170E-02	.554E-02	.855E-02	.113E-01	.131E-01	.150E-01

TABLE I (CONT.D)

ABSORPTION COEFFICIENTS OF H2O
K (PER CM AT STP)

1/CM	300 K	600 K	1000 K	1500 K	2000 K	2500 K	3000 K
7500.	.175E-02	.140E-02	.385E-02	.595E-02	.803E-02	.945E-02	.120E-01
7525.	.772E-03	.751E-03	.384E-02	.575E-02	.537E-02	.594E-02	.800E-02
7550.	.491E-03	.600E-03	.301E-02	.453E-02	.380E-02	.434E-02	.600E-02
7575.	.275E-03	.410E-03	.193E-02	.366E-02	.319E-02	.332E-02	.500E-02
7600.	.185E-03	.280E-03	.131E-02	.232E-02	.247E-02	.256E-02	.420E-02
7625.	.101E-03	.160E-03	.915E-03	.150E-02	.186E-02	.197E-02	.370E-02
7650.	.691E-04	.110E-03	.565E-03	.114E-02	.205E-02	.192E-02	.340E-02
7675.	.476E-04	.750E-04	.114E-02	.124E-02	.175E-02	.187E-02	.320E-02
7700.	.305E-04	.590E-04	.529E-03	.114E-02	.160E-02	.185E-02	.300E-02
7725.	.240E-04	.480E-04	.293E-03	.842E-03	.141E-02	.184E-02	.290E-02
7750.	.170E-04	.360E-04	.122E-03	.435E-03	.124E-02	.182E-02	.290E-02
7775.	.120E-04	.240E-04	.121E-03	.435E-03	.118E-02	.187E-02	.291E-02
7800.	.810E-05	.170E-04	.103E-03	.439E-03	.126E-02	.192E-02	.295E-02
7825.	.550E-05	.120E-04	.866E-04	.367E-03	.119E-02	.193E-02	.300E-02
7850.	.390E-05	.900E-05	.716E-04	.351E-03	.116E-02	.194E-02	.303E-02
7875.	.295E-05	.830E-05	.373E-04	.254E-03	.114E-02	.196E-02	.310E-02
7900.	.230E-05	.800E-05	.465E-04	.298E-03	.117E-02	.201E-02	.320E-02
7925.	.225E-05	.820E-05	.367E-04	.252E-03	.116E-02	.205E-02	.330E-02
7950.	.220E-05	.840E-05	.371E-04	.268E-03	.127E-02	.211E-02	.340E-02
7975.	.223E-05	.920E-05	.396E-04	.273E-03	.128E-02	.216E-02	.355E-02
8000.	.235E-05	.103E-04	.415E-04	.263E-03	.121E-02	.221E-02	.365E-02
8025.	.280E-05	.125E-04	.633E-04	.363E-03	.136E-02	.231E-02	.380E-02
8050.	.310E-05	.150E-04	.979E-04	.492E-03	.150E-02	.241E-02	.400E-02
8075.	.370E-05	.180E-04	.120E-03	.580E-03	.167E-02	.251E-02	.410E-02
8100.	.420E-05	.200E-04	.987E-04	.509E-03	.171E-02	.257E-02	.420E-02
8125.	.510E-05	.240E-04	.134E-03	.547E-03	.173E-02	.267E-02	.440E-02
8150.	.600E-05	.270E-04	.121E-03	.534E-03	.172E-02	.274E-02	.457E-02
8175.	.720E-05	.300E-04	.204E-03	.684E-03	.184E-02	.285E-02	.468E-02
8200.	.820E-05	.330E-04	.276E-03	.819E-03	.199E-02	.297E-02	.479E-02
8225.	.100E-04	.380E-04	.317E-03	.859E-03	.214E-02	.308E-02	.485E-02

TABLE I (CONT.D)

ABSORPTION COEFFICIENTS OF H2O
K (PER CM AT STP)

1/CM	300 K	600 K	1000 K	1500 K	2000 K	2500 K	3000 K
8250.	.125E-04	.420E-04	.240E-03	.818E-03	.220E-02	.317E-02	.490E-02
8275.	.145E-04	.500E-04	.452E-03	.109E-02	.238E-02	.293E-02	.499E-02
8300.	.175E-04	.560E-04	.301E-03	.941E-03	.243E-02	.342E-02	.500E-02
8325.	.198E-04	.630E-04	.280E-03	.107E-02	.260E-02	.353E-02	.501E-02
8350.	.230E-04	.710E-04	.276E-03	.109E-02	.272E-02	.365E-02	.502E-02
8375.	.280E-04	.830E-04	.369E-03	.127E-02	.295E-02	.377E-02	.501E-02
8400.	.330E-04	.890E-04	.430E-03	.139E-02	.306E-02	.385E-02	.500E-02
8425.	.360E-04	.950E-04	.371E-03	.135E-02	.306E-02	.384E-02	.499E-02
8450.	.390E-04	.980E-04	.434E-03	.147E-02	.316E-02	.385E-02	.495E-02
8475.	.400E-04	.990E-04	.397E-03	.143E-02	.318E-02	.384E-02	.490E-02
8500.	.400E-04	.980E-04	.364E-03	.141E-02	.317E-02	.381E-02	.480E-02
8525.	.390E-04	.940E-04	.390E-03	.142E-02	.314E-02	.376E-02	.475E-02
8550.	.380E-04	.900E-04	.380E-03	.145E-02	.318E-02	.375E-02	.463E-02
8575.	.330E-04	.750E-04	.358E-03	.138E-02	.310E-02	.372E-02	.455E-02
8600.	.300E-04	.680E-04	.343E-03	.136E-02	.309E-02	.369E-02	.443E-02
8625.	.270E-04	.580E-04	.382E-03	.143E-02	.315E-02	.369E-02	.433E-02
8650.	.240E-04	.500E-04	.343E-03	.136E-02	.306E-02	.363E-02	.420E-02
8675.	.200E-04	.450E-04	.309E-03	.134E-02	.306E-02	.359E-02	.408E-02
8700.	.180E-04	.400E-04	.281E-03	.127E-02	.294E-02	.341E-02	.395E-02
8725.	.170E-04	.360E-04	.276E-03	.124E-02	.290E-02	.336E-02	.380E-02
8750.	.160E-04	.310E-04	.272E-03	.122E-02	.283E-02	.323E-02	.367E-02
8775.	.140E-04	.280E-04	.241E-03	.117E-02	.273E-02	.309E-02	.351E-02
8800.	.120E-04	.250E-04	.237E-03	.115E-02	.269E-02	.297E-02	.338E-02
8825.	.100E-04	.220E-04	.218E-03	.111E-02	.259E-02	.284E-02	.323E-02
8850.	.920E-05	.198E-04	.206E-03	.105E-02	.246E-02	.269E-02	.310E-02
8875.	.810E-05	.170E-04	.205E-03	.100E-02	.235E-02	.257E-02	.295E-02
8900.	.720E-05	.160E-04	.177E-03	.921E-03	.220E-02	.245E-02	.280E-02
8925.	.650E-05	.150E-04	.172E-03	.834E-03	.205E-02	.232E-02	.268E-02
8950.	.590E-05	.130E-04	.147E-03	.735E-03	.194E-02	.218E-02	.253E-02
8975.	.510E-05	.110E-04	.120E-03	.629E-03	.177E-02	.203E-02	.240E-02

TABLE I (CONT.D)

ABSORPTION COEFFICIENTS OF H2O
K (PER CM AT STP)

1/CM	300 K	600 K	1000 K	1500 K	2000 K	2500 K	3000 K
9000.	.460E-05	.950E-05	.960E-04	.513E-03	.154E-02	.180E-02	.238E-02
9025.	.420E-05	.800E-05	.578E-04	.314E-03	.123E-02	.154E-02	.218E-02
9050.	.380E-05	.720E-05	.529E-04	.292E-03	.114E-02	.137E-02	.207E-02
9075.	.330E-05	.660E-05	.485E-04	.269E-03	.102E-02	.122E-02	.197E-02
9100.	.290E-05	.580E-05	.430E-04	.239E-03	.896E-03	.107E-02	.187E-02
9125.	.270E-05	.520E-05	.259E-04	.193E-03	.784E-03	.944E-03	.179E-02
9150.	.240E-05	.450E-05	.316E-04	.207E-03	.671E-03	.848E-03	.171E-02
9175.	.220E-05	.400E-05	.444E-05	.602E-04	.516E-03	.750E-03	.163E-02
9200.	.190E-05	.360E-05	.324E-05	.460E-04	.439E-03	.688E-03	.156E-02
9225.	.170E-05	.320E-05	.180E-05	.321E-04	.384E-03	.653E-03	.149E-02
9250.	.140E-05	.280E-05	.171E-05	.344E-04	.340E-03	.616E-03	.143E-02
9275.	.130E-05	.250E-05	.299E-05	.600E-04	.343E-03	.619E-03	.138E-02
9300.	.120E-05	.220E-05	.299E-05	.600E-04	.343E-03	.619E-03	.133E-02

TABLE II

FINE STRUCTURE PARAMETER (1/DLR) FOR H2O

1/CM	600 K	1000 K	1500 K	2000 K	2500 K	3000 K
1150.	.439E 00	.983E 00	.293E 01	.110E 02	.442E 02	.205E 03
1175.	.327E 00	.767E 00	.238E 01	.936E 01	.384E 02	.178E 03
1200.	.434E 00	.951E 00	.267E 01	.106E 02	.423E 02	.203E 03
1225.	.440E 00	.969E 00	.270E 01	.107E 02	.431E 02	.203E 03
1250.	.328E 00	.784E 00	.238E 01	.964E 01	.394E 02	.183E 03
1275.	.497E 00	.939E 00	.234E 01	.758E 01	.286E 02	.125E 03
1300.	.296E 00	.717E 00	.226E 01	.909E 01	.378E 02	.176E 03
1325.	.361E 00	.800E 00	.229E 01	.889E 01	.355E 02	.164E 03
1350.	.486E 00	.949E 00	.245E 01	.801E 01	.310E 02	.137E 03
1375.	.403E 00	.869E 00	.239E 01	.730E 01	.239E 02	.854E 02
1400.	.474E 00	.957E 00	.229E 01	.607E 01	.161E 02	.434E 02
1425.	.507E 00	.966E 00	.209E 01	.496E 01	.110E 02	.247E 02
1450.	.260E 00	.642E 00	.165E 01	.459E 01	.101E 02	.195E 02
1475.	.552E 00	.898E 00	.175E 01	.444E 01	.121E 02	.350E 02
1500.	.653E 00	.871E 00	.139E 01	.248E 01	.500E 01	.116E 02
1525.	.377E 00	.773E 00	.182E 01	.354E 01	.758E 01	.126E 02
1550.	.388E 00	.787E 00	.177E 01	.368E 01	.718E 01	.123E 02
1575.	.277E 00	.695E 00	.208E 01	.472E 01	.104E 02	.193E 02
1600.	.341E 00	.781E 00	.227E 01	.657E 01	.209E 02	.631E 02
1625.	.394E 00	.100E 01	.308E 01	.635E 01	.136E 02	.237E 02
1650.	.295E 00	.817E 00	.244E 01	.592E 01	.115E 02	.186E 02
1675.	.258E 00	.712E 00	.216E 01	.534E 01	.108E 02	.188E 02
1700.	.357E 00	.812E 00	.208E 01	.527E 01	.112E 02	.248E 02
1725.	.222E 00	.581E 00	.169E 01	.474E 01	.125E 02	.262E 02
1750.	.340E 00	.794E 00	.213E 01	.534E 01	.129E 02	.276E 02
1775.	.385E 00	.775E 00	.194E 01	.481E 01	.138E 02	.368E 02
1800.	.444E 00	.917E 00	.239E 01	.645E 01	.194E 02	.583E 02
1825.	.358E 00	.758E 00	.200E 01	.550E 01	.165E 02	.492E 02
1850.	.432E 00	.878E 00	.224E 01	.598E 01	.203E 02	.563E 02
1875.	.204E 00	.540E 00	.171E 01	.494E 01	.149E 02	.359E 02

TABLE II (CONT.D)

FINE STRUCTURE PARAMETER (1/DLR) FOR H2O

1/CM	600 K	1000 K	1500 K	2000 K	2500 K	3000 K
1900.	.228E 00	.587E 00	.181E 01	.537E 01	.160E 02	.409E 02
1925.	.306E 00	.693E 00	.196E 01	.541E 01	.143E 02	.415E 02
1950.	.353E 00	.779E 00	.209E 01	.521E 01	.135E 02	.330E 02
1975.	.153E 00	.442E 00	.150E 01	.435E 01	.111E 02	.257E 02
2000.	.170E 00	.446E 00	.141E 01	.389E 01	.981E 01	.244E 02
2025.	.213E 00	.496E 00	.146E 01	.360E 01	.913E 01	.233E 02
2050.	.192E 00	.484E 00	.152E 01	.403E 01	.101E 02	.261E 02
2075.	.217E 00	.551E 00	.175E 01	.447E 01	.115E 02	.281E 02
2100.	.261E 00	.574E 00	.166E 01	.413E 01	.124E 02	.348E 02
2125.	.389E 00	.683E 00	.170E 01	.364E 01	.110E 02	.358E 02
2150.	.421E 00	.128E 01	.273E 01	.495E 01	.168E 02	.654E 02
2175.	.433E 00	.101E 01	.208E 01	.401E 01	.144E 02	.890E 02
2200.	.449E 00	.109E 01	.247E 01	.488E 01	.190E 02	.117E 03
2225.	.462E 00	.113E 01	.267E 01	.532E 01	.209E 02	.125E 03
2250.	.480E 00	.116E 01	.289E 01	.581E 01	.230E 02	.133E 03
2275.	.496E 00	.120E 01	.313E 01	.634E 01	.254E 02	.141E 03
2300.	.522E 00	.124E 01	.338E 01	.691E 01	.279E 02	.151E 03
2325.	.530E 00	.128E 01	.366E 01	.755E 01	.308E 02	.161E 03
2350.	.548E 00	.132E 01	.396E 01	.823E 01	.339E 02	.171E 03
2375.	.565E 00	.137E 01	.428E 01	.898E 01	.374E 02	.182E 03
2400.	.585E 00	.141E 01	.463E 01	.980E 01	.412E 02	.194E 03
2425.	.602E 00	.146E 01	.501E 01	.106E 02	.454E 02	.207E 03
2450.	.625E 00	.151E 01	.542E 01	.116E 02	.500E 02	.221E 03
2475.	.646E 00	.156E 01	.587E 01	.127E 02	.550E 02	.235E 03
2500.	.668E 00	.161E 01	.635E 01	.138E 02	.607E 02	.251E 03
2525.	.690E 00	.166E 01	.686E 01	.151E 02	.668E 02	.267E 03
2550.	.718E 00	.171E 01	.743E 01	.165E 02	.736E 02	.284E 03
2575.	.674E 00	.163E 01	.707E 01	.158E 02	.694E 02	.260E 03
2600.	.632E 00	.156E 01	.673E 01	.152E 02	.654E 02	.237E 03
2625.	.592E 00	.148E 01	.641E 01	.146E 02	.616E 02	.217E 03

TABLE II (CONT.D)

FINE STRUCTURE PARAMETER (1/DLR) FOR H2O

1/CM	600 K	1000 K	1500 K	2000 K	2500 K	3000 K
2650.	.556E 00	.141E 01	.610E 01	.140E 02	.581E 02	.198E 03
2675.	.522E 00	.135E 01	.580E 01	.135E 02	.547E 02	.181E 03
2700.	.489E 00	.128E 01	.553E 01	.129E 02	.516E 02	.165E 03
2725.	.471E 00	.122E 01	.526E 01	.124E 02	.486E 02	.151E 03
2750.	.454E 00	.117E 01	.501E 01	.119E 02	.458E 02	.137E 03
2775.	.438E 00	.113E 01	.477E 01	.114E 02	.432E 02	.125E 03
2800.	.422E 00	.109E 01	.454E 01	.110E 02	.407E 02	.115E 03
2825.	.409E 00	.104E 01	.432E 01	.105E 02	.383E 02	.105E 03
2850.	.393E 00	.100E 01	.411E 01	.101E 02	.361E 02	.960E 02
2875.	.380E 00	.969E 00	.391E 01	.977E 01	.341E 02	.876E 02
2900.	.368E 00	.930E 00	.372E 01	.938E 01	.321E 02	.800E 02
2925.	.355E 00	.895E 00	.354E 01	.901E 01	.302E 02	.730E 02
2950.	.342E 00	.864E 00	.337E 01	.865E 01	.285E 02	.667E 02
2975.	.332E 00	.836E 00	.321E 01	.831E 01	.268E 02	.609E 02
3000.	.320E 00	.805E 00	.306E 01	.798E 01	.253E 02	.556E 02
3025.	.311E 00	.786E 00	.291E 01	.766E 01	.239E 02	.508E 02
3050.	.303E 00	.759E 00	.277E 01	.736E 01	.225E 02	.464E 02
3075.	.294E 00	.736E 00	.264E 01	.707E 01	.212E 02	.424E 02
3100.	.284E 00	.710E 00	.251E 01	.679E 01	.200E 02	.387E 02
3125.	.278E 00	.688E 00	.239E 01	.652E 01	.188E 02	.353E 02
3150.	.270E 00	.675E 00	.227E 01	.626E 01	.177E 02	.323E 02
3175.	.262E 00	.659E 00	.217E 01	.601E 01	.167E 02	.295E 02
3200.	.255E 00	.640E 00	.206E 01	.577E 01	.157E 02	.269E 02
3225.	.249E 00	.625E 00	.196E 01	.554E 01	.148E 02	.246E 02
3250.	.243E 00	.609E 00	.203E 01	.469E 01	.109E 02	.266E 02
3275.	.238E 00	.592E 00	.202E 01	.449E 01	.958E 01	.229E 02
3300.	.232E 00	.580E 00	.191E 01	.462E 01	.966E 01	.173E 02
3325.	.228E 00	.567E 00	.184E 01	.413E 01	.879E 01	.170E 02
3350.	.222E 00	.554E 00	.167E 01	.400E 01	.859E 01	.137E 02
3375.	.217E 00	.542E 00	.172E 01	.396E 01	.841E 01	.136E 02

TABLE II (CONT.D)

FINE STRUCTURE PARAMETER (1/DLR) FOR H2O

1/CM	600 K	1000 K	1500 K	2000 K	2500 K	3000 K
3400.	.214E 00	.533E 00	.159E 01	.384E 01	.817E 01	.124E 02
3425.	.208E 00	.525E 00	.159E 01	.397E 01	.761E 01	.107E 02
3450.	.205E 00	.516E 00	.141E 01	.320E 01	.629E 01	.958E 01
3475.	.201E 00	.509E 00	.141E 01	.318E 01	.643E 01	.101E 02
3500.	.199E 00	.500E 00	.148E 01	.372E 01	.685E 01	.103E 02
3525.	.195E 00	.498E 00	.140E 01	.405E 01	.779E 01	.132E 02
3550.	.178E 00	.491E 00	.145E 01	.406E 01	.809E 01	.159E 02
3575.	.211E 00	.548E 00	.156E 01	.424E 01	.894E 01	.185E 02
3600.	.347E 00	.802E 00	.200E 01	.440E 01	.842E 01	.140E 02
3625.	.256E 00	.695E 00	.189E 01	.421E 01	.717E 01	.941E 01
3650.	.233E 00	.624E 00	.171E 01	.392E 01	.709E 01	.100E 02
3675.	.227E 00	.635E 00	.176E 01	.403E 01	.669E 01	.877E 01
3700.	.162E 00	.448E 00	.133E 01	.342E 01	.742E 01	.129E 02
3725.	.366E 00	.687E 00	.166E 01	.413E 01	.157E 02	.447E 02
3750.	.155E 01	.193E 01	.326E 01	.434E 01	.987E 01	.201E 02
3775.	.843E 00	.112E 01	.179E 01	.337E 01	.652E 01	.158E 02
3800.	.282E 00	.662E 00	.185E 01	.435E 01	.122E 02	.245E 02
3825.	.165E 00	.520E 00	.173E 01	.448E 01	.902E 01	.136E 02
3850.	.340E 00	.700E 00	.188E 01	.387E 01	.824E 01	.126E 02
3875.	.354E 00	.745E 00	.173E 01	.347E 01	.730E 01	.116E 02
3900.	.263E 00	.665E 00	.173E 01	.360E 01	.679E 01	.889E 01
3925.	.184E 00	.530E 00	.154E 01	.360E 01	.710E 01	.930E 01
3950.	.191E 00	.559E 00	.165E 01	.403E 01	.791E 01	.108E 02
3975.	.177E 00	.565E 00	.175E 01	.451E 01	.763E 01	.994E 01
4000.	.169E 00	.552E 00	.179E 01	.484E 01	.804E 01	.116E 02
4025.	.786E-01	.363E 00	.171E 01	.569E 01	.118E 02	.179E 02
4050.	.170E 00	.550E 00	.205E 01	.585E 01	.144E 02	.295E 02
4075.	.191E 00	.556E 00	.198E 01	.516E 01	.122E 02	.277E 02
4100.	.155E 00	.482E 00	.220E 01	.885E 01	.228E 02	.404E 02
4125.	.144E 00	.288E 00	.247E 01	.132E 02	.249E 02	.286E 02

TABLE II (CONT.D)

FINE STRUCTURE PARAMETER (1/DLR) FOR H2O

1/CM	600 K	1000 K	1500 K	2000 K	2500 K	3000 K
4150.	.126E 00	.379E 00	.275E 01	.162E 02	.328E 02	.691E 02
4175.	.121E 00	.432E 00	.306E 01	.179E 02	.376E 02	.794E 02
4200.	.119E 00	.491E 00	.340E 01	.198E 02	.430E 02	.912E 02
4225.	.121E 00	.559E 00	.378E 01	.219E 02	.492E 02	.104E 03
4250.	.124E 00	.635E 00	.421E 01	.242E 02	.563E 02	.120E 03
4275.	.127E 00	.723E 00	.468E 01	.267E 02	.644E 02	.138E 03
4300.	.136E 00	.823E 00	.521E 01	.295E 02	.737E 02	.159E 03
4325.	.158E 00	.936E 00	.580E 01	.326E 02	.843E 02	.182E 03
4350.	.185E 00	.106E 01	.645E 01	.360E 02	.964E 02	.209E 03
4375.	.218E 00	.121E 01	.717E 01	.399E 02	.110E 03	.241E 03
4400.	.256E 00	.137E 01	.798E 01	.440E 02	.126E 03	.277E 03
4425.	.228E 00	.122E 01	.693E 01	.394E 02	.112E 03	.251E 03
4450.	.202E 00	.108E 01	.601E 01	.352E 02	.994E 02	.228E 03
4475.	.180E 00	.957E 00	.522E 01	.314E 02	.882E 02	.207E 03
4500.	.160E 00	.847E 00	.452E 01	.281E 02	.783E 02	.189E 03
4525.	.142E 00	.750E 00	.393E 01	.251E 02	.694E 02	.171E 03
4550.	.126E 00	.664E 00	.341E 01	.225E 02	.616E 02	.156E 03
4575.	.112E 00	.588E 00	.296E 01	.201E 02	.547E 02	.141E 03
4600.	.100E 00	.521E 00	.257E 01	.179E 02	.485E 02	.128E 03
4625.	.893E-01	.461E 00	.223E 01	.160E 02	.430E 02	.117E 03
4650.	.792E-01	.408E 00	.193E 01	.143E 02	.382E 02	.106E 03
4675.	.705E-01	.362E 00	.168E 01	.128E 02	.339E 02	.967E 02
4700.	.628E-01	.320E 00	.145E 01	.114E 02	.301E 02	.879E 02
4725.	.558E-01	.284E 00	.126E 01	.102E 02	.267E 02	.799E 02
4750.	.173E 00	.428E 00	.123E 01	.442E 01	.220E 02	.817E 02
4775.	.156E 00	.396E 00	.121E 01	.510E 01	.206E 02	.871E 02
4800.	.244E 00	.461E 00	.119E 01	.407E 01	.193E 02	.103E 03
4825.	.175E 00	.396E 00	.118E 01	.465E 01	.202E 02	.100E 03
4850.	.151E 00	.368E 00	.117E 01	.462E 01	.193E 02	.894E 02
4875.	.134E 00	.337E 00	.115E 01	.401E 01	.174E 02	.770E 02

TABLE II (CONT.D)

FINE STRUCTURE PARAMETER (1/DLR) FOR H2O

1/CM	600 K	1000 K	1500 K	2000 K	2500 K	3000 K
4900.	.148E 00	.349E 00	.114E 01	.369E 01	.153E 02	.706E 02
4925.	.962E-01	.286E 00	.112E 01	.394E 01	.166E 02	.628E 02
4950.	.782E-01	.258E 00	.111E 01	.412E 01	.169E 02	.612E 02
4975.	.616E-01	.230E 00	.110E 01	.474E 01	.187E 02	.691E 02
5000.	.465E-01	.205E 00	.107E 01	.464E 01	.165E 02	.466E 02
5025.	.462E-01	.202E 00	.106E 01	.464E 01	.170E 02	.507E 02
5050.	.726E-01	.258E 00	.110E 01	.460E 01	.169E 02	.541E 02
5075.	.601E-01	.228E 00	.102E 01	.443E 01	.163E 02	.499E 02
5100.	.786E-01	.261E 00	.104E 01	.431E 01	.156E 02	.507E 02
5125.	.978E-01	.302E 00	.117E 01	.452E 01	.173E 02	.581E 02
5150.	.140E 00	.382E 00	.135E 01	.465E 01	.176E 02	.596E 02
5175.	.144E 00	.399E 00	.149E 01	.492E 01	.187E 02	.641E 02
5200.	.735E-01	.260E 00	.127E 01	.464E 01	.190E 02	.615E 02
5225.	.316E-01	.162E 00	.108E 01	.480E 01	.183E 02	.534E 02
5250.	.336E-01	.159E 00	.100E 01	.422E 01	.140E 02	.455E 02
5275.	.280E-01	.138E 00	.907E 00	.383E 01	.135E 02	.423E 02
5300.	.436E-01	.170E 00	.913E 00	.365E 01	.146E 02	.531E 02
5325.	.483E-01	.184E 00	.955E 00	.394E 01	.153E 02	.583E 02
5350.	.749E-01	.241E 00	.111E 01	.471E 01	.197E 02	.947E 02
5375.	.341E 00	.510E 00	.151E 01	.668E 01	.438E 02	.716E 03
5400.	.673E 00	.702E 00	.180E 01	.881E 01	.110E 03	.333E 04
5425.	.343E 00	.465E 00	.148E 01	.807E 01	.888E 02	.242E 04
5450.	.592E 00	.569E 00	.128E 01	.519E 01	.201E 02	.727E 03
5475.	.175E 00	.346E 00	.110E 01	.408E 01	.129E 02	.108E 03
5500.	.134E 00	.313E 00	.109E 01	.421E 01	.134E 02	.873E 02
5525.	.931E-01	.275E 00	.109E 01	.400E 01	.132E 02	.519E 02
5550.	.104E 00	.310E 00	.122E 01	.450E 01	.157E 02	.610E 02
5575.	.963E-01	.340E 00	.146E 01	.528E 01	.168E 02	.463E 02
5600.	.744E-01	.331E 00	.174E 01	.707E 01	.246E 02	.611E 02
5625.	.683E-01	.334E 00	.191E 01	.981E 01	.315E 02	.955E 02

TABLE II (CONT.D)

FINE STRUCTURE PARAMETER (1/DLR) FOR H2O

1/CM	600 K	1000 K	1500 K	2000 K	2500 K	3000 K
5650.	.604E-01	.316E 00	.195E 01	.112E 02	.420E 02	.129E 03
5675.	.646E-01	.345E 00	.216E 01	.132E 02	.496E 02	.158E 03
5700.	.691E-01	.377E 00	.240E 01	.155E 02	.584E 02	.194E 03
5725.	.742E-01	.413E 00	.266E 01	.182E 02	.689E 02	.238E 03
5750.	.793E-01	.451E 00	.294E 01	.215E 02	.812E 02	.292E 03
5775.	.850E-01	.493E 00	.326E 01	.253E 02	.958E 02	.358E 03
5800.	.912E-01	.539E 00	.362E 01	.298E 02	.112E 03	.440E 03
5825.	.976E-01	.589E 00	.401E 01	.351E 02	.133E 03	.539E 03
5850.	.104E 00	.644E 00	.445E 01	.413E 02	.156E 03	.661E 03
5875.	.112E 00	.704E 00	.493E 01	.487E 02	.184E 03	.811E 03
5900.	.119E 00	.770E 00	.547E 01	.573E 02	.218E 03	.994E 03
5925.	.128E 00	.841E 00	.606E 01	.675E 02	.257E 03	.121E 04
5950.	.137E 00	.919E 00	.672E 01	.794E 02	.302E 03	.149E 04
5975.	.147E 00	.100E 01	.745E 01	.936E 02	.357E 03	.183E 04
6000.	.157E 00	.109E 01	.826E 01	.110E 03	.420E 03	.224E 04
6025.	.152E 00	.105E 01	.783E 01	.104E 03	.398E 03	.213E 04
6050.	.146E 00	.100E 01	.743E 01	.988E 02	.376E 03	.201E 04
6075.	.141E 00	.963E 00	.704E 01	.936E 02	.356E 03	.191E 04
6100.	.136E 00	.922E 00	.668E 01	.887E 02	.336E 03	.181E 04
6125.	.132E 00	.882E 00	.634E 01	.840E 02	.318E 03	.171E 04
6150.	.127E 00	.844E 00	.601E 01	.795E 02	.301E 03	.162E 04
6175.	.123E 00	.808E 00	.570E 01	.753E 02	.284E 03	.154E 04
6200.	.119E 00	.774E 00	.541E 01	.713E 02	.269E 03	.146E 04
6225.	.114E 00	.740E 00	.513E 01	.676E 02	.254E 03	.138E 04
6250.	.110E 00	.708E 00	.487E 01	.640E 02	.240E 03	.131E 04
6275.	.107E 00	.678E 00	.462E 01	.606E 02	.227E 03	.124E 04
6300.	.103E 00	.648E 00	.438E 01	.574E 02	.215E 03	.117E 04
6325.	.997E-01	.621E 00	.415E 01	.544E 02	.203E 03	.111E 04
6350.	.963E-01	.594E 00	.394E 01	.515E 02	.192E 03	.105E 04
6375.	.929E-01	.568E 00	.374E 01	.488E 02	.182E 03	.100E 04

TABLE II (CONT.D)

FINE STRUCTURE PARAMETER (1/DLR) FOR H2O

1/CM	600 K	1000 K	1500 K	2000 K	2500 K	3000 K
6400.	.898E-01	.544E 00	.354E 01	.462E 02	.172E 03	.949E 03
6425.	.867E-01	.520E 00	.336E 01	.438E 02	.163E 03	.900E 03
6450.	.836E-01	.498E 00	.319E 01	.414E 02	.154E 03	.852E 03
6475.	.808E-01	.477E 00	.302E 01	.393E 02	.145E 03	.808E 03
6500.	.780E-01	.456E 00	.287E 01	.372E 02	.137E 03	.765E 03
6525.	.752E-01	.436E 00	.272E 01	.352E 02	.130E 03	.725E 03
6550.	.726E-01	.418E 00	.258E 01	.333E 02	.123E 03	.687E 03
6575.	.702E-01	.400E 00	.245E 01	.316E 02	.116E 03	.651E 03
6600.	.677E-01	.382E 00	.232E 01	.299E 02	.110E 03	.617E 03
6625.	.654E-01	.366E 00	.220E 01	.283E 02	.104E 03	.584E 03
6650.	.631E-01	.350E 00	.209E 01	.269E 02	.986E 02	.553E 03
6675.	.609E-01	.335E 00	.198E 01	.254E 02	.933E 02	.524E 03
6700.	.588E-01	.321E 00	.188E 01	.241E 02	.882E 02	.497E 03
6725.	.568E-01	.307E 00	.178E 01	.228E 02	.834E 02	.471E 03
6750.	.548E-01	.294E 00	.169E 01	.216E 02	.789E 02	.446E 03
6775.	.422E-01	.277E 00	.197E 01	.175E 02	.657E 02	.220E 03
6800.	.476E-01	.276E 00	.170E 01	.130E 02	.552E 02	.180E 03
6825.	.538E-01	.286E 00	.179E 01	.101E 02	.447E 02	.143E 03
6850.	.741E-01	.322E 00	.187E 01	.798E 01	.394E 02	.130E 03
6875.	.103E 00	.395E 00	.211E 01	.834E 01	.381E 02	.138E 03
6900.	.757E-01	.338E 00	.199E 01	.884E 01	.371E 02	.130E 03
6925.	.453E-01	.245E 00	.172E 01	.922E 01	.434E 02	.164E 03
6950.	.670E-01	.325E 00	.208E 01	.954E 01	.431E 02	.150E 03
6975.	.398E-01	.244E 00	.190E 01	.105E 02	.447E 02	.151E 03
7000.	.408E-01	.244E 00	.183E 01	.108E 02	.476E 02	.173E 03
7025.	.635E-01	.311E 00	.202E 01	.105E 02	.505E 02	.200E 03
7050.	.694E-01	.296E 00	.163E 01	.732E 01	.328E 02	.126E 03
7075.	.437E-01	.224E 00	.154E 01	.745E 01	.318E 02	.113E 03
7100.	.258E-01	.160E 00	.132E 01	.705E 01	.321E 02	.111E 03
7125.	.258E-01	.162E 00	.132E 01	.746E 01	.323E 02	.111E 03

TABLE II (CONT.D)

FINE STRUCTURE PARAMETER (1/DLR) FOR H2O

1/CM	600 K	1000 K	1500 K	2000 K	2500 K	3000 K
7150.	.208E-01	.143E 00	.127E 01	.835E 01	.381E 02	.140E 03
7175.	.183E-01	.130E 00	.117E 01	.788E 01	.342E 02	.122E 03
7200.	.154E-01	.107E 00	.101E 01	.752E 01	.434E 02	.204E 03
7225.	.253E-01	.152E 00	.123E 01	.845E 01	.460E 02	.218E 03
7250.	.320E-01	.181E 00	.139E 01	.908E 01	.502E 02	.236E 03
7275.	.274E-01	.175E 00	.141E 01	.798E 01	.328E 02	.106E 03
7300.	.230E-01	.151E 00	.129E 01	.723E 01	.334E 02	.120E 03
7325.	.314E-01	.193E 00	.146E 01	.592E 01	.189E 02	.421E 02
7350.	.563E-01	.265E 00	.158E 01	.534E 01	.160E 02	.356E 02
7375.	.567E-01	.286E 00	.188E 01	.794E 01	.302E 02	.872E 02
7400.	.710E-01	.367E 00	.234E 01	.151E 02	.763E 02	.340E 03
7425.	.804E-01	.490E 00	.370E 01	.253E 02	.135E 03	.612E 03
7450.	.909E-01	.654E 00	.585E 01	.423E 02	.241E 03	.110E 04
7475.	.102E 00	.872E 00	.924E 01	.708E 02	.428E 03	.197E 04
7500.	.116E 00	.116E 01	.145E 02	.118E 03	.763E 03	.355E 04